HAW HAMBURG

Master Thesis

Conditions for Passenger Aircraft Minimum Fuel Consumption, Direct Operating Costs and Environmental Impact

Author: Brecht Caers

Supervisor: Prof. Dr.-Ing. Dieter Scholz, MSME
Submitted: 2019-07-28

Faculty of Engineering and Computer Science
Department of Automotive and Aeronautical Engineering

DOI:
https://doi.org/10.15488/9323

URN:
https://nbn-resolving.org/urn:nbn:de:gbv:18302-aero2019-07-28.013

Associated URLs:
https://nbn-resolving.org/html/urn:nbn:de:gbv:18302-aero2019-07-28.013

Any further request may be directed to:
Prof. Dr.-Ing. Dieter Scholz, MSME
E-Mail see: http://www.ProfScholz.de

This work is part of:
Digital Library - Projects & Theses - Prof. Dr. Scholz
http://library.ProfScholz.de

Published by
Aircraft Design and Systems Group (AERO)
Department of Automotive and Aeronautical Engineering
Hamburg University of Applied Science

This report is deposited and archived:
- Deutsche Nationalbiliothek (https://www.dnb.de)
- Repositorium der Leibniz Universität Hannover (https://www.repo.uni-hannover.de)
- Internet Archive (https://archive.org)
  Item: https://archive.org/details/TextCaers.pdf

This report has associated published data in Harvard Dataverse:
https://doi.org/10.7910/DVN/DLZSDK

Abstract

Purpose – Find optimal flight and design parameters for three objectives: minimum fuel consumption, Direct Operating Costs (DOC), and environmental impact of a passenger jet aircraft.
Approach – Combining multiple models (this includes aerodynamics, specific fuel consumption, DOC, and equivalent CO_2 mass) into one generic model. In this combined model, each objective's importance is determined by a weighting factor. Additionally, the possibility of further optimizing this model by altering an aircraft's wing loading is analyzed.
Findings – When optimizing for a compromise between economic and ecologic benefits, the general outcome is a reduction in cruise altitude and an unaltered cruise Mach number compared to common practice. Decreasing cruise speed would benefit the environmental impact but has a negative effect on seat-mile cost. An increase in wing loading could further optimize the general outcome. Albeit at the cost of a greater required landing distance, therefore limiting the operational opportunities of this aircraft.
Research limitations – Most models use estimating equations based on first principles and statistical data.
Practical implications – The optimal cruise altitude and speed for a specific objective can be approximated for any passenger jet aircraft.
Social implications – By using a simple approach, the discussion of optimizing aircraft opens up to a level where everyone can participate.
Value – To find a general answer on how to optimize aviation, operational and design-wise, by using a simple approach.

Table of Contents

List of Figures

List of Tables

List of Symbols

a	Speed of sound
A	Aspect ratio
c	Thrust specific fuel consumption
C_D	Drag coefficient
C_{D0}	Zero lift drag coefficient
ΔC_{Dw}	Wave drag increment

C_L	Lift coefficient
$C_{L,md}$	Lift coefficient for minimum drag
$C_{L,max,L}$	Maximum lift coefficient during landing
e	Oswald factor
E	Aerodynamic efficiency
f	Fuel consumption
f_{MTOW}	Fuel consumption per kg of aircraft MTOW
f_{NM}	Fuel consumption per nautical mile
g	Gravity of Earth
H	Altitude
H_f	Net heating value of the fuel
k_H	Humidity correction factor
k_L	Landing field length correction factor
k_{INF}	Inflation factor
M	Mach number
$m_{CO2,eq}$	Equivalent CO_2 mass
m_f	Onboard fuel mass
m_{ML}	Maximum landing mass
m_{MTO}	Maximum take-off mass
M	Mach number
M_{CR}	Cruise Mach number
M_{crit}	Critical Mach number
M_{DD}	Drag divergence Mach number
n_{seat}	Number of seats
$n_{t,a}$	Number of flights per year
p_{INF}	Annual mean inflation rate
R	Range
R_{DOC}	DOC range
R_{NM}	Range in nautical mile
r_a	Specific air range
s	Forcing factor
S	Relevant surface area
s_{LFL}	Landing field length
S_{wet}	Wetted surface area
T	Ambient temperature
T_N	Net thrust of all installed engines
t_b	Block time
t_f	Flight time
$U_{a,f}$	Annual aircraft utilization
V	True airspeed
V_{md}	Speed for minimum drag

V_{MSR}	Speed for maximum specific air range
W_f	Uncorrected fuel flow
W_{ff}	Corrected fuel flow
x	Still air distance

Greek Symbols

γ	Flight path angle
δ	Pressure ratio
η_0	Overall engine efficiency
θ	Temperature ratio
ρ	Air density
σ	Density ratio
$\varphi_{25,w}$	Wing sweep angle

List of Abbreviations

AEA	Association of European Airlines
AIC	Aircraft-Induced Cloudiness
ATC	Air Traffic Control
BADA	Base of Aircraft Data
BPR	Bypass Ratio
CF	Characterization Factor
DOC	Direct Operating Costs
ECON	Economy cruise speed
EI	Emission Index
EIA	U.S. Energy Information Administration
FCOM	Flight Crew Operating Manual
FL	Flight Level
FMC	Flight Management Computer
FOB	Fuel On Board
GWP	Global Warming Potential
IAS	Indicated Airspeed
IATA	International Air Transport Association
ICAO	International Civil Aviation Organization
IPCC	Intergovernmental Panel on Climate Change
ISO	International Organization for Standardization
LRC	Long Range Cruise speed

LTO	Landing and Take-Off (cycle)
MRC	Maximum Range Cruise speed
MTOW	Maximum Take-Off Weight
NM	Nautical Mile
ROC	Rate Of Climb
ROD	Rate Of Descent
RVSM	Reduced Vertical Separation Minima
SAR	Specific Air Range
SGR	Specific Ground Range
SGTP	Sustained Global Temperature Potential
TAS	True Airspeed
TSFC	Thrust Specific Fuel Consumption

List of Definitions

Airway
: A defined zone of heavy air traffic (**Whitelegg 2000**).

Block time
: This the flight time with added ground times (such as due to the push back of the aircraft, taxi prior to take-off and after landing, or waiting on the ground for clearance). (**Scholz 2015**).

Critical Mach number
: The free-stream Mach number at which localized regions of supersonic flow on the aircraft's geometry first appear (**Young 2018**).

Cruise flight
: Portion of a flight from the point where the aircraft has leveled off following a climb to its initial cruising altitude until the point where it commences its descent (**Young 2018**).

Direct operating costs
: Costs that include the entire operating costs of the aircraft (**Scholz 2015**).

Drag divergence Mach number
: The Mach number at which the wave drag amounts to 0.002 (**Scholz 2015**).

Emission index
: The mass of species emitted per kilogram of fuel burned (**Van Endert 2017**).

Flight time

Time that commences when an aircraft moves under its own power for the purpose of flight and ends when the aircraft comes to a rest after landing (**FAR Part 1 2005**)

Landing field length

The landing distance of an aircraft multiplied by a safety factor (**Scholz 2015**).

Specific air range

Still air distance traveled per unit of fuel mass consumed (**Young 2018**).

Sustained global temperature potential

A climate change metric that treats gas emissions as persistent events and not as one-time events (**Neubauer 2015**).

Thrust specific fuel consumption

Is the mass of fuel burned per unit of time, divided by the thrust (**Young 2018**).

True airspeed

The velocity of the aircraft relative to the atmosphere (**Hull 2007**)

Wing loading

The maximum take-off weight of an aircraft over its wing surface area (**Scholz 2015**).

1 Introduction

1.1 Motivation

Optimizing aircraft and flight parameters for economic reasons goes back more than a century. People have been trying to minimize fuel consumption and the cost of flying since the invention of the very first aircraft. And nowadays the search still continues for more fuel-efficient engines, lighter structures or optimized routes for airlines. Economic reasons drive most, if not all, decisions in aircraft design and in operating procedures for airlines.

In the most recent decades, following the growing worldwide attention to climate change, the amount of research on the environmental effects of aircraft has ramped up significantly. This is further augmented by the recent focus of regulatory organizations (e.g. ICAO) on decreasing the climate impact of the aviation industry. Nevertheless, attention to the environmental impact of aviation was and still is lagging behind on the automotive industry.

The main issue with existing research is that optimization models are mostly kept behind closed doors by manufacturers and airlines to guard them from the competition. This makes it difficult for outsiders to gain any insight in realistic operating data of modern passenger jet aircraft. The aim here is to open up the discussion to more people by working with first principles, simple equations, and publicly available data.

This thesis is written with a reader with a basic engineering background in mind. All aviation-related terms and abbreviations are defined in the list of definitions and list of abbreviations or elaborated in the body of the text.

1.2 Title Terminology

"Conditions for Passenger Aircraft Minimum Fuel Consumption, Direct Operating Costs and Environmental Impact"

Passenger aircraft: An aircraft which main goal is to transport passengers. In this thesis passenger aircraft will be narrowed down to passenger jet aircraft.

Fuel Consumption: The mass of fuel burned per unit of time or distance.

Direct Operating Costs: The costs directly associated with operating the aircraft.

Environmental Impact: The direct or indirect impact on the environment of operating an aircraft.

1.3 Objectives

The main objective of this thesis is to deliver an overview of the influence of different flight and design parameters on an aircraft's fuel consumption, direct operating costs, and environmental impact. The influence of cruise speed Mach number, altitude, and wing loading will be analyzed. The aim is to make these models as generic as possible by minimizing the input of aircraft specific data.

The first step is to review and analyze some fundamental methods for calculating fuel consumption, DOC, and environmental impact separately and the methods needed to calculate all relevant parameters. All models are based on first principles, simple equations, and statistical data.

The models are then implemented in an Excel tool which calculates each of the previously mentioned goals and the most important parameters to reach them. The influence of each of these parameters is further analyzed and compared to real-world flight operation practices when possible.

The final step is to combine all separate models into one model to find and optimum cruise Mach number and altitude for minimum fuel consumption, DOC and environmental impact combined. These results are then recalculated for the same aircraft with a higher wing loading in order to analyze the impact of this design parameter. The final result is a combined value which can be altered for greater economic or ecologic importance by means of weighting factors.

1.4 Previous Research

Several cruise speed options to obtain minimum fuel consumption are discussed by **Young 2018**. Specific air range is defined and calculated and by use of this parameter, three different cruise speed options are considered and compared with each other. Furthermore, an optimum cruise altitude for minimum fuel consumption is defined as cruise-climb and the commonly used stepped approximation of the cruise-climb maneuver is discussed.

An important parameter for calculating fuel consumption is the thrust specific fuel consumption. The TSFC's dependency on flight altitude, speed and thrust setting is discussed in **Bensel 2018**. A model for calculating the TSFC is made by **Herrmann 2010** and is used in the fuel consumption model in later chapters.

Direct operating costs have been researched by a multitude of organizations. For the model in this thesis, a method by **Scholz 2015** will be used which is mostly based on the AEA1989

methods. This method is fully elaborated in the lecture notes by Scholz, therefore only results and some relevant equations will be mentioned in this thesis.

The environmental impact of the aviation industry has gained more attention recently, providing enhanced research. The first comprehensive report on this subject was written by the IPCC, called “Aviation and the Global Atmosphere” (**Penner 1999**). It handles the direct and indirect effects of the aviation industry on the climate. These effects are put into quantitative results by using radiative forcing, albeit with rather high levels of uncertainty. A differentiation is made between subsonic and supersonic aviation and their estimated future impacts. The report also lists multiple options to reduce the impact of aviation.

One area where the IPCC report lacks in is accuracy of the impact of aircraft-induced cloudiness. This includes contrail formation and aircraft-induced cirrus clouds. In an update (**Sausen 2005**) to the IPCC report, the radiative forcing of aircraft-induced cloudiness was strongly reduced, while increasing the accuracy of the results. In a report by **Fichter 2005**, the influence of cruise altitude on contrail formation is discussed.

The master thesis by **Van Endert 2017** introduces the concept of ecolabels for aircraft. Altitude dependency of NO_x and contrail formation are calculated and the concept of equivalent CO_2 mass is used as an alternative metric for radiative forcing. Most equations and data used were originally produced by **Schwarz 2011**, but have been simplified and compiled to generate one value in the form of equivalent CO_2 mass.

1.5 Structure of the Work

Chapter 2: Overview of existing research and results as an introduction to the subject. Emphasis on fuel consumption and environmental impact.

Chapter 3: Brief review of the models used in this thesis for aerodynamics, TSFC, DOC, the atmosphere, and equivalent CO_2 mass.

Chapter 4: Explanation of the Excel tool used to calculate all results for Chapter 5 to 8.

Chapter 5: Model for minimal fuel consumption and its most influential parameters.

Chapter 6: Model for minimal direct operating costs and its most influential parameters.

Chapter 7: Model for minimal environmental impact and its most influential parameters. Split into resource depletion and engine emissions.

Chapter 8: Combined model of DOC and environmental impact. Includes a subchapter about the influence of wing loading.

Chapter 9: Conclusions and recommendations.

2 Literature Review

2.1 Cruise Speed for Minimum Fuel Consumption

The minimum fuel consumption case can be seen as a maximum range case. Minimum fuel consumption is considered as burning a minimum amount of fuel for a maximum distance, while maximum range can be described as covering a maximum distance on a minimum amount of fuel. These two definitions boil down to the same idea.

For normal commercial aircraft operations, the cruise flight phase spans the majority of the total flight time. Taking this into consideration, most models only calculate optimum speed values for cruise flight. In addition, climb and descend speed can only be varied lightly due to different restricting parameters (e.g. ATC restrictions or runway length).

Young 2018 gives an overview of different possible cruise speeds. These cruise speeds are based on the specific air range r_a, which can be defined as:

$$r_a = \frac{dx}{-dm_f} = \frac{\frac{dx}{dt}}{\frac{-dm_f}{dt}} = \frac{V}{W_f} = \frac{V}{c \cdot T_N} = \frac{V}{c \cdot D} \tag{2.1}$$

From this equation the theoretical speed for maximum r_a, noted as V_{MSR}, can be derived. The specific air range depends on the true airspeed V, the TSFC c and the drag D. The TSFC c is assumed constant and the drag D can be expressed in function of speed V:

$$D = \left[\frac{C_{D0} \cdot \rho \cdot S}{2}\right] \cdot V^2 + \left[\frac{2 \cdot (m \cdot g)^2}{\pi \cdot A \cdot e \cdot \rho \cdot S}\right] \cdot \frac{1}{V^2} \tag{2.2}$$

Or simplified:

$$D = A_D \cdot V^2 + B_D \cdot \frac{1}{V^2} \tag{2.3}$$

To find the highest SAR in function of speed (with a TSFC assumed constant), the ratio V/D should be maximized. The following derivation is made:

$$\frac{d}{dV}\left(\frac{V}{D}\right) = 0 \tag{2.4}$$

This results in:

$$V_{MSR} = \sqrt[4]{3} \cdot \sqrt{\frac{B_D}{A_D}} = \sqrt[4]{3} \cdot V_{md} \tag{2.5}$$

With: V_{md} the speed for minimum drag (or maximum aerodynamic efficiency).

Continuing with Eq. (2.1), r_a can be defined based on the TSFC. By integrating the resulting equation for r_a the still air range R can be achieved.

$$r_a = \frac{V \cdot E}{c \cdot m \cdot g} \tag{2.6}$$

$$R = \frac{1}{g} \cdot \int_{m2}^{m1} \frac{V \cdot E}{c \cdot m} dm \tag{2.7}$$

With: m_1 the start-of-cruise aircraft mass
m_2 the end-of-cruise aircraft mass

2.1.1 Analytical Integration

An analytical integration of Eq. (2.7) can be done if the assumption is made that the TSFC does not change during cruise. The result is a reasonable approximation, but assuming a constant TSFC is the most important shortcoming in these simplified models for cruise speed and altitude. In the following integrations a mean constant value for the TSFC will be used, noted as $\bar{c}$.

The approach used by **Young 2018** and **Hull 2007** is to first establish boundary conditions for three different scenarios. Integrations can be found in the aforementioned literature, only the relevant results in terms of operation of the aircraft will be mentioned here:

1) Cruise at constant H and constant C_L

   Considering the equation for the lift coefficient in steady level flight:

$$C_L = \frac{2 \cdot m \cdot g}{\rho \cdot V^2 \cdot S} \tag{2.8}$$

   It is clear that to keep the altitude (related to ρ) and C_L constant, V should decrease with decreasing m. Which means the engine thrust F_N must also decrease constantly, making this an unviable solution for the flight crew.

2) Cruise at constant V and constant C_L

This situation is known as cruise-climb. The resulting expression after integrating is known as the Breguet range equation:

$$R = \frac{V \cdot E}{\bar{c} \cdot g} \cdot \ln\left(\frac{m_1}{m_2}\right) \tag{2.9}$$

For non-steady level flight Eq. (2.8) turns into:

$$C_L = \frac{2 \cdot m \cdot g \cdot \cos\gamma}{\rho \cdot V^2 \cdot S} \tag{2.10}$$

During cruise climb the flight angle γ is very small, which leads to $\cos\gamma \cong 1$. As V and C_L are to be held constant, the ratio m/ρ should also remain constant. This implies that ρ (and thus the altitude) should increase with decreasing m. Consequently, the altitude should be increased slowly during the whole cruise phase, a cruise-climb maneuver.

3) Cruise at constant H and constant V

In this case the integration can be solved if it is assumed that the drag can be modelled by the transonic drag polar (Eq. (3.1)). During cruise the lift coefficient in this scenario will reduce with time (due to its dependency on mass, which in turn decreases with the consumption of fuel). This means that the drag coefficient will also reduce. Considering the following equation for aircraft drag during cruise:

$$T_N = D = \frac{1}{2} \cdot \rho \cdot V^2 \cdot S \cdot C_D \tag{2.12}$$

A reducing drag coefficient means reducing drag, which in term means the crew must constantly reduce the thrust to maintain a constant V.

2.1.2 Maximum Range Cruise Speed

Young 2018 describes the following three cruise speed options. The first is the maximum range cruise speed: MRC. This is the speed that results in the maximum SAR, which is (theoretically) $V_{MSR} = \sqrt[4]{3} \cdot V_{md}$. This speed decreases slightly while the aircraft becomes lighter due to fuel consumption during the flight, as illustrated in Figure 2.1:

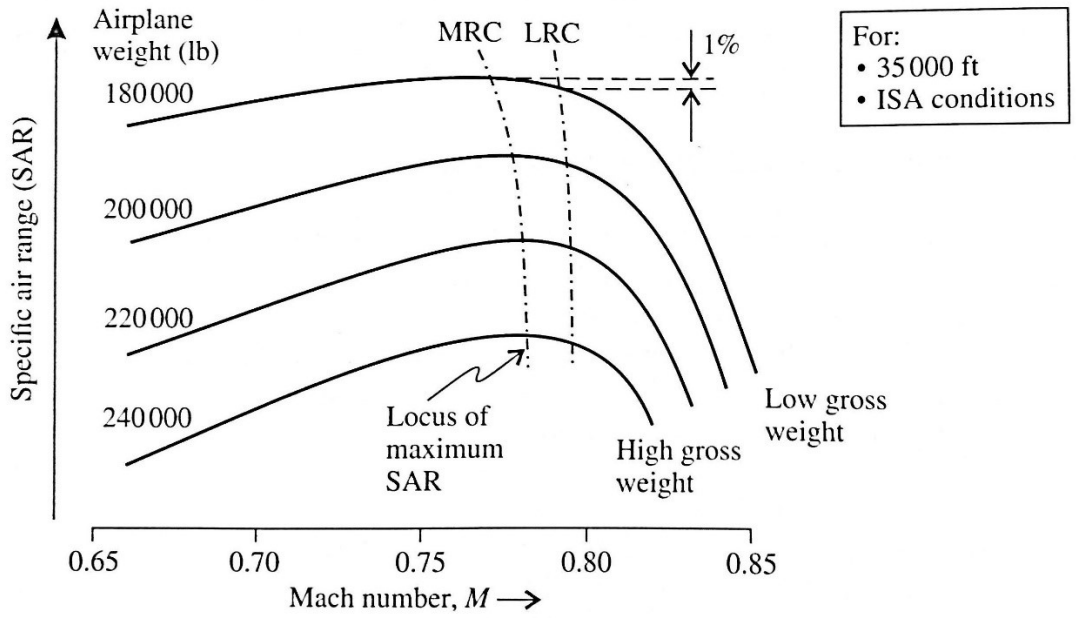

Figure 2.1: MRC and LRC speed (**Young 2018**)

The MRC speed depends on an aircraft's gross weight, cruising altitude and the ambient air temperature and is the speed which corresponds with the lowest fuel cost.

2.1.3 Economy Cruise Speed

The cruise speed used in practice by most airlines is called economy cruise speed: ECON. It is a little faster than the MRC speed, therefore using a small amount more fuel but also arriving at the destination in a shorter time. Time is an important factor in calculating the trip cost as the time-dependent costs can be substantial. The ECON speed is usually calculated (by iteration) before each flight with the most recent cost index (CI) from the airline (**Roberson 2007**). This cost index is different for each operator and aircraft.

The ECON speed is the speed for the lowest direct operating cost (and not just the lowest fuel cost). This time dependency of the direct operating cost can be seen in the seat-mile cost, modelled in Chapter 6.

2.1.4 Long-Range Cruise Speed

The long-range cruise speed LRC is a simplified approach to the ECON speed. For calculating the LRC speed it is not necessary to have any knowledge of the airline's cost structure. The LRC speed is determined by allowing a 1% reduction from the peak SAR and selecting the faster of the two resulting speeds (**Airbus 2002**). The advantage is that 1% of range is

traded for 3 to 5% higher cruise speed (**Hurt 1965**), which in turn leads to a shorter flight time. The difference between MRC and LRC speed is illustrated in Figure 2.2.

2.1.5 Comparison

The following figure illustrates how the different costs vary with increasing Mach number in cruise flight. As stated before, the MRC speed corresponds with the lowest possible fuel cost and the ECON speed with the lowest possible total cost. When time-dependent costs are considered, ECON speed is always higher than MRC speed. The LRC speed is typically about 2-5% faster than the MRC speed according to **Roberson 2007** and **Seto 2009**.

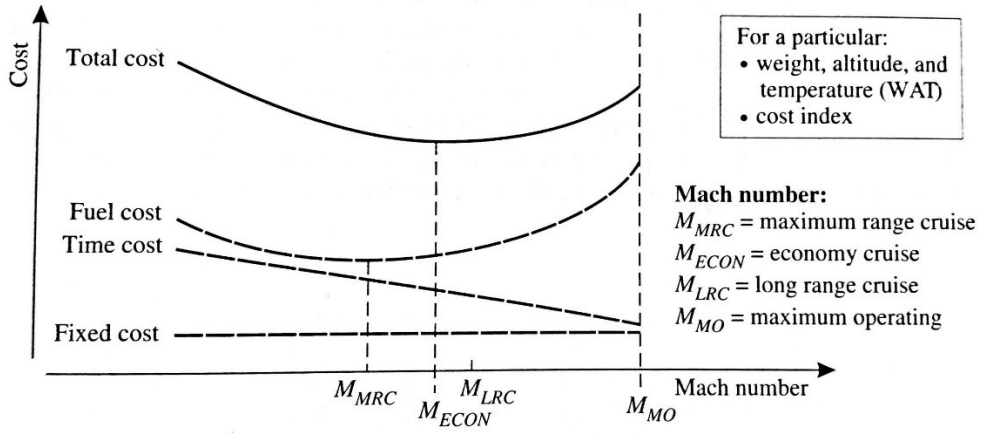

Figure 2.2: Cost overview for the different cruise speeds (**Young 2018**)

Another thing to note is that the LRC speed is calculated for zero wind conditions, while the ECON speed usually takes wind speed into account when entered into the FMC. This means that the ECON speed will be lowered in a strong tailwind and increased when headwind is present, making optimal use of weather conditions (**Roberson 2007**).

2.2 Cruise Altitude for Minimum Fuel Consumption

The optimum cruise altitude is the altitude that results in the greatest SAR for a particular aircraft weight, ambient air temperature and Mach number. These data are determined by flight testing and published in the aircraft's FCOM by the manufacturer. For many aircraft models, flight testing data shows that the optimum altitude tends to increase quasi linear with decreasing aircraft weight. To fly at the optimum altitude during the whole flight would mean increasing altitude constantly for the duration of the cruise (see Chapter 2.1.1, scenario 2). This maneuver is called cruise-climb and is forbidden by ATC due to flight level restrictions.

Flight levels (FL) are used to assure safe air traffic by separating aircraft into certain altitude zones. They are used starting from a certain transition altitude above the ground (depending on country). The altitude is calculated by measuring the ambient pressure and is standardized to the ISA pressure at sea level of 101 325 Pa. This standardization guarantees that every aircraft perceives flight levels at the same altitude, regardless of local variations in ambient pressure. Most modern aircraft are certified for reduced vertical separation minima (RVSM). This reduces the minimum flight level separation from 2 000 ft to 1 000 feet and allows aircraft to safely fly more optimum routes, reducing fuel consumption and increasing airspace capacity (**FAA 2017**). Even though the minimum separation has been reduced, aircraft are still not allowed to constantly change flight level during their flight. That is why in practice jet aircraft fly a stepped approximation of the cruise-climb maneuver, illustrated in Figure 2.3:

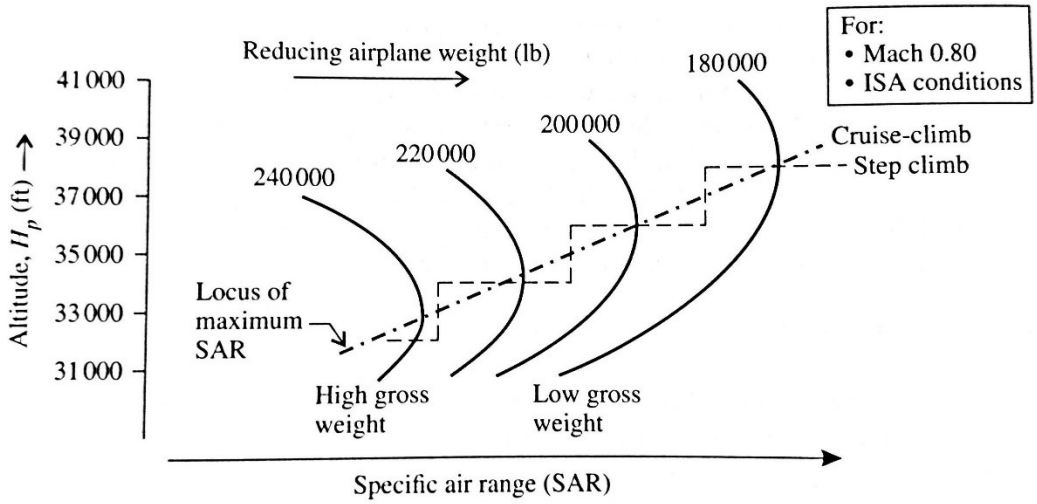

Figure 2.3: Step-climb approximation for cruise-climb (**Young 2018**)

2.3 Direct Operating Costs

The direct operating costs are all costs made by an operator of an aircraft (e.g. airline) in order to operate the aircraft. The DOC can be split up into time-independent/accountancy costs like depreciation and interest, and into time-dependent costs. These time-dependent costs are called the cost index and include fuel, maintenance, crew, and fees and handling. Fuel price can be considered highly time-dependent (see Figure 2.4) and can alter a DOC model based on the date of calculation.

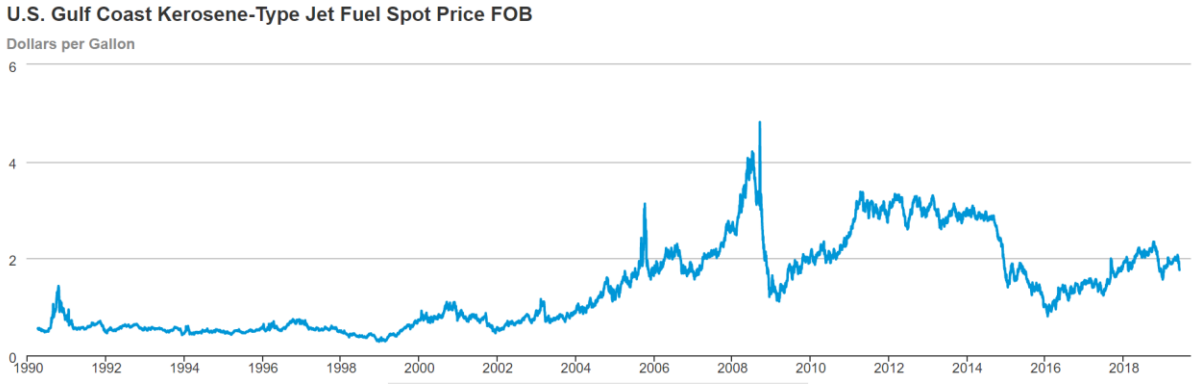

Figure 2.4: Variation in jet fuel prices throughout the recent decades (**EIA 2019**)

The method used in this thesis is described in the lecture notes by **Scholz 2015**. It is based on the methods defined in AEA 1989a and AEA 1989b. The AEA 1989a variation is for short- and medium-range aircraft and the b variation for long-range aircraft. The output can be represented as the annual cost of one aircraft, denoted as: $C_{a/c,a}$ or the seat-mile cost $C_{s,m}$.

2.4 Environmental Impact

The environmental impact of an aircraft in cruise flight can be divided into resource depletion and engine emissions with their impact on the global atmosphere. Noise pollution and local air quality will not be considered here since only cruise flight is covered in this thesis.

2.4.1 Resource Depletion

Resource depletion will be limited to the depletion caused by an aircraft's fuel consumption. It could be seen in a broader context that includes the materials that were used to manufacture, transport and assemble different parts of an aircraft. However, the aim here is to treat the operational aspect of the aircraft only. Therefore, resource depletion can be set equal to the fuel consumption of the aircraft. Jet fuel (kerosene) is distilled from crude oil, which is considered the resource in this model.

2.4.2 Aviation and the Global Atmosphere

The environmental impact of aviation has been researched thoroughly by the IPCC in their 1999 report titled "Aviation and the Global Atmosphere" (**Penner 1999**). The following summary is based on this report.

There are a number of different ways in which operating a jet aircraft impacts the environment. Within the scope of this thesis only the impact of actually flying the aircraft will be considered, no indirect impact or emissions from ground transport at airports for example. First, there is the measurable emission from the combustion of jet fuel. This consists of carbon dioxide (CO_2), water vapor (H_2O), nitrogen oxides (NO_x) and other particulates like sulfur oxides (SO_x) and soot. These gases and particles are emitted directly into the atmosphere around the tropopause level (see Chapter 3.4 for the tropopause).

Subsequently, there is the climate impact of these emissions. This is a lot harder to measure, but by means of radiative forcing (RF) the climate impact of emission components can be compared mutually or to the climate impact of other industries. Radiative forcing (RF) is the difference between the energy which the Earth absorbs from the Sun and the energy which is radiated back into space. It is defined in units of watt per square meter. A positive radiative forcing will cause warming of the Earth, a negative one will cause cooling. This balance between absorbed and reflected energy determines the average global temperature and can be influenced by greenhouse gasses (among other factors). Radiative forcing makes it possible to measure climate change in a quantitative way. The drawback of using radiative forcing is that it cannot be applied to calculate the influence of a single flight, only the total influence of all aviation emissions during a period of time. In most cases this period is defined as 100 years (**Jardine 2005**). For this reason, the metric of equivalent CO_2 mass will be used (elaborated in Chapter 3.5).

The following table gives an overview of each emission component's direct or indirect impact on the environment:

Table 2.1: Climate impact of different emission components (**Penner 1999**)

Emitted Species	Role and Major Effect at Earth's Surface
CO_2	*Troposphere and Stratosphere* Direct radiative forcing ⟶ warming
H_2O	*Troposphere* Direct radiative forcing ⟶ warming Increased contrail formation ⟶ radiative forcing ⟶ warming *Stratosphere* Direct radiative forcing ⟶ warming Enhanced PSC formation ⟶ O_3 depletion ⟶ enhanced UV-B Modifies O_3 chemistry ⟶ O_3 depletion ⟶ enhanced UV-B
NO_x	*Troposphere* O_3 formation in upper troposphere ⟶ radiative forcing ⟶ warming ⟶ reduced UV-B Decrease in CH_4 ⟶ less radiative forcing ⟶ cooling *Stratosphere* O_3 formation below 18-20 km ⟶ reduced UV-B O_3 formation above 18-20 km ⟶ enhanced UV-B Enhanced PSC formation ⟶ O_3 depletion ⟶ enhanced UV-B
SO_xO and H_2SO_4	*Troposphere* Enhanced sulfate aerosol concentrations Direct radiative forcing ⟶ cooling Contrail formation ⟶ radiative forcing ⟶ warming Increased cirrus cloud cover ⟶ radiative forcing ⟶ warming Modifies O_3 chemistry *Stratosphere* Modifies O_3 chemistry
Soot	*Troposphere* Direct radiative forcing ⟶ warming Contrail formation ⟶ radiative forcing ⟶ warming Increased cirrus cloud cover ⟶ radiative forcing ⟶ warming Modifies O_3 chemistry *Stratosphere* Modifies O_3 chemistry

In 2005, an update to the 1999 report (by **Sausen 2005**, based on the TRADEOFF project) was published to present several new values for the radiative forcing of emission components. Especially the RF value of contrails is strongly reduced by a factor of three to four. The following figure shows a comparison of RF values for different components:

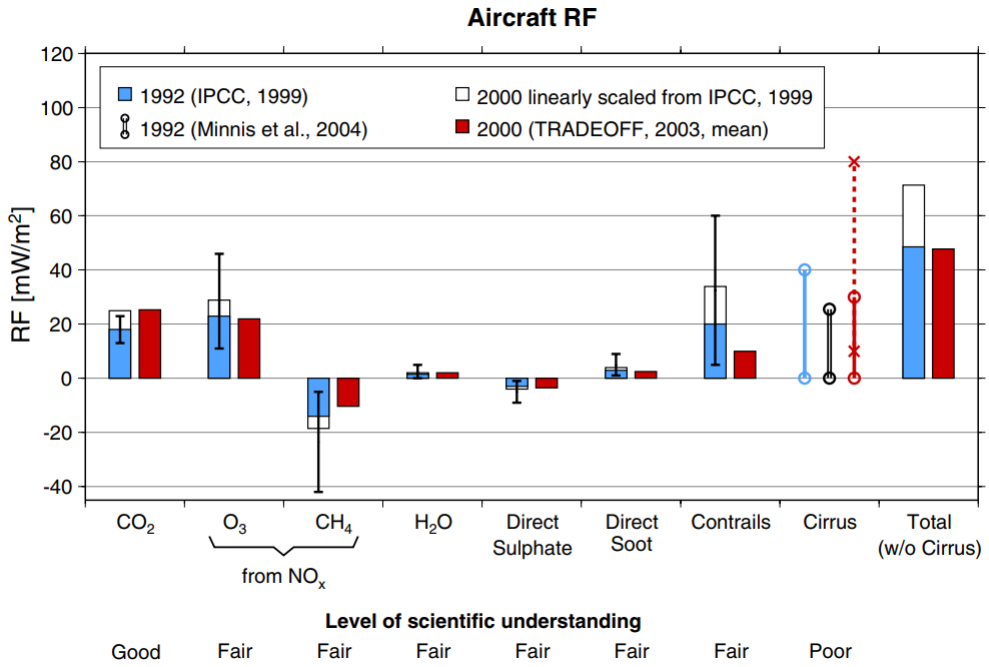

Figure 2.5: Comparison of radiative forcing values for emission components (**Sausen 2005**)

Out of all emission components, only contrails and nitrogen oxides (NO_x) are found to be dependent on the cruise altitude (**Fichter 2005**). CO_2 emission depends primarily on the fuel consumption of the aircraft. These three components will be used in the environmental impact model in Chapter 7. The other components have a smaller environmental impact and will not be considered.

2.4.3 Contrails and Aviation-Induced Cirrus Clouds

Contrails are the result of water vapor in the engine exhaust gasses of a jet aircraft flying at common cruise altitudes. The ambient temperature at this altitude is around -56° C, which means the water vapor freezes into tiny ice crystals (further augmented by sulfur oxides and soot). This formation of ice crystals forms the well-known white lines that trail after aircraft and can be seen from the ground. The initially thin lines can last long and spread to widths of more than 10 km. In the so-called airways over the North Atlantic Ocean and Europe, contrails can cover 5% of the sky area annually. Below these airways, contrails could have a bigger environmental impact than all greenhouse gasses combined (**Whitelegg 2000**).

The presence of contrails can also induce the formation of cirrus clouds which would not naturally occur there. These are called aviation-induced cirrus clouds and are believed to have a strong warming effect on the atmosphere (**Jardine 2005**). In the 2005 update to the IPCC report, multiple studies concerning the radiative forcing of these cirrus clouds were analyzed. Cirrus clouds could account for the same amount of radiative forcing as all other emission components combined. The conclusion however is that there is too much uncertainty over the

actual RF value to include cirrus clouds in the total RF value of all emission components (**Sausen 2005**). This lack of scientific understanding is mentioned in Figure 2.5 as well.

The formation of contrails (and thus aviation-induced cirrus clouds) depends upon the following factors: humidity, temperature, pressure, the emission index of water vapor, and the overall propulsion efficiency of the aircraft. Furthermore, the atmosphere must be supersaturated with respect to ice to make ice crystal growth possible. Another significant factor is the influence of latitude and the seasonal cycle, which can be seen clearly in Figure 2.6 and Figure 2.7 (**Fichter 2005**).

The TRADEOFF study following up on the aforementioned IPCC report tried to find quantitative results for the impact of cruise altitude changes on the global coverage of contrails and the radiative forcing they cause (**Fichter 2005**). The results of the report are summarized below, describing the method used and the results:

The study applied a parameterization for line-shaped contrails by **Ponater 2002**. This model is based on the thermodynamic theory of contrail formation (Schmidt-Appleman theory), which takes into account that contrails can only form if the air is supersaturated with respect to ice. To calculate the actual contrail coverage from the potential contrail coverage, the distance travelled was used instead of the amount of fuel used. The base case of mean contrail coverage was determined by using satellite observations. And all climate change effects caused by contrails are measured as radiative forcing.

Generally, a decrease in altitude results in a decrease in global contrail coverage. The relationship between the two is almost linear up to a maximum decrease of 45 % in coverage at an altitude of 6 000 ft under the base case. On the other hand, an increase in fuel consumption can also be seen by flying at a lower cruise altitude (further discussed in Chapter 5 and 7). The report also analyzes the impact of an increase in cruise altitude. In this case there is a slight increase in global contrail coverage and a small decrease in fuel consumption.

Table 2.2: Effect of cruise altitude on contrails and fuel consumption (**Fichter 2005**)

Inventory	Flown Distance [*10^9 km/yr]	Fuel Consumption [Tg/yr]	Global Mean Contrail Coverage [%]	Net RF by Contrails [mW/m^2]
DLR2	18.0	112.2	0.052 (distance) 0.057 (fuel)	2.1 (3.2) 2.3 (3.5)
TRADEOFF base case	17.1	111.5	0.047 (distance) 0.052 (fuel)	1.9 (2.9) 2.0 (3.1)
TRADEOFF +2 kft	17.1	111.0	0.050 (distance)	2.0 (3.1)
TRADEOFF –2 kft	17.1	114.5	0.041 (distance)	1.6 (2.5)
TRADEOFF –4 kft	17.1	115.5	0.034 (distance)	1.3 (2.0)
TRADEOFF –6 kft	17.1	118.0	0.026 (distance)	1.0 (1.6)

The values given in the table above are all average global values. However, due to the dependency on latitude and the seasonal cycle, the local values of contrail coverage vary widely over the globe. This is visible on the following figures:

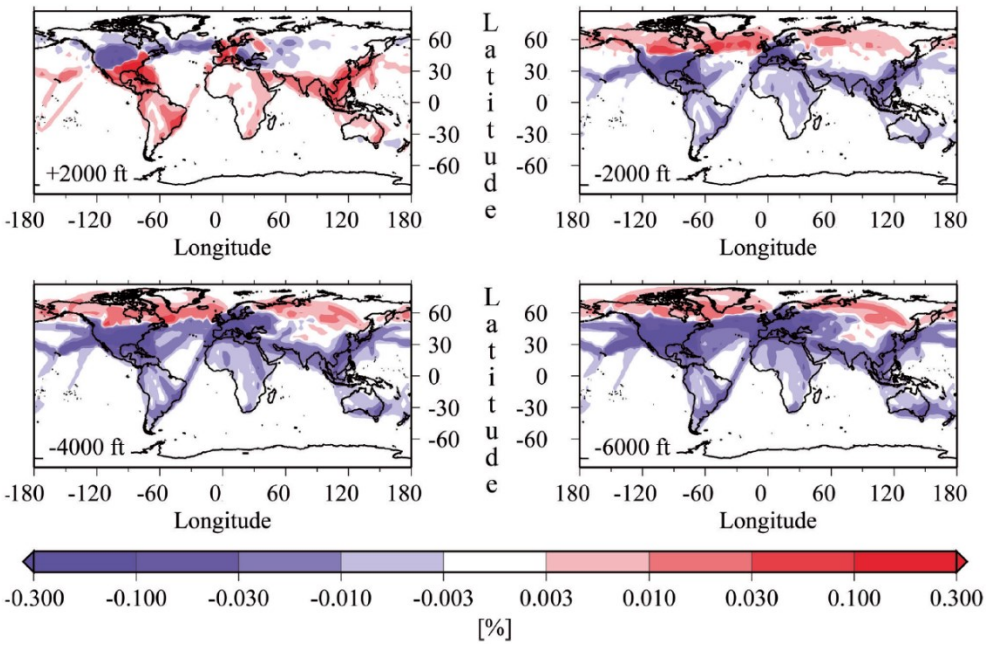

Figure 2.6: Contrail coverage variation in function of altitude changes (% in relation to the base case) (**Fichter 2005**)

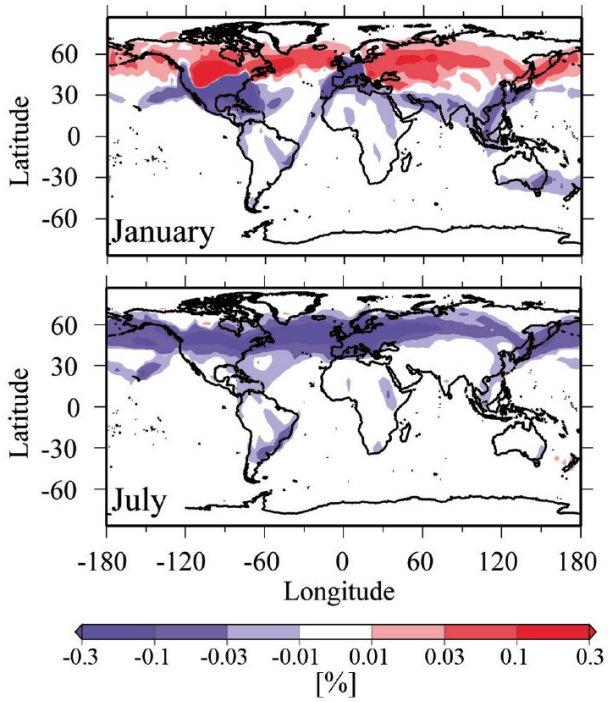

Figure 2.7: Seasonal influence on contrail coverage (6000 ft under the base case) (**Fichter 2005**)

3 Fundamental Models

3.1 Aerodynamics

3.1.1 Drag Coefficient

The drag polar expresses the relationship between lift and drag coefficient. For low-speed subsonic flight, a single line can represent the drag polar. When flying at higher transonic speeds, the drag polar consists of multiple lines. Each of these lines represent a different cruise Mach number. A generic high speed drag polar is given in the following figure:

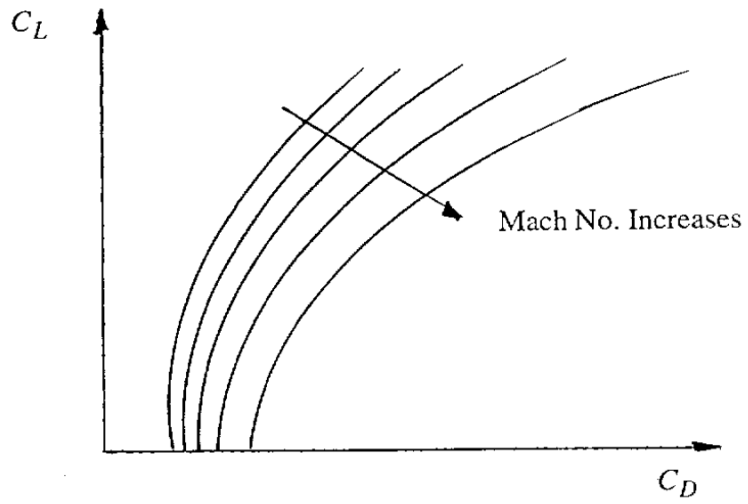

Figure 3.1: Generic Drag polar for the transonic region (**Young 2001**)

In the transonic region (where $M > M_{crit}$), the drag coefficient consists of the following terms:

$$C_D = C_{D0} + \Delta C_{Dw} + K \cdot C_L^2 \tag{3.1}$$

With:

$$K = \frac{1}{\pi \cdot A \cdot e} \tag{3.2}$$

The zero lift drag coefficient C_{D0} depends mostly on geometric aircraft parameters and can be estimated with the method in Chapter 3.1.2. The wave drag increment ΔC_{Dw} is highly dependent on the aircraft speed and is discussed in Chapter 3.1.3. The final component $K \,.\, C_L^2$ is the lift dependent part of the drag coefficient. The Oswald factor must be known in order to calculate it. This is discussed in Chapter 3.1.4.

In the following subchapters, a lot of approximations will be made in the calculation of drag components. The reason being that aircraft manufactures try to keep most of their exact aircraft data classified. This means that only people in the industry can use exact data and generate an accurate result. In the academic world this data is seldomly available and calculations must be made with approximating equations and statistical data.

3.1.2 Zero Lift Drag Coefficient

The zero lift drag coefficient represents the drag that is present when zero lift force is applied on an aircraft. It depends mostly on geometric aircraft parameters and material choice (roughness). It can be used to judge a design on its aerodynamic properties.

There are a number of different options for calculating or estimating C_{D0}. Three different methods can be found in **Scholz 2015.** The method which is the most generally applicable is to calculate C_{D0} based on E_{max} and the Oswald factor e (described in 3.1.4):

$$C_{D0} = \frac{\pi \cdot A \cdot e}{4 \cdot E_{max}} \tag{3.3}$$

With:

$$E_{max} = k_E \cdot \sqrt{\frac{A}{S/S_{wet}}} \tag{3.4}$$

With: $k_E = 15.8$
$S/S_{wet} = 6.2$

Other methods include estimating C_{D0} from the wetted area of the aircraft or a more detailed approach by using the individual drag of aircraft components. Both methods can be found in **Scholz 2015**.

3.1.3 Wave Drag Increment

The wave drag increment is a term which is added to the drag coefficient equation to account for shock effects present at transonic speeds. Generally, the wave drag increment has a very small influence at low speed and only starts to gain importance when closing in on the drag divergence Mach number.

This drag divergence Mach number M_{dd} is an important parameter in wave drag calculation. The so-called Boeing definition will be used here. It states that M_{dd} corresponds to the speed where drag increases by 20 drag counts above the baseline condition (**Blake 2009**). 20 drag counts (CTS) equals a wave drag increment of: $\Delta C_{Dw} = 0.0020$.

The design philosophy of Boeing and Airbus is to set $M_{DD} = M_{CR}$ (**Scholz 2015**). But if desired, M_{dd} can be calculated with a method explained in **Scholz 2015**. Continuing with the previously mentioned design philosophy, the wave drag increment can be approximated based on statistical data:

$$\Delta C_{Dw} = A \cdot \tan\left(B \cdot \left(\frac{M}{M_{crit}}\right) - B\right) \cdot cos^3\left(\varphi_{25,w}\right) \tag{3.5}$$

With:

$$M_{crit} = \frac{B \cdot M_{DD}}{tan^{-1}\left(\frac{0.002}{A \cdot cos^3\left(\varphi_{25,w}\right)}\right) + B} \tag{3.6}$$

An important restriction for the Mach number in Eq. (3.5) is the following:

$$M < M_{crit} \cdot \left(1 + \frac{\pi}{2\,B}\right) \tag{3.7}$$

A and B in these equations are constants that are based on an analysis of several aircraft. The values in Table 3.1 can be used when calculating one of the aircraft mentioned in the table. When calculating any other aircraft, the averaged values in Table 3.2 should be used. The Excel tool uses the constants from Table 3.2 as default. Table 3.1 clearly shows that the parameters can vary widely between different aircraft models, which means that the average statistical values used in the Excel tool make the model slightly less accurate.

Table 3.1: Statistically derived values for A and B for a number of aircraft (**Scholz 2015**)

	A 320-200	**B727-200**	**B737-800**	**C-130H**	**BAe 146**
A	0.000885	0.000766	0.001171	0.001201	0.001765
B	3.734	5.257	3.543	3.126	3.457

Table 3.2: Statistically derived values for A and B for any aircraft type (**Scholz 2015**)

	Result
A	0.001272
B	3.477

3.1.4 Oswald Factor

The Oswald factor or Oswald efficiency number is a value which, together with the aspect ratio, defines the rate of change of the drag coefficient with a varying lift coefficient. It is used to calculate the induced drag.

For an estimation of the Oswald factor e a method from **Scholz 2015** will be used. Because the estimated e is used in the calculation of C_{D0} (see Chapter 3.1.2), the method to estimate e should not rely on the value of C_{D0}. Thus, 'method 1' is used without the input of C_{D0}. The Oswald factor is composed of the following factors:

$$e = e_{theo} \cdot k_{e,F} \cdot k_{e,D0} \cdot k_{e,M} \tag{3.8}$$

The limiting factor here is the correction factor for losses due to the compressibility effects on induced drag: $k_{e,M}$. It is dependent on the flight Mach number and is calculated as follows:

$$k_{e,M} = a_e \cdot \left(\frac{M}{M_{comp}} - 1\right)^{b_e} + c_e \tag{3.9}$$

With: $b_e = 10.82$
$c_e = 1$
$M_{comp} = 0.3$

And:

$$a_e = \frac{-1}{\left(\frac{M + 0.08}{M_{comp}} - 1\right)^{b_e}} \tag{3.10}$$

Equations for the other factors can be found in **Scholz 2015**.

3.2 Thrust Specific Fuel Consumption

The TSFC is defined as the mass of fuel burned per unit of time, divided by the thrust. It is an important performance parameter for a jet engine. A smaller TSFC means a better effeciency of the engine (**Young 2018**).

In theory TSFC is dependent on altitude (overall engine efficiency), thrust and speed. The overall engine efficiency depends partially on the difference between maximum internal air temperature and outside air temperature. Implying that overall engine efficiency increases with rising altitude. However, most commercial jet aircraft cruise in the stratosphere where

the temperature is invariable with altitude (see Chapter 3.4). In the altitude range of cruise flight for these aircraft, the variation in TSFC varies between 1% and 2%. Thus, the dependency on altitude can be neglected according to **Bensel 2018**.

The dependency on thrust can also be considered small enough to neglect. This is proven by **Bensel 2018** by retrofitting data from 4 different turbojet engines to visualize a general trend of very small variation in TSFC with varying amounts of thrust during cruise (see Figure 3.2). With thrust variatons of up to 25 %, the change in TSFC is less than 5 %. This conclusion is shared by **Young 2018**.

As a result of this, TSFC would only be dependent of aircraft speed. An important note to make here is that in the study by Bensel the aircraft are considered to be flying at common cruise altitudes for commercial jet aircraft. For the scope of this thesis this is not always the case. This means that the altitude-dependency will be taken into account in the TSFC model in Chapter 5.

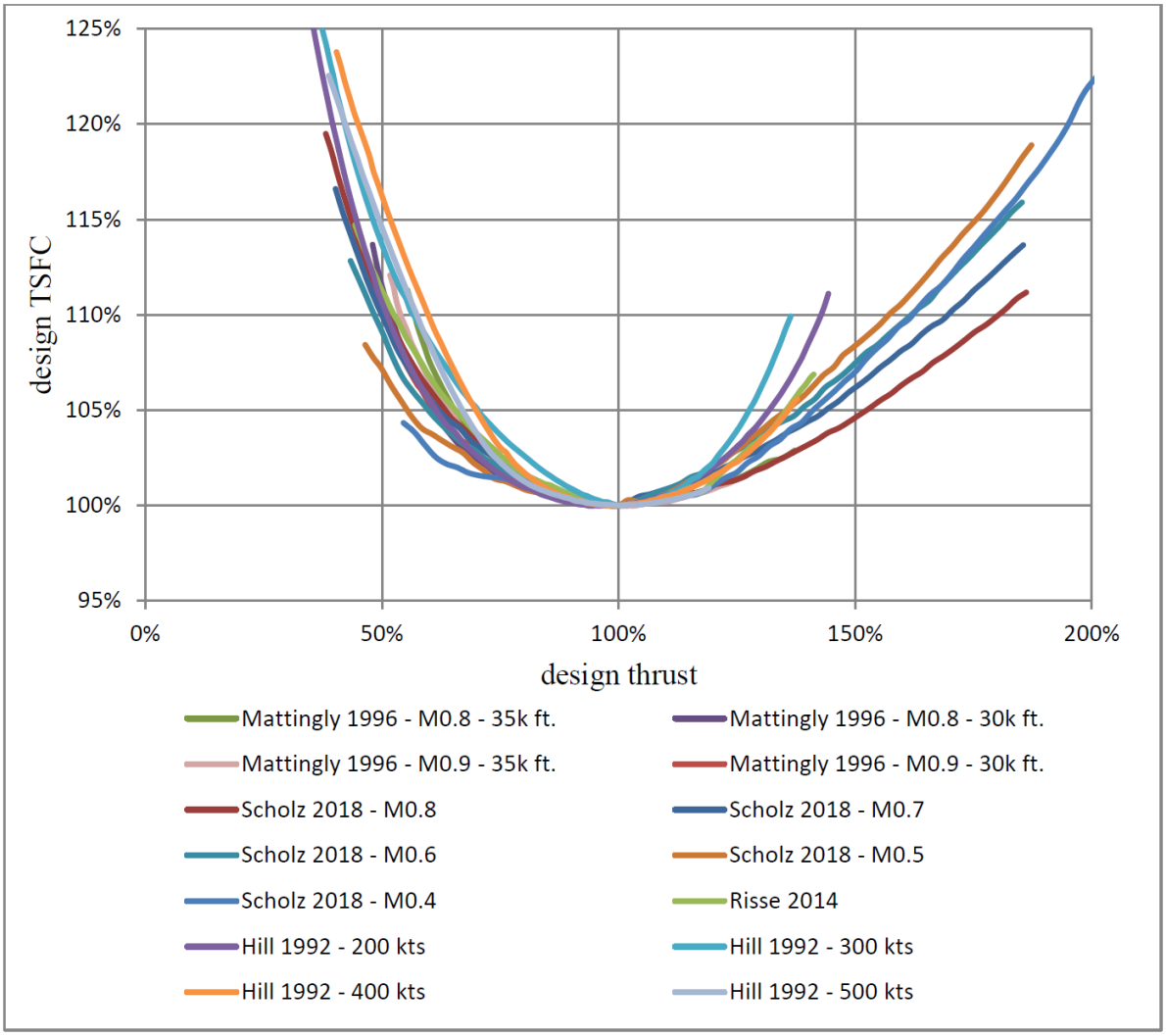

Figure 3.2: Design TSFC in function of design thrust (**Bensel 2018**)

The TSFC variation with speed can be modelled linearly according to the model from **Roux 2002** and **Scholz 2017** or the non-linear model by **Herrmann 2010**. Taking into consideration that most modern turbofan engines have a relatively high bypass ratio, **Bensel 2018** concluded that the non-linear Herrmann model fits closer to the actual TSFC characteristics of a high-BPR turbofan engine. The input variables are also easier to obtain than those for the linear model. The non-linear model does include the impact of altitude on the TSFC as well. Therefore, the Herrmann model will be used for all further TSFC calculations in this thesis.

All equations used in the model by **Herrmann 2010** can be found in Appendix A.

The input variables are:

- Cruise Mach number
- Cruise altitude
- Bypass ratio
- Take-off thrust (one engine)
- Overall pressure ratio (if known)
- Turbine entry temperature

As an output TSFC in kg/Ns is generated.

3.3 Direct Operating Costs

The DOC is calculated with a method from **Scholz 2015** based on the AEA1989 method. Essentially, direct operating costs only contain aircraft-related costs and can be divided into 7 categories and several subcategories. These categories are then added up to form one DOC value, expressed as an annual DOC cost for one aircraft. However, the more accurate way to compare multiple aircraft with different design and flight missions is by using the seat-mile cost:

$$C_{s,m} = \frac{C_{a/c,a}}{n_{seat} \cdot n_{t,a} \cdot R_{DOC}} \tag{3.11}$$

The full list of categories and subcategories:

- Depreciation C_{DEP}
- Interest C_{INT}
- Insurance C_{INS}
- Fuel C_F
- Maintenance C_M:
    - Airframe maintenance $C_{M,AF}$
    - Power plant maintenance $C_{M,PP}$
- Crew C_C:
    - Cockpit crew $C_{C,CO}$
    - Cabin crew $C_{C,CA}$
- Fees and charges C_{FEE}:
    - Landing fees $C_{FEE,LD}$
    - ATC or navigation fees $C_{FEE,NAV}$
    - Ground handling fees $C_{FEE,GND}$

All equations and necessary data can be found in **Scholz 2015** or in the Excel tool as an applied model.

3.4 Atmosphere

From a flight mechanics point of view the atmosphere is often modelled by the standard atmosphere. This is an idealized, steady-state representation of the Earth's atmosphere constructed by different organizations: ISO with ISO 2533:1975, ICAO with the International Standard Atmosphere and the United States government with the US Standard Atmosphere. Up to an altitude of 32 km all three models are identical **(NASA, 1976)**. Within the scope of this thesis, the layers of interest are the two lowest layers of the Earth's atmosphere: the troposphere and stratosphere, which are divided by the tropopause.

Note that the further mentioned altitude of the tropopause of 11 000 m (36 089 ft) is an average value used in the standard atmosphere model. The actual altitude of the boundary between troposphere and stratosphere varies significantly between the Equator and the poles.

The following mathematical approach is summarized from **Young 2001**:

1) Troposphere:

This is the region which spans from sea level up to the tropopause at 11 000 m (36 089 ft). The temperature is assumed to be exactly 288.15 K at sea level and to decrease linearly with 0.0065 K/m for increasing altitude.

Temperature, pressure, and density are generally given as ratios of the ambient condition to the condition at sea level (denoted with subscript 0).

$$\theta = \frac{T}{T_0} \; with: \; T = T_0 - L \cdot H \tag{3.12}$$

$$\delta = \frac{p}{p_0} = \left[1 - \frac{L \cdot H}{T_0}\right]^{\frac{g}{R \cdot L}} \tag{3.13}$$

$$\sigma = \frac{\rho}{\rho_0} = \left[1 - \frac{L \cdot H}{T_0}\right]^{\frac{g}{R \cdot L}-1} \tag{3.14}$$

With: T_0 = 288.15 K
L = 0.0065 K/m
p_0 = 101 325 Pa
ρ_0 = 1.2250 kg/m^3
g = 9.80665 m/s^2
R = 287.053 m^2/s^2/K

2) Stratosphere:

This is the region above the troposphere. The focus here is the part of the stratosphere from the tropopause at 11 000 m up to 20 000 m (65 617 ft). Within this zone it is assumed that the temperature is a constant 216.65 K.

In this case temperature, pressure, and density are given as ratios of the ambient condition to the conditions at tropopause level (denoted with subscript t). This simplifies into two equations:

$$T = T_t = 216.65 \; K \tag{3.15}$$

$$\frac{p}{p_t} = \frac{\rho}{\rho_t} = e^{\frac{-g}{R \cdot T_t} \cdot (H - H_t)} \tag{3.16}$$

With: p_t = 22 657 Pa
ρ_t = 0.36392 kg/m^3
H_t = 11 000 m
g = 9.80665 m/s^2
R = 287.053 m^2/s^2/K

The following figure illustrates the behavior of the three main atmospheric parameters in function of altitude up to 15 000 m:

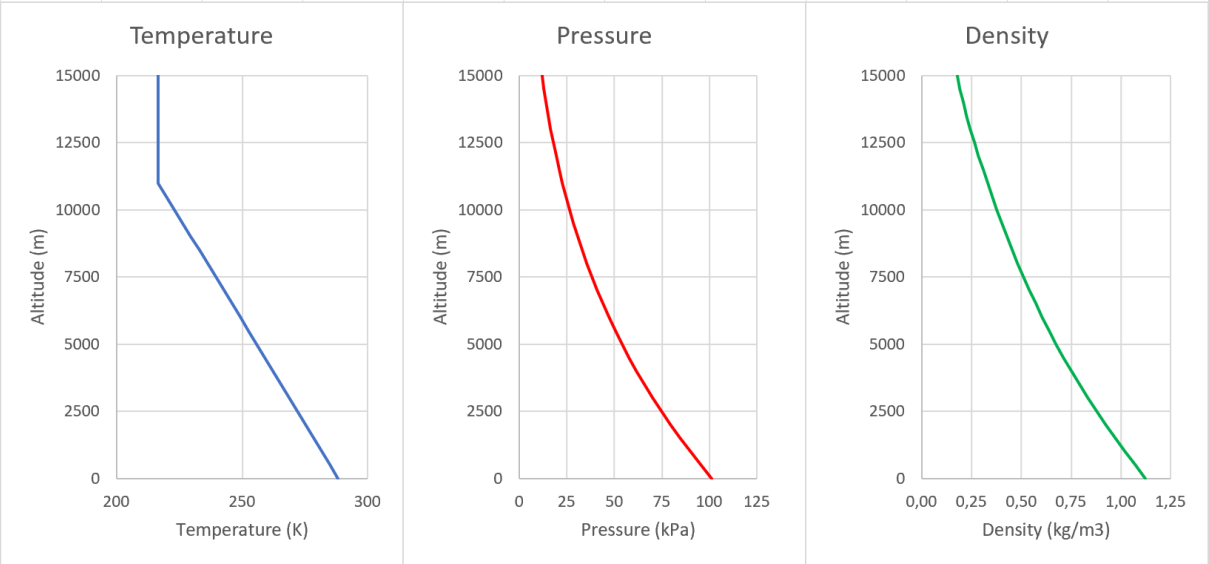

Figure 3.3: Distribution of atmospheric parameters in function of altitude

3.5 Equivalent CO_2 Mass

The equivalent CO_2 mass or $m_{CO2,eq}$ is a metric used to express the environmental impact of engine emissions in a quantitative way. Introduced in **Schwarz 2011**, it combines the effects of the three biggest emission contributors: CO_2, NO_x, and aircraft-induced cloudiness (AIC). AIC includes contrails and aircraft-induced cirrus clouds (see Chapter 2.4.3). The equation is made as generic as possible by dividing equivalent CO_2 mass by the number of seats on the aircraft. This results in units of kg CO_2 per NM flown, per seat:

$$m_{CO2,eq} = \frac{EI_{CO2} \cdot f_{NM}}{n_{seat}} \cdot 1 + \frac{EI_{NOx} \cdot f_{NM}}{n_{seat}} \cdot CF_{midpoint,NOx} + \frac{R_{NM}}{R_{NM} \cdot n_{seat}} \cdot CF_{midpoint,AIC} \quad (3.17)$$

To get a better understanding of this equation, it is displayed with its units only:

$$\frac{kg\ CO2}{NM \cdot n_{seat}} =$$

$$\frac{kg\ CO2/kg\ fuel \cdot kg\ fuel/NM}{n_{seat}} \cdot 1 + \frac{kg\ NOx/kg\ fuel \cdot kg\ fuel/NM}{n_{seat}} \cdot \frac{kg\ CO2}{kg\ NOx} + \frac{NM}{NM \cdot n_{seat}} \cdot \frac{kg\ CO2}{NM} \quad (3.18)$$

The equation is made up of two types of unknown parameters: Emission indices (EI) and characterization factors (CF). The emission index is the mass amount of the specie emitted per mass amount of fuel burned. The emission index of CO_2 is equal to 3.16 kg CO_2 per kg of fuel burned and is independent of the aircraft's altitude (**Schwarz 2011**). The emission index of NO_x is a variable value that does depend on the altitude. It is calculated using the Boeing fuel flow method 2 (**Baughcum 1996**).

The Boeing fuel flow method 2 (BFFM2) is a method for calculating the emission index of NO_x based on fuel flow and emission index data from the ICAO Aircraft Engine Emissions Databank (**ICAO 2019**). The method is adjusted for atmospheric effects at different altitudes and represents a relationship between fuel flow and the emission index of NO_x. Essentially, it starts from the actual fuel flow of the considered aircraft (calculated from its fuel consumption and TAS) and corrects it for the reference condition. Then, EI of NO_x and fuel flow values from the ICAO databank are corrected by a factor defined by Boeing and plotted in a log-log plot for several different flight stages. The next step is to derive an equation for EI NO_x in function of fuel flow by curve fitting the log-log plot. The final step is to correct the EI NO_x value for actual atmospheric conditions. The method is described in more detail in Appendix B and in an applied form for the Excel tool in Chapter 4.7.

The characterization factor (CF) may be considered as a conversion factor from NO_x or AIC emissions to the equivalent CO_2 emission. Both are altitude dependent by introducing a forcing factor s. The result has units of kg of CO_2 per kg of NO_x and kg of CO_2 per NM flown respectively:

$$CF_{midpoint,NOx} =$$

$$\frac{SGTP_{03s,100}}{SGTP_{CO2,100}} \cdot s_{O3s}(H) + \frac{SGTP_{03L,100}}{SGTP_{CO2,100}} \cdot s_{O3L}(H) + \frac{SGTP_{CH4,100}}{SGTP_{CO2,100}} \cdot s_{CH4}(H) \quad (3.19)$$

$$CF_{midpoint,AIC} = \frac{SGTP_{contrails,100}}{SGTP_{CO2,100}} \cdot s_{contrails}(H) + \frac{SGTP_{cirrus,100}}{SGTP_{CO2,100}} \cdot s_{cirrus}(H) \quad (3.20)$$

The SGTP factor stands for sustained global temperature potential. Environmental impact is generally measured in global warming potential (GWP), which uses radiative forcing to express the impact of a system. Radiative forcing however is not the best metric for estimating the impact of a single flight (see Chapter 2.4.2). Instead SGTP is used as an alternative metric.

It expresses an average temperature increase or decrease (over 100 years) in Kelvin per unit of the respective specie. Units are K per relevant unit for each of the emission contributors (per kg CO_2, per kg NO_x or per NM for AIC). SGTP values can be found in the following table:

Table 3.3: SGTP values (**Schwarz 2009**)

Species	$SGTP_{i,100}$
CO_2 (K/kg CO_2)	$3{,}58 \cdot 10^{-14}$
Short O_3 (K/kg NO_x)	$7{,}79 \cdot 10^{-12}$
Long O_3 (K/NO_x)	$-9{,}14 \cdot 10^{-13}$
CH_4 (K/kg NO_x)	$-3{,}90 \cdot 10^{-12}$
Contrails (K/NM)	$2{,}54 \cdot 10^{-13}$
Contrails (K/km)	$1{,}37 \cdot 10^{-13}$
Cirrus (K/NM)	$7{,}63 \cdot 10^{-13}$
Cirrus (K/km)	$4{,}12 \cdot 10^{-13}$

The forcing factor *s* introduces the altitude dependency in Eq. (3.19) and (3.20). The forcing factors for short ozone, long ozone and methane increase with increasing altitude. The AIC forcing factor reveals a clear peak around the common cruise altitude for jet aircraft and turns to almost zero at lower altitudes (see Figure 3.4). Exact values for all forcing factors are extracted in **Van Endert 2017** and can be found in the Excel tool and in Appendix C.

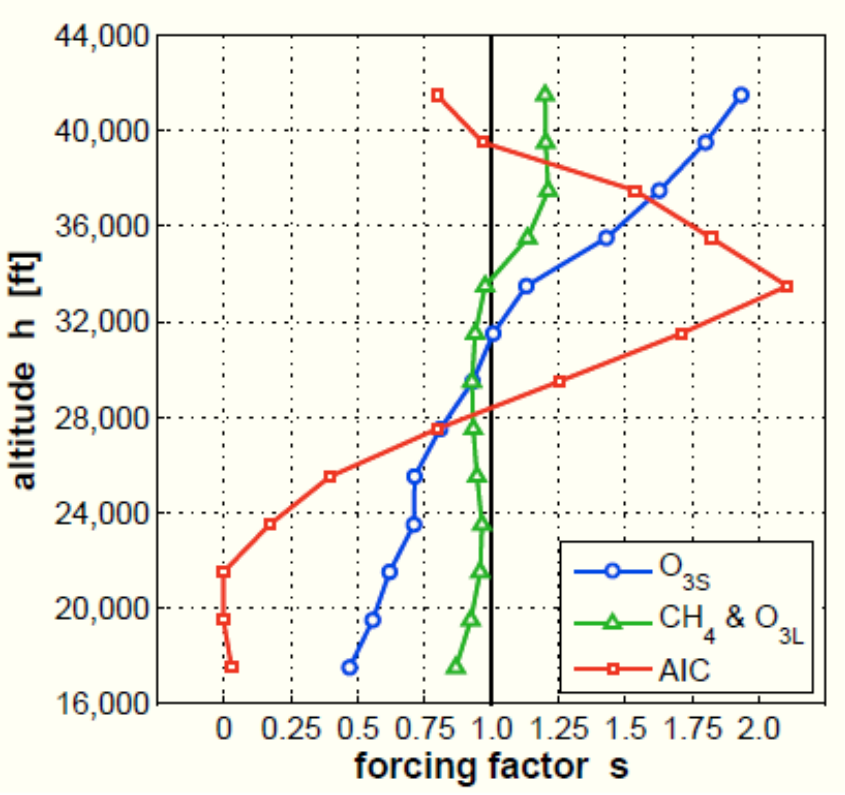

Figure 3.4: Forcing factor s in function of altitude (**Schwarz 2011**)

4 Excel Tool

4.1 General

In the four following chapters calculations will be made to come up with results for the different models. To keep an overview, all this is done in an Excel tool which will be added to this thesis. This chapter delivers a brief overview of the tool. Each subchapter, starting from Chapter 4.4, is dedicated to one sheet of the Excel tool. Most of the calculations in the tool are done by macros in the form of buttons. All these macros can be executed separately, there is no need to calculate them in any order. For ease of use, the following color code is used consistently throughout the Excel tool:

Table 4.1: Color code used in the Excel tool

User input value	Bold black on green background
Calculated input value	Green on white background
Important result	Black on orange background
Result represented in plot	Black on blue background

An important note for the user is that the tool was written in an Excel version that uses a comma as a decimal separator instead of a dot. This means that all results acquired from the tool will be displayed with a comma as decimal separator.

4.2 Case Study: Airbus A320-200

As a representative example the Airbus A320-200 (weight variant 000) will be used in all models. This is a popular aircraft at the time of publication an has been for some time, meaning that a great amount of aircraft data can be found relatively easy. Furthermore, it is a single aisle aircraft. This is the group of aircraft with the biggest global market share by far right now and probably will be in the near future (69 % of all passenger aircraft and growing) according to **Boeing 2018**. All aircraft data used in the models is found in **Airbus 2005a** and **Jackson 2007**.

4.3 Macro for Calculation

All calculations are done with macros programmed in Visual Basic in Excel. This is a quick example of the standard loop code that is used to calculate the matrix style output values. In this way the user can insert additional restrictions or alter the code. The if statement inside the

loop is meant as a safety to prevent output values being displayed for Mach numbers greater than the maximum operating Mach number of the aircraft.

```
Sub Calculate_fuelcons()

For i = 52 To 71


    For j = 3 To 13


        Sheets("Inputs_Outputs").Cells(i, 2).Copy
Sheets("Inputs_Outputs").Cells(3, 10)

        Sheets("Inputs_Outputs").Cells(51, j).Copy
Sheets("Inputs_Outputs").Cells(2, 10)

        If Sheets("Inputs_Outputs").Cells(51, j).Value <
Sheets("Inputs_Outputs").Cells(14, 2).Value Then

        Sheets("Fuel").Cells(39, 9).Copy

        Sheets("Inputs_Outputs").Cells(i, j).PasteSpecial xlPasteValues

        Else

        Sheets("Inputs_Outputs").Cells(i, j).Value = ""

        End If

    Next j

Next i

End Sub
```

4.4 Inputs and Outputs

The inputs are divided into categories: aircraft parameters, engine parameters, flight parameters, and constants.

- Aircraft parameters: these parameters are used for all outputs and should be filled in as thorough as possible.

- Engine parameters: are used for TSFC calculation and for calculating maintenance costs and engine price in the DOC.

- Flight parameters: contain the two main inputs in this model: Mach number and altitude. All other parameters (except range) change with varying Mach number and altitude. The range is needed for DOC calculation.

- Constants: the values are taken from **Young 2001** and can be left as is.

Below the input categories, all outputs are shown. From top to bottom are four different categories and from left to right in general the main parameter followed by the most influential parameters for each category and/or the normalized value of the main parameter. The following lay-out is used:

Table 4.2: Lay-out of the outputs in the Excel tool

Lift coefficient	Drag coefficient	Oswald factor	Wave drag increment
Fuel consumption	TSFC	Aerodynamic efficiency	Fuel consumption *normalized*
Seat-mile cost	Annual DOC per aircraft	Flight time	Seat-mile cost *normalized*
Environmental impact	Equivalent CO_2 mass	EI_NO_x	Equivalent CO_2 mass *normalized*
Combined values			

Note that the input Mach number goes up to 0.9, but the displayed results are limited by the chosen aircraft's maximum operating Mach number. All outputs for a higher Mach number will be left blank.

At the bottom of the sheet, four weighting factors can be found. Both the environmental impact model and the combined model are made up of different values with a weighting factor each. The environmental impact model is composed of resource depletion (fuel consumption) and equivalent CO_2 mass. The combined model is composed of seat-mile cost and environmental impact. All weighting factors are set to 0.5 by default, which means that each component has the same importance. The user can change the influence of each component on the total result by altering the weighting factors.

All outputs that are multiplied with a weighting factor are normalized values. Calculation results are first normalized between 0 and 1, then multiplied with their respective weighting factor and finally added up to get a combined value between 0 and 1:

$$combined\ value =$$

$$(wf\ 1 \cdot normalized\ val.\ 1) + (wf\ 2 \cdot normalized\ val.\ 2) + \cdots \qquad (4.1)$$

4.5 Fuel

The fuel consumption sheet is used to calculate all aerodynamic parameters on the left: Oswald factor, wave drag increment, lift- and drag coefficient, and the aerodynamic efficiency. On the right side TSFC is calculated with the method from **Herrmann 2010**.

In this sheet no user input is necessary. Its main purpose is to elaborate the calculation methods for each parameter of the fuel consumption calculation.

4.6 DOC

This sheet is used to calculate the annual DOC and the seat-mile cost. It also generates a visualization of the weight of each category from the total DOC by using a pie chart. This is located under the total annual DOC value.

At the bottom of the sheet is a table with matching bar graph. Here the user can enter four different flight scenarios (Mach and altitude) and compare the DOC distribution for each scenario.

The following user input is required for this sheet:

1. The current year of calculation must be entered for a correct inflation factor.

2. A selection must be made between a short/medium-range aircraft or a long-range aircraft.

3. The current price for jet A-1 fuel (kerosene) must be entered from **EIA 2019** or another source (must be FOB price).

4.7 Environmental

In this sheet the environmental impact of the aircraft is calculated. This is the combination of equivalent CO_2 mass per Nm flown per seat and resource depletion (as fuel consumption). At the bottom of the sheet the user has the option to compare four flight scenarios (Mach number and altitude) and the corresponding impact of each emission component.

There is some user input required in this sheet to calculate the emission index for NOx. This is done by using the Boeing fuel flow method 2 (BFFM2) (**Baughcum 1996**). Based on the fuel flow and EI_NO_x values from the ICAO Aircraft Engines Emission Database (**ICAO**

2019). The full method is introduced in Chapter 3.5 and fully explained in Appendix B. In the Excel tool the following steps must be taken by the user:

1. The unadapted fuel flow and EI_NO_x values for T/O, C/O, App and Idle must be obtained from **ICAO 2019** for the appropriate engine and filled in in the following table (green columns only):

Table 4.3: ICAO engine data (**ICAO 2019**)

Flight stage	Wf_unadapted	r	Wf_adapte	EI_NOx
T/O	**1,166**	1,01	1,17766	**28,7**
C/O	**0,961**	1,013	0,973493	**23,3**
App	**0,326**	1,02	0,33252	**10**
Idle	**0,107**	1,1	0,1177	**4,3**

2. The graph accompanying the table shows the correlation between adapted fuel flow and the corresponding EI_NO_x values, including a trendline for this correlation (see Figure 4.1). The trendline function should be filled in in cell C45 (also changing the x variable in the function to cell C43) to get an uncorrected EI_NO_x value for the cruise stage. With some further calculations following the Boeing fuel flow method 2, the final corrected EI_NO_x value is presented in cell C51.

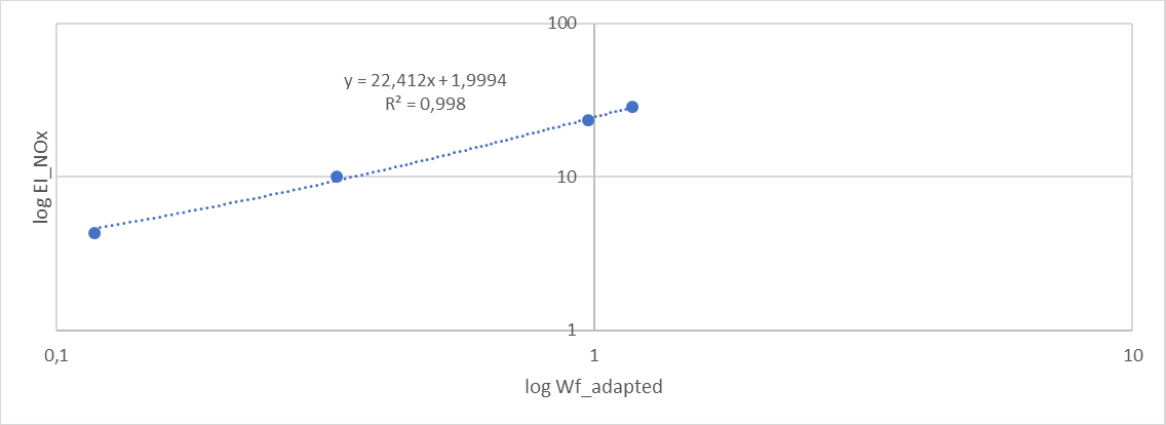

Figure 4.1: Correlation between adapted fuel flow and EI_NO_x

4.8 Flight Time

The flight time sheet is used to generate an approximating model for a generic passenger jet aircraft. No user input is required. BADA data (**Eurocontrol 1998**) is presented for four aircraft: Airbus A320-200, Airbus A340, Boeing 737-200, and Boeing 747-400. This data is presented in graphs and is used to calculate an averaged model. The averaged model is then compared to the results generated by using Eq. 6.1 (a simple flight time calculation). All corresponding graphs can be found in Appendix D as well.

4.9 Extra Information

This sheet includes a linear interpolation model for the forcing factor data (see Appendix C), the Airbus A320-200 payload-range diagram with a simple fuel consumption calculation (see Chapter 5.1), and the Airbus A320-200 drag polar based on data from the fuel consumption sheet. No user input is required in this sheet.

5 Flight Parameter Optimization: Minimum Fuel Consumption

In the following four chapters all optimization results are generated for an Airbus A320-200 (weight variant 000) as a representative example but the models are made for any passenger jet aircraft.

5.1 General

In this chapter a simple model will be designed and utilized to calculate an aircraft's fuel consumption. It is mostly based on aerodynamic parameters and TSFC, in function of the aircraft's cruise Mach number and altitude.

As mentioned in Chapter 2.1, minimum fuel consumption during cruise is related with maximum specific air range r_a. The equation for the SAR (Eq. (2.6)) can be altered so it contains the Mach number:

$$r_a = \frac{V \cdot E}{c \cdot m \cdot g} = \frac{M \cdot a \cdot E}{c \cdot m \cdot g} \tag{5.1}$$

The SAR is expressed in units of km/kg fuel, which means the inverse $f = 1/r_a$ can be defined as the fuel consumption in units of kg fuel per km (or NM) flown. Nautical mile will be used throughout the model instead of kilometer. The mass of fuel is used instead of the volume because the density of fuel changes with altitude. Fuel consumption can be calculated with the following equation:

$$f = \frac{c \cdot m \cdot g}{M \cdot a \cdot E} \tag{5.2}$$

With g as a constant, m depending on the aircraft and mission, and all other parameters depending on flight parameters. However, to make the model as generic as possible f will be divided by m (which is the MTOW in this case). This results in the following equation in units of kg fuel per NM flown, per kg of MTOW:

$$f_{MTOW} = \frac{c \cdot g}{M \cdot a \cdot E} \tag{5.3}$$

An alternative way to Eq. (5.2) to calculate fuel consumption is by calculating the specific air range with the aircraft's payload-range diagram. This should be used as an estimation rather than a real calculation. Or it could be used to check the order of magnitude of a calculated fuel

consumption result. The drawback of this option is that the required values for range and payload mass are read from a diagram, which comes with a certain level of inaccuracy.

The method is based on calculating specific air range by using maximum range and range for maximum payload with their respective payloads. The specific air range is defined as:

$$r_a = \frac{R_2 - R_1}{m_1 - m_2} \tag{5.4}$$

With R and m values depicted on the following example of a payload-range diagram:

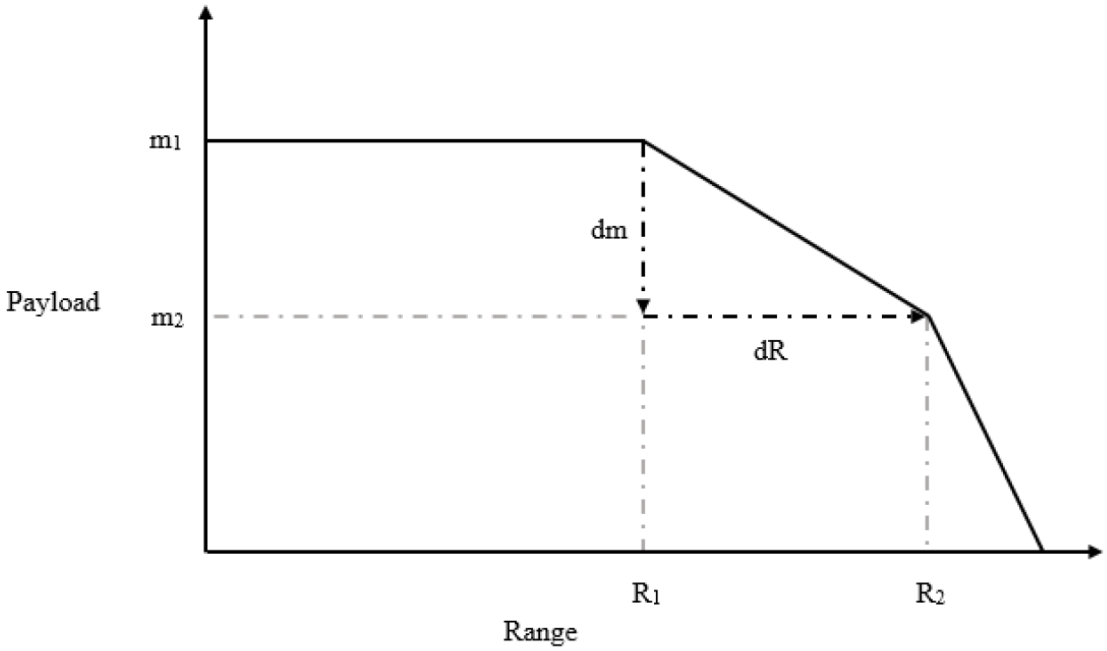

Figure 5.1: Illustrative example of a payload-range diagram (**Van Endert 2017**)

With: R_1 = range at maximum payload
R_2 = maximum range
m_1 = maximum payload
m_2 = payload at maximum range

An aircraft's payload-range diagram is usually found in the publicly available "documents for airport planning". As an example, the Airbus A320 document for airport planning (**Airbus 2005a**) can be used for the Airbus A320-200 payload-range diagram.

Continuing with Eq. (5.2) to calculate fuel consumption: M and C_L were expected to be the inputs in this model according to the task sheet. These two parameters are mutually dependent, with the altitude H as the link between them. The lift coefficient C_L is defined as:

$$C_L = \frac{2 \cdot m \cdot g}{\rho \cdot M^2 \cdot a^2 \cdot S} \tag{5.5}$$

This equation implicates that the relationship between M and C_L depends on ρ, a and S. The first two parameters are in turn dependent on the altitude H. The dependency of the density ρ is given in Chapter 3.4 and for a in Chapter 5.2.1. Using the following set of equations:

$$a = \sqrt{\gamma \cdot R \cdot T} \tag{5.6}$$

$$T = T_0 - L \cdot H \tag{3.12}$$

$$\rho = \rho_0 \cdot \left[1 - \frac{L \cdot H}{T_0}\right]^{\frac{g}{R \cdot L} - 1} \tag{3.14}$$

Eq. (5.5) can be solved for the altitude H:

$$H = -\frac{T_0}{L} \cdot \left(\left(\frac{2 \cdot m \cdot g}{\rho_0 \cdot T_0 \cdot M^2 \cdot \gamma \cdot R \cdot S \cdot C_L}\right)^{R \cdot L / g} - 1\right) \tag{5.7}$$

The problem with this model is that the mutual dependency of M and C_L is also influenced by the wing surface area S. And because S is different for every aircraft, the model would become less generally applicable. For this reason, the choice has been made to deviate from the original task description and use the Mach number M and the altitude H as inputs in all models.

5.2 Important Parameters

The most important parameters for calculating fuel consumption according to Eq. (5.3) are displayed in the following diagram. Inputs are green, important intermediate parameters blue and the final result in grey.

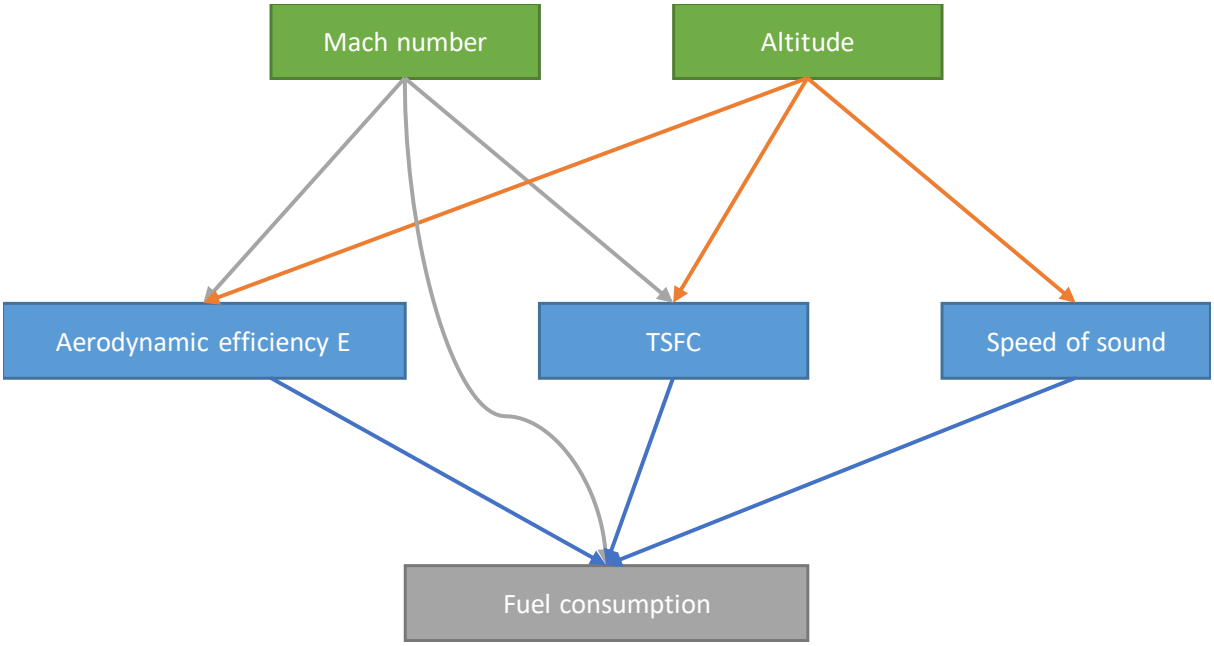

Figure 5.2: Flowchart of fuel consumption calculation

5.2.1 Speed of Sound

The speed of sound a is dependent on the ambient temperature and can be calculated as follows:

$$a = \sqrt{\gamma \cdot R \cdot T} \tag{5.8}$$

With: $\gamma = 1.4$
$R = 287.053\ \mathrm{m^2/s^2K}$
T = ambient temperature in K

Due to the change of temperature with varying height (see Chapter 3.4), the speed of sound is dependent on cruise altitude.

5.2.2 Aerodynamic Efficiency

The aerodynamic efficiency E is the ratio between lift and drag, and can be written in several different ways:

$$E = \frac{L}{D} = \frac{2 \cdot \rho \cdot S \cdot V^2 \cdot C_L}{2 \cdot \rho \cdot S \cdot V^2 \cdot C_D} = \frac{C_L}{C_D} \tag{5.9}$$

By introducing Eq. (3.1), E can be written as:

$$E = \frac{C_L}{C_{D0} + \Delta C_{Dw} + K \cdot C_L^2} \tag{5.10}$$

With:

$$K = \frac{1}{\pi \cdot A \cdot e} \tag{3.2}$$

A model must be used to calculate C_{D0}, ΔC_{Dw}, and e. This is accomplished by using different methods from **Scholz 2015** (see Chapter 3.1). The lift coefficient C_L is defined as:

$$C_L = \frac{2 \cdot m \cdot g}{\rho \cdot M^2 \cdot a^2 \cdot S} \tag{5.5}$$

This equation and Eq. (3.2) imply that the aerodynamic efficiency E is partially dependent on geometric aircraft design parameters including the aspect ratio A and the surface area S.

5.2.3 Mach Number

The Mach number M is considered as an input in this model. It can be derived from true airspeed and local speed of sound if need be:

$$M = \frac{V}{a} \tag{5.11}$$

5.2.4 Specific Fuel Consumption

The calculation of the specific fuel consumption c is accomplished with the non-linear method provided in **Herrmann 2010**. This method is introduced and further elaborated in Chapter 3.2. All necessary equations can be found in Appendix A.

5.3 Results Fuel Consumption

The results are presented as generic as possible. By calculating fuel consumption as kg of fuel per NM flown and per kg of aircraft MTOW, aircraft of different sizes and for different flight missions can be compared. Even an aircraft to be designed can be used without knowledge of its MTOW. On the other hand, the most common units used in relevant literature are kg of

fuel per 100 km flown per seat (comparable to the units used in the automotive industry). This representation will be included as well.

5.3.1 TSFC

Thrust specific fuel consumption is represented as kg of fuel used per Newton of thrust per second. And this in function of Mach number and altitude. The lower the value is, the better.

		Mach number								
		0,4	**0,45**	**0,5**	**0,55**	**0,6**	**0,65**	**0,7**	**0,75**	**0,8**
Altitude (m)	**3000**	1,08E-05	1,15E-05	1,22E-05	1,3E-05	1,39E-05	1,49E-05	1,6E-05	1,73E-05	1,87E-05
	3500	1,08E-05	1,15E-05	1,22E-05	1,3E-05	1,39E-05	1,48E-05	1,59E-05	1,71E-05	1,85E-05
	4000	1,08E-05	1,15E-05	1,22E-05	1,3E-05	1,38E-05	1,47E-05	1,58E-05	1,7E-05	1,83E-05
	4500	1,08E-05	1,15E-05	1,22E-05	1,29E-05	1,37E-05	1,47E-05	1,57E-05	1,68E-05	1,81E-05
	5000	1,08E-05	1,15E-05	1,21E-05	1,29E-05	1,37E-05	1,46E-05	1,56E-05	1,67E-05	1,79E-05
	5500	1,08E-05	1,15E-05	1,21E-05	1,28E-05	1,36E-05	1,45E-05	1,55E-05	1,65E-05	1,78E-05
	6000	1,08E-05	1,14E-05	1,21E-05	1,28E-05	1,36E-05	1,44E-05	1,54E-05	1,64E-05	1,76E-05
	6500	1,08E-05	1,14E-05	1,21E-05	1,28E-05	1,35E-05	1,44E-05	1,53E-05	1,63E-05	1,74E-05
	7000	1,08E-05	1,14E-05	1,21E-05	1,28E-05	1,35E-05	1,43E-05	1,52E-05	1,62E-05	1,73E-05
	7500	1,08E-05	1,14E-05	1,21E-05	1,27E-05	1,35E-05	1,42E-05	1,51E-05	1,61E-05	1,71E-05
	8000	1,08E-05	1,14E-05	1,20E-05	1,27E-05	1,34E-05	1,42E-05	1,50E-05	1,60E-05	1,70E-05
	8500	1,08E-05	1,14E-05	1,20E-05	1,27E-05	1,34E-05	1,41E-05	1,50E-05	1,59E-05	1,69E-05
	9000	1,08E-05	1,14E-05	1,20E-05	1,26E-05	1,33E-05	1,41E-05	1,49E-05	1,58E-05	1,67E-05
	9500	1,09E-05	1,14E-05	1,20E-05	1,26E-05	1,33E-05	1,40E-05	1,48E-05	1,57E-05	1,66E-05
	10000	1,09E-05	1,14E-05	1,20E-05	1,26E-05	1,33E-05	1,40E-05	1,48E-05	1,56E-05	1,65E-05
	10500	1,09E-05	1,14E-05	1,20E-05	1,26E-05	1,32E-05	1,39E-05	1,47E-05	1,55E-05	1,64E-05
	11000	1,09E-05	1,14E-05	1,20E-05	1,26E-05	1,32E-05	1,39E-05	1,46E-05	1,54E-05	1,63E-05
	11500	1,09E-05	1,14E-05	1,20E-05	1,26E-05	1,32E-05	1,39E-05	1,46E-05	1,54E-05	1,63E-05
	12000	1,09E-05	1,14E-05	1,20E-05	1,26E-05	1,32E-05	1,39E-05	1,46E-05	1,54E-05	1,63E-05
	12500	1,09E-05	1,14E-05	1,20E-05	1,26E-05	1,32E-05	1,39E-05	1,46E-05	1,54E-05	1,63E-05

Figure 5.3: Results TSFC in kg of fuel per N of thrust per second

TSFC increases with increasing Mach number and decreasing altitude (except for the case of Mach 0.4, which stays almost constant). TSFC depends on the overall engine efficiency η_0 which is a combination of five engine component efficiencies according to the model by **Herrmann 2010** (see Appendix A): inlet, fan, compressor, turbine, and nozzle. Four of these (all except inlet efficiency) are directly influenced by the cruise Mach number in a negative way. The gas generator efficiency equation and the final equation for calculating the TSFC are also directly influenced by the Mach number. Altitude influences the TSFC model by means of the ambient temperature. Ambient temperature has an influence on the gas generator function and on the final TSFC equation.

Apart from ambient temperature, altitude influences the TSFC in another more profound way which is possibly not as visible by representing results in the style of Figure 5.3. The speed of sound varies with altitude and by using Mach number instead of TAS as columns, the TAS does not remain constant throughout one column. An increase in altitude means a decrease in

TAS for a certain Mach number. This explains the trend of lower TSFC at higher altitude: the TSFC is lower because the TAS is lower for an equal Mach number.

The relationship between TSFC and TAS is displayed in Figure 5.4. Starting from the bottom left corner, the three different shapes which are on almost the same horizontal level represent the TSFC at one Mach number. Moving to a higher speed, the TSFC increases with decreasing altitude for an equal Mach number. At a TAS of 0 knot, the TSFC is not equal to zero (engine on idle). The lower the TAS goes to 0, the closer together all TSFC values are, independent of altitude. This effect is visible in the results on Figure 5.3 as well.

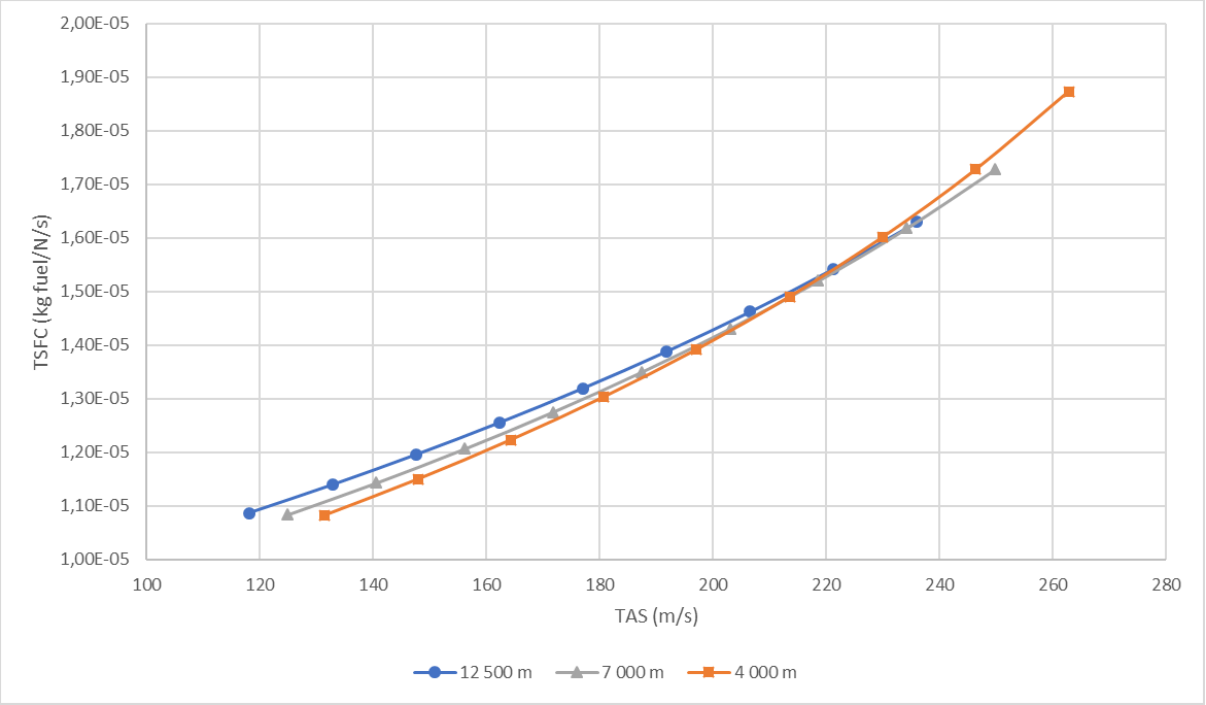

Figure 5.4: TSFC in function of true airspeed for three different altitudes

The calculated output for the Airbus A320 with CFM56-5B4 engines at regular flight conditions (Mach 0.78 at an altitude of 11 500 m) is $1.59 \cdot 10^{-5}$ kg/Ns, which corresponds with the value range found in **Jenkinson 1999** for the CFM56 engine family: $1.54 \cdot 10^{-5} - 1.89 \cdot 10^{-5}$ kg/Ns. This validates the accuracy of the TSFC model to a certain extent.

5.3.2 Aerodynamic Efficiency

The aerodynamic efficiency E is a dimensionless parameter. The higher it is, the better.

		Mach number								
		0,4	**0,45**	**0,5**	**0,55**	**0,6**	**0,65**	**0,7**	**0,75**	**0,8**
Altitude (m)	**3000**	18,59	19,47	19,46	18,89	17,96	16,71	15,38	13,90	11,88
	3500	18,19	19,32	19,55	19,16	18,39	17,23	15,95	14,49	12,45
	4000	17,73	19,08	19,55	19,37	18,75	17,71	16,50	15,07	13,02
	4500	17,22	18,77	19,47	19,51	19,06	18,14	17,02	15,64	13,59
	5000	16,65	18,39	19,31	19,56	19,29	18,52	17,50	16,18	14,16
	5500	16,05	17,94	19,06	19,52	19,44	18,84	17,93	16,70	14,71
	6000	15,41	17,42	18,73	19,39	19,51	19,08	18,31	17,18	15,25
	6500	14,75	16,85	18,32	19,18	19,49	19,24	18,62	17,60	15,76
	7000	14,07	16,24	17,84	18,87	19,37	19,30	18,85	17,96	16,22
	7500	13,38	15,58	17,30	18,48	19,16	19,28	18,99	18,25	16,64
	8000	12,68	14,90	16,69	18,01	18,85	19,15	19,03	18,46	17,00
	8500	11,98	14,19	16,04	17,47	18,45	18,92	18,98	18,58	17,29
	9000	11,29	13,47	15,35	16,86	17,97	18,60	18,83	18,60	17,49
	9500	10,61	12,74	14,63	16,20	17,41	18,18	18,57	18,51	17,60
	10000	9,95	12,01	13,89	15,50	16,79	17,68	18,22	18,32	17,61
	10500	9,30	11,29	13,13	14,76	16,10	17,10	17,77	18,03	17,52
	11000	9,38	11,37	13,22	14,85	16,19	17,17	17,82	18,07	17,54
	11500	8,75	10,66	12,46	14,08	15,46	16,53	17,29	17,68	17,35
	12000	8,15	9,96	11,71	13,31	14,70	15,83	16,69	17,21	17,07
	12500	7,58	9,30	10,98	12,54	13,94	15,10	16,03	16,65	16,69

Figure 5.5: Results aerodynamic efficiency

The aerodynamic efficiency E has an optimum zone that follows a rising Mach number - rising altitude pattern. E is defined as $E = C_L/C_D$ and this ratio clarifies the pattern. Looking at the following two figures for lift coefficient and drag coefficient, the optimum zone for E is associated with moderate values for both coefficients (yellow zone). This is because a high lift coefficient has a high drag coefficient as a result and vice versa, which alters the ratio between the two.

		Mach number								
		0,4	**0,45**	**0,5**	**0,55**	**0,6**	**0,65**	**0,7**	**0,75**	**0,8**
Altitude (m)	**3000**	0,818	0,647	0,524	0,433	0,364	0,310	0,267	0,233	0,205
	3500	0,873	0,689	0,558	0,461	0,388	0,330	0,285	0,248	0,218
	4000	0,931	0,736	0,596	0,492	0,414	0,353	0,304	0,265	0,233
	4500	0,994	0,785	0,636	0,526	0,442	0,376	0,325	0,283	0,248
	5000	1,062	0,839	0,680	0,562	0,472	0,402	0,347	0,302	0,266
	5500	1,136	0,898	0,727	0,601	0,505	0,430	0,371	0,323	0,284
	6000	1,216	0,961	0,778	0,643	0,541	0,461	0,397	0,346	0,304
	6500	1,303	1,030	0,834	0,689	0,579	0,493	0,425	0,371	0,326
	7000	1,397	1,104	0,894	0,739	0,621	0,529	0,456	0,397	0,349
	7500	1,500	1,185	0,960	0,793	0,667	0,568	0,490	0,427	0,375
	8000	1,612	1,274	1,032	0,853	0,716	0,610	0,526	0,458	0,403
	8500	1,734	1,370	1,109	0,917	0,770	0,657	0,566	0,493	0,433
	9000	1,866	1,475	1,195	0,987	0,830	0,707	0,609	0,531	0,467
	9500	2,012	1,589	1,287	1,064	0,894	0,762	0,657	0,572	0,503
	10000	2,170	1,715	1,389	1,148	0,965	0,822	0,709	0,617	0,543
	10500	2,344	1,852	1,500	1,240	1,042	0,888	0,766	0,667	0,586
	11000	2,323	1,836	1,487	1,229	1,033	0,880	0,759	0,661	0,581
	11500	2,514	1,986	1,609	1,330	1,117	0,952	0,821	0,715	0,628
	12000	2,720	2,149	1,741	1,439	1,209	1,030	0,888	0,774	0,680
	12500	2,943	2,325	1,884	1,557	1,308	1,115	0,961	0,837	0,736

Figure 5.6: Results lift coefficient

The lift coefficient is influenced by density and true airspeed V (which is made up of Mach number and the speed of sound):

$$C_L = \frac{2 \cdot m \cdot g}{\rho \cdot M^2 \cdot a^2 \cdot S} \tag{5.5}$$

This implies an increase in lift coefficient with an increase in altitude (because of the decreasing pressure). The second effect is that of true airspeed. A higher TAS results in a lower lift coefficient. A maximum TAS can be found at the highest Mach number and lowest altitude because of the increase of speed of sound with decreasing altitude. And in the same way a minimum TAS at the lowest Mach number and highest altitude. This effect can also be seen in Figure 5.6. An important thing to note is that there is no pursuit for maximum lift coefficient during cruise flight, as this results in a high drag coefficient. The optimal lift coefficient values can be found in the yellow or orange zone on Figure 5.6.

		Mach number								
		0,4	**0,45**	**0,5**	**0,55**	**0,6**	**0,65**	**0,7**	**0,75**	**0,8**
Altitude (m)	**3000**	0,044	0,033	0,027	0,023	0,020	0,019	0,017	0,017	0,017
	3500	0,048	0,036	0,029	0,024	0,021	0,019	0,018	0,017	0,018
	4000	0,053	0,039	0,030	0,025	0,022	0,020	0,018	0,018	0,018
	4500	0,058	0,042	0,033	0,027	0,023	0,021	0,019	0,018	0,018
	5000	0,064	0,046	0,035	0,029	0,024	0,022	0,020	0,019	0,019
	5500	0,071	0,050	0,038	0,031	0,026	0,023	0,021	0,019	0,019
	6000	0,079	0,055	0,042	0,033	0,028	0,024	0,022	0,020	0,020
	6500	0,088	0,061	0,046	0,036	0,030	0,026	0,023	0,021	0,021
	7000	0,099	0,068	0,050	0,039	0,032	0,027	0,024	0,022	0,022
	7500	0,112	0,076	0,056	0,043	0,035	0,029	0,026	0,023	0,023
	8000	0,127	0,085	0,062	0,047	0,038	0,032	0,028	0,025	0,024
	8500	0,145	0,097	0,069	0,052	0,042	0,035	0,030	0,027	0,025
	9000	0,165	0,110	0,078	0,059	0,046	0,038	0,032	0,029	0,027
	9500	0,190	0,125	0,088	0,066	0,051	0,042	0,035	0,031	0,029
	10000	0,218	0,143	0,100	0,074	0,057	0,046	0,039	0,034	0,031
	10500	0,252	0,164	0,114	0,084	0,065	0,052	0,043	0,037	0,033
	11000	0,248	0,161	0,112	0,083	0,064	0,051	0,043	0,037	0,033
	11500	0,287	0,186	0,129	0,094	0,072	0,058	0,047	0,040	0,036
	12000	0,334	0,216	0,149	0,108	0,082	0,065	0,053	0,045	0,040
	12500	0,388	0,250	0,172	0,124	0,094	0,074	0,060	0,050	0,044

Figure 5.7: Results drag coefficient

The drag coefficient consists of three contributors: zero lift drag coefficient, wave drag increment, and induced drag coefficient. The induced drag coefficient is highly influenced by the lift coefficient as stated before. It is also the most important contributor, as can be seen on Figure 5.8. This figure shows the importance of each contributor that makes up the drag coefficient of an Airbus A320-200 at regular flight conditions (Mach 0.78 at 11 500 m altitude).

The wave drag increment has a small influence on the total drag coefficient. It's near zero at the lower Mach numbers and ramps up quickly when reaching the optimum cruise Mach number for this type of aircraft. But even when at maximum value, it makes up less than 10 % of the total drag coefficient. The only effect that is visible is that the drag coefficient stays at a constant value around the optimum cruise Mach number, instead of decreasing due to a decreasing lift coefficient.

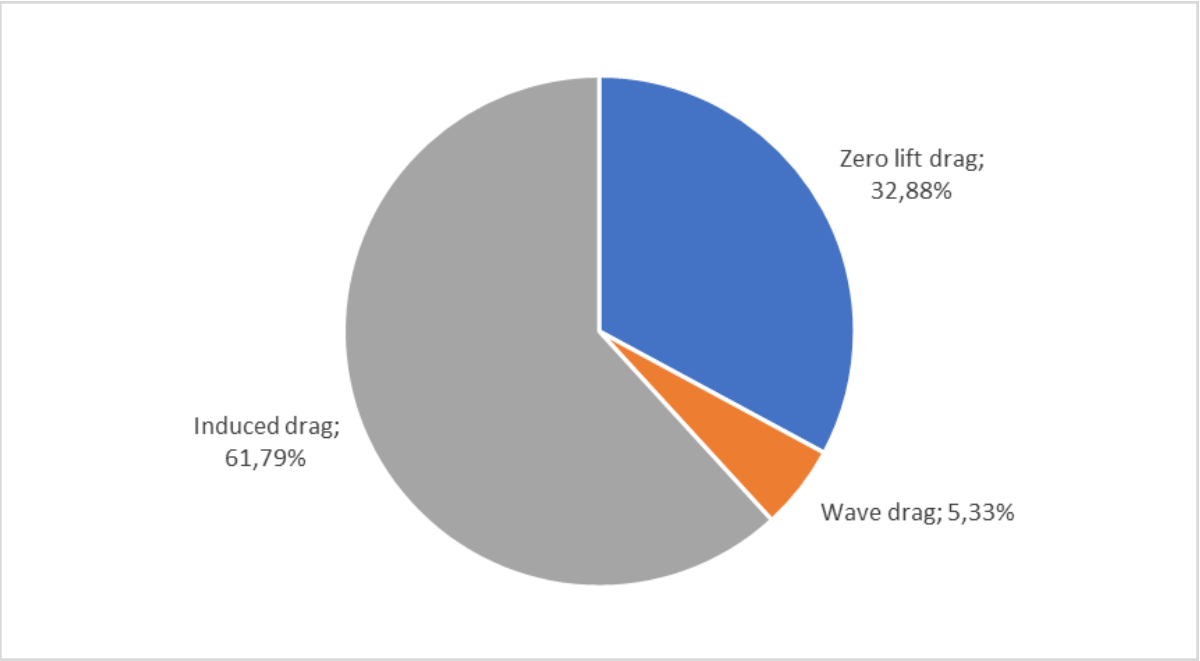

Figure 5.8: Drag component contribution on the Airbus A320-200

Due to the choice of method 1 for calculating the zero lift drag coefficient in the Excel tool (see Chapter 3.1.2), its calculation is mostly influenced by the Oswald factor. This means a decrease in C_{D0} when the Mach number increases, which corresponds with the theory: looking at the following equation (derived in Chapter 2), drag can be divided into two components which are influenced by speed in opposite ways:

$$D = A_D \cdot V^2 + B_D \cdot \frac{1}{V^2} \tag{2.3}$$

These components are called parasitic drag and induced drag respectively. Parasitic drag depends on the zero lift drag coefficient and induced drag on the lift coefficient. Their behavior in function of speed is shown graphically in Figure 5.9:

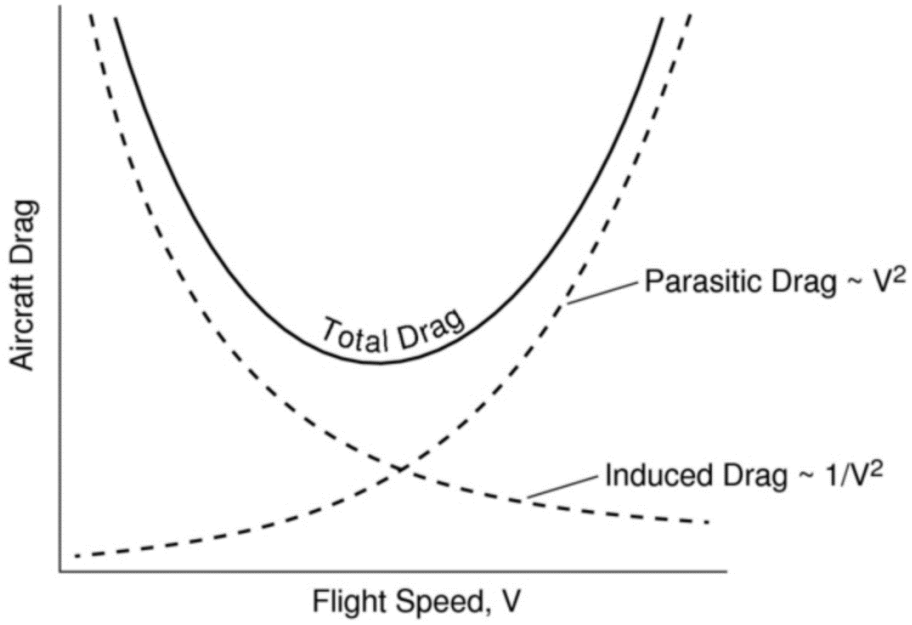

Figure 5.9: Aircraft drag in function of flight speed (**Spakovszky 2006**)

5.3.3 Fuel Consumption

The following table and accompanying contour plot show the fuel consumption as kg of fuel per NM flown, per kg of aircraft MTOW. And this in function of Mach number and altitude.

		Mach number								
		0,4	**0,45**	**0,5**	**0,55**	**0,6**	**0,65**	**0,7**	**0,75**	**0,8**
Altitude (m)	**3000**	8,05E-05	7,26E-05	6,95E-05	6,94E-05	7,14E-05	7,59E-05	8,23E-05	9,16E-05	1,09E-04
	3500	8,28E-05	7,35E-05	6,95E-05	6,86E-05	6,99E-05	7,36E-05	7,92E-05	8,76E-05	1,03E-04
	4000	8,54E-05	7,48E-05	6,98E-05	6,80E-05	6,86E-05	7,16E-05	7,65E-05	8,40E-05	9,84E-05
	4500	8,85E-05	7,64E-05	7,03E-05	6,78E-05	6,77E-05	7,00E-05	7,41E-05	8,07E-05	9,38E-05
	5000	9,21E-05	7,85E-05	7,13E-05	6,79E-05	6,70E-05	6,86E-05	7,20E-05	7,79E-05	8,97E-05
	5500	9,62E-05	8,09E-05	7,25E-05	6,82E-05	6,67E-05	6,76E-05	7,03E-05	7,53E-05	8,60E-05
	6000	1,01E-04	8,38E-05	7,42E-05	6,90E-05	6,66E-05	6,68E-05	6,89E-05	7,32E-05	8,28E-05
	6500	1,06E-04	8,71E-05	7,62E-05	7,00E-05	6,69E-05	6,64E-05	6,78E-05	7,13E-05	7,99E-05
	7000	1,12E-04	9,10E-05	7,87E-05	7,15E-05	6,76E-05	6,63E-05	6,70E-05	6,99E-05	7,74E-05
	7500	1,19E-04	9,54E-05	8,16E-05	7,33E-05	6,86E-05	6,66E-05	6,66E-05	6,88E-05	7,54E-05
	8000	1,26E-04	1,00E-04	8,50E-05	7,56E-05	6,99E-05	6,72E-05	6,66E-05	6,80E-05	7,37E-05
	8500	1,34E-04	1,06E-04	8,90E-05	7,83E-05	7,17E-05	6,82E-05	6,69E-05	6,76E-05	7,24E-05
	9000	1,44E-04	1,13E-04	9,35E-05	8,15E-05	7,40E-05	6,96E-05	6,75E-05	6,76E-05	7,16E-05
	9500	1,54E-04	1,20E-04	9,87E-05	8,53E-05	7,67E-05	7,15E-05	6,86E-05	6,80E-05	7,11E-05
	10000	1,65E-04	1,28E-04	1,05E-04	8,97E-05	7,99E-05	7,38E-05	7,02E-05	6,88E-05	7,11E-05
	10500	1,78E-04	1,37E-04	1,11E-04	9,47E-05	8,36E-05	7,66E-05	7,22E-05	7,01E-05	7,15E-05
	11000	1,78E-04	1,37E-04	1,11E-04	9,47E-05	8,36E-05	7,65E-05	7,21E-05	7,01E-05	7,15E-05
	11500	1,91E-04	1,46E-04	1,18E-04	9,98E-05	8,76E-05	7,95E-05	7,44E-05	7,16E-05	7,23E-05
	12000	2,05E-04	1,56E-04	1,26E-04	1,06E-04	9,21E-05	8,30E-05	7,71E-05	7,36E-05	7,35E-05
	12500	2,21E-04	1,68E-04	1,34E-04	1,12E-04	9,71E-05	8,70E-05	8,02E-05	7,60E-05	7,52E-05

Figure 5.10: Results fuel consumption in kg fuel per NM flown, per kg of aircraft MTOW

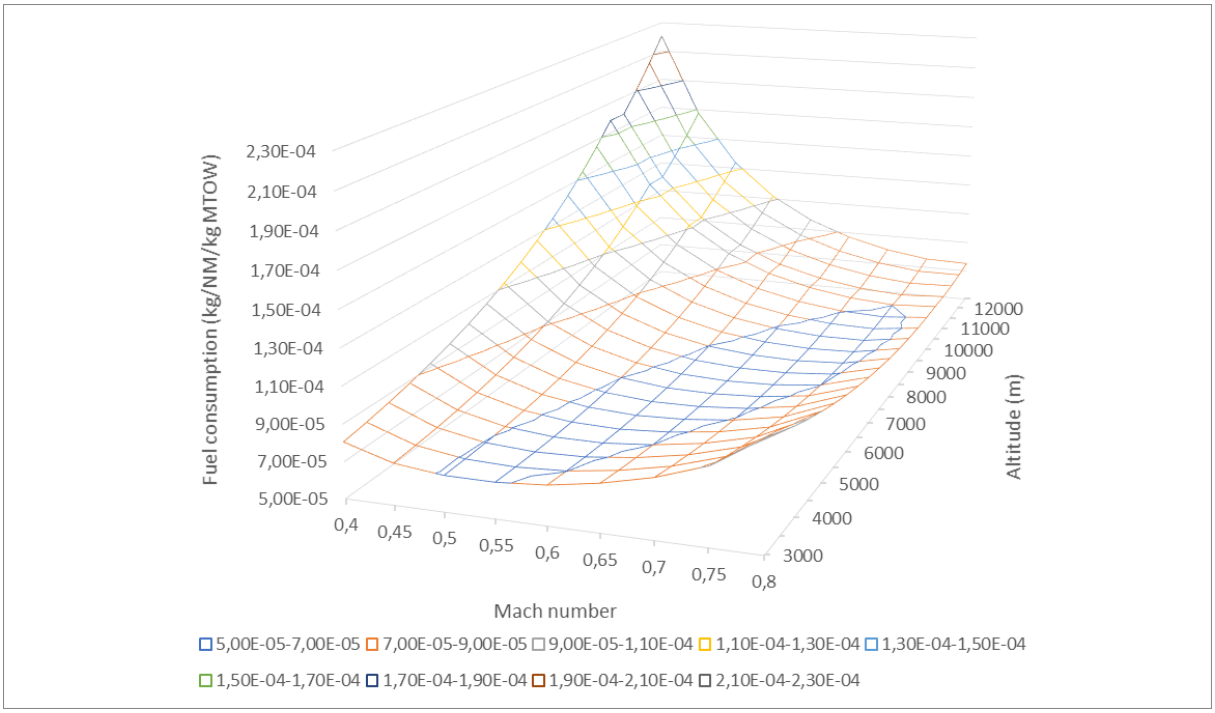

Figure 5.11: Contour plot of the fuel consumption results

The color pattern of the aerodynamic efficiency results from Chapter 5.3.2 can clearly be recognized in the fuel consumption results. The pattern is shifted towards higher Mach number because of the Mach number's presence in the denominator of the fuel consumption equation (Eq. (5.3)). There is also a shift towards higher altitudes, caused by the decreasing TSFC (found in the nominator) with increasing altitude.

$$f_{MTOW} = \frac{c \cdot g}{M \cdot a \cdot E} \tag{5.3}$$

Fuel consumption can also be represented in units of kg of fuel per 100 km flown, per seat.

		Mach number								
		0,4	**0,45**	**0,5**	**0,55**	**0,6**	**0,65**	**0,7**	**0,75**	**0,8**
Altitude (m)	**3000**	2,13	1,92	1,84	1,84	1,89	2,01	2,18	2,42	2,88
	3500	2,19	1,94	1,84	1,81	1,85	1,95	2,10	2,32	2,74
	4000	2,26	1,98	1,85	1,80	1,82	1,90	2,02	2,22	2,60
	4500	2,34	2,02	1,86	1,79	1,79	1,85	1,96	2,14	2,48
	5000	2,44	2,08	1,89	1,80	1,77	1,82	1,91	2,06	2,37
	5500	2,55	2,14	1,92	1,81	1,76	1,79	1,86	1,99	2,28
	6000	2,67	2,22	1,96	1,82	1,76	1,77	1,82	1,94	2,19
	6500	2,81	2,30	2,02	1,85	1,77	1,76	1,79	1,89	2,11
	7000	2,96	2,41	2,08	1,89	1,79	1,76	1,77	1,85	2,05
	7500	3,14	2,52	2,16	1,94	1,81	1,76	1,76	1,82	1,99
	8000	3,33	2,66	2,25	2,00	1,85	1,78	1,76	1,80	1,95
	8500	3,55	2,81	2,35	2,07	1,90	1,80	1,77	1,79	1,92
	9000	3,80	2,98	2,47	2,16	1,96	1,84	1,79	1,79	1,89
	9500	4,07	3,17	2,61	2,26	2,03	1,89	1,82	1,80	1,88
	10000	4,38	3,39	2,77	2,37	2,11	1,95	1,86	1,82	1,88
	10500	4,72	3,63	2,95	2,50	2,21	2,03	1,91	1,85	1,89
	11000	4,72	3,63	2,94	2,50	2,21	2,03	1,91	1,85	1,89
	11500	5,06	3,87	3,13	2,64	2,32	2,10	1,97	1,89	1,91
	12000	5,43	4,14	3,33	2,79	2,44	2,20	2,04	1,95	1,94
	12500	5,84	4,43	3,55	2,96	2,57	2,30	2,12	2,01	1,99

Figure 5.12: Results fuel consumption in kg fuel per 100 km flown, per seat

As a comparison to these results, an average car can be said to consume about 6 l of gasoline per 100 km driven on the highway. With an average density of gasoline of about 0.755 kg/l, this equals 4.53 kg of gasoline. This means that one person driving in a car would consume more fuel than one person traveling on this aircraft at optimal flight conditions or even regular fight conditions (Mach 0.78 at 11 500 m). Keep in mind that this is greatly simplified: the LTO cycle is not accounted, an aircraft is used for longer ranges than a car in general, transport to and from the airport is not accounted, etc.

5.4 Conclusion Fuel Consumption

In this chapter fuel consumption is calculated by use of aerodynamic parameters and the aircraft's TSFC. With the aerodynamic parameters based on flight parameters and (a minimum of) geometric parameters of the aircraft. The TSFC is based on flight parameters and basic engine parameters. All results are for an Airbus A320-200, but the methods used are meant for any passenger jet aircraft.

All models used for calculating aerodynamic parameters have one or more factors based on statistical data. This introduces a certain level of inaccuracy in the values of individual results (e.g. one result for a certain Mach number of altitude). However, the scope of this work is not to generate exact data for fuel consumption, but to visualize the trend of fuel consumption

variation when altering flight parameters. This goal is still accomplished because the same models and statistical factors are used for each individual result, ensuring that the fuel consumption variation stays credible. In addition to this, TSFC results seem to be within bounds of actual engine data (see Chapter 5.3.1) and the fuel consumption results are within the expected order of magnitude for a single aisle aircraft.

The fuel consumption results in Chapter 5.3.3 show a big influence of the aerodynamic efficiency E. They follow the colored shape of the optimal ratio of lift coefficient to drag coefficient. Aerodynamic efficiency can be optimized by increasing the lift coefficient while reducing the drag coefficient. The TSFC, Mach number, and local speed of sound have a smaller influence on fuel consumption.

The optimal flight parameters for minimal fuel consumption of an Airbus A320-200, calculated with the methods present, are Mach 0.65 at an altitude of 7000 m. However, the whole dark green zone in Figure 5.10 only differs from this minimum with up to 2.45 %. When looking at the regular flight parameters of Mach 0.78 at 11 500 m, the fuel consumption differs 7.01 % from the minimum.

The importance of considering fuel consumption in function of Mach number and altitude is that both flight parameters can be changed without changing anything to the aircraft's design. At least for small variations in cruise speed or altitude. When flying at greatly reduced altitudes in comparison to common jet cruise altitudes, the wing loading of the aircraft could be changed to further reduce fuel consumption. This scenario is discussed in Chapter 8.3.

6 Flight Parameter Optimization: DOC

6.1 General

The direct operating costs represent the economic impact of operating an aircraft. In this chapter DOC will be represented as an annual cost and as the seat-mile cost. DOC is composed of seven categories and several subcategories as explained in Chapter 3.3. The aim is to visualize the economic impact of flying at varying flight parameters. To have a generic model and maintain the option to compare different aircraft, the seat-mile cost will be used as the primary metric.

6.2 Important Parameters

The most influential parameters in DOC calculation are represented in Figure 6.1. Inputs are green, important intermediate parameters in blue and the final results in grey. DOC is divided into time-independent and time-dependent costs (see Chapter 3.3). The time-independent costs in blue on the left are only influenced by the type of aircraft, and airframe- and engine prices. The type of aircraft determines the depreciation period and interest rate. The time-dependent costs are influenced by flight time, fuel price, crew and maintenance costs, and different fees and charges. Only flight time and fuel price are actually varying. Crew and maintenance costs and fees are fixed 1989 values which are adjusted for inflation.

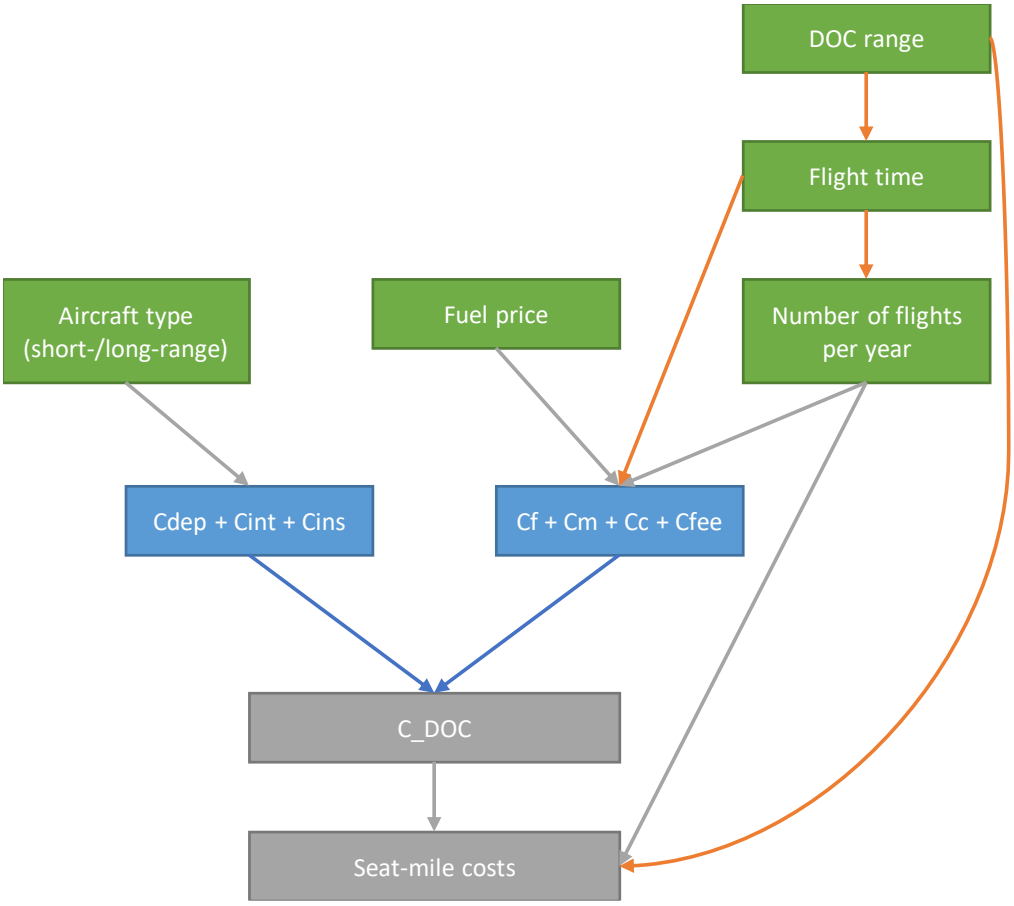

Figure 6.1: Flowchart of DOC calculation

6.2.1 DOC Range

The DOC range R_{DOC} is considered as a typical range for the type of aircraft considered. It is defined as 50 % of the range for maximum payload in **Scholz 2015**. The range for maximum payload can be found on the aircraft's payload-range diagram, which is publicly available in the aircraft's "Documents for airport planning" (see **Airbus 2005a** for the A320 document). Range has a big influence on DOC in two main ways: it influences flight time and it influences fuel consumption. Its influence on flight time is discussed in Chapter 6.2.2. The influence on fuel consumption can be visualized with the so-called bath tub curve (Figure 6.2).

This curve displays the relationship between fuel consumption and range. At short range, fuel consumption is relatively high due to the necessary amount of reserve fuel and alternate fuel that must be on board independent of range. With increasing range, fuel consumption decreases up to an optimum range and starts increasing again slightly after this point. From the optimum point on, the aircraft must take on more fuel in order to transport the fuel required for the longer range. At a certain point fuel consumption increases in a steep way due to payload restrictions. At this point the aircraft must reduce payload (passengers or cargo) in order to stay under the maximum take-off weight (**Burzlaff 2017**).

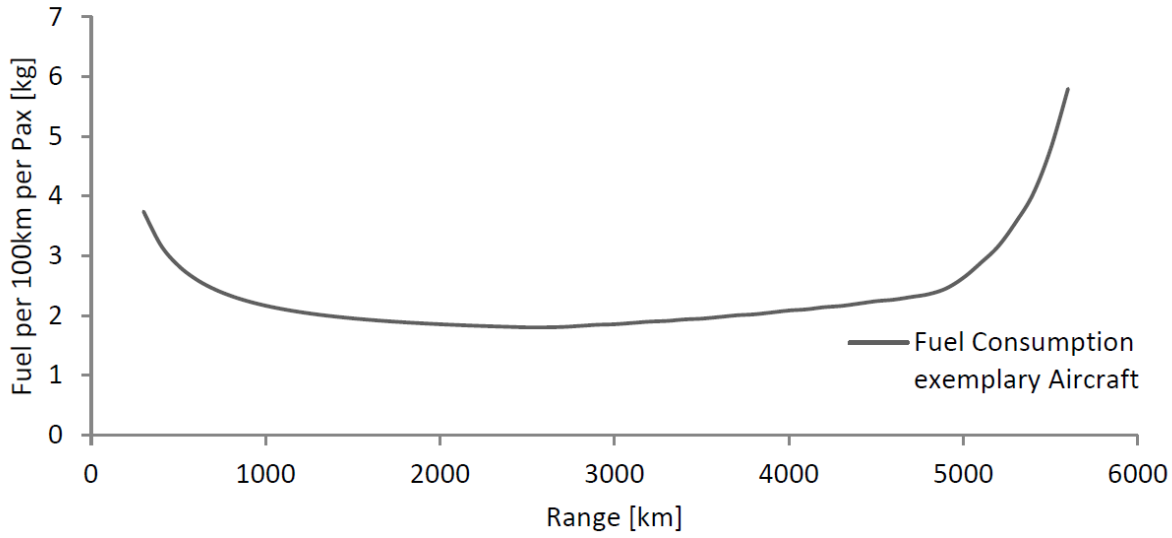

Figure 6.2: Bath tub curve of an exemplary aircraft (**Burzlaff 2017**)

6.2.2 Flight Time

Flight time t_f is the most important parameter when considering seat-mile cost. The flight time in hours could be considered as only dependent on true airspeed and DOC range and could be calculated as follows:

$$t_f = \frac{R_{DOC}}{V} \tag{6.1}$$

However, this equation is a simplification. It calculates the flight time as if the whole range would be flown at cruise speed. A more correct approach is to include the speed differences during the climb and descend flight stages (take-off and landing only take up a very small amount of time compared to the total flight time and will be neglected). Especially for short ranges climb and descent time takes up a considerable share of the total flight time. The added flight time can be calculated from the climb rate and descend rate at certain altitude zones with the corresponding speeds. These rates and speeds are aircraft-dependent and regulated by the authorities.

Two ways to calculate flight time are discussed here. The first one is to look for aircraft specific data in the aircraft performance database by **Eurocontrol 2019** or their (less up-to-date) BADA tables (**Eurocontrol 1998**) and calculate the flight time per colored segment. See Figure 6.3 for the Airbus A320-200 performance data.

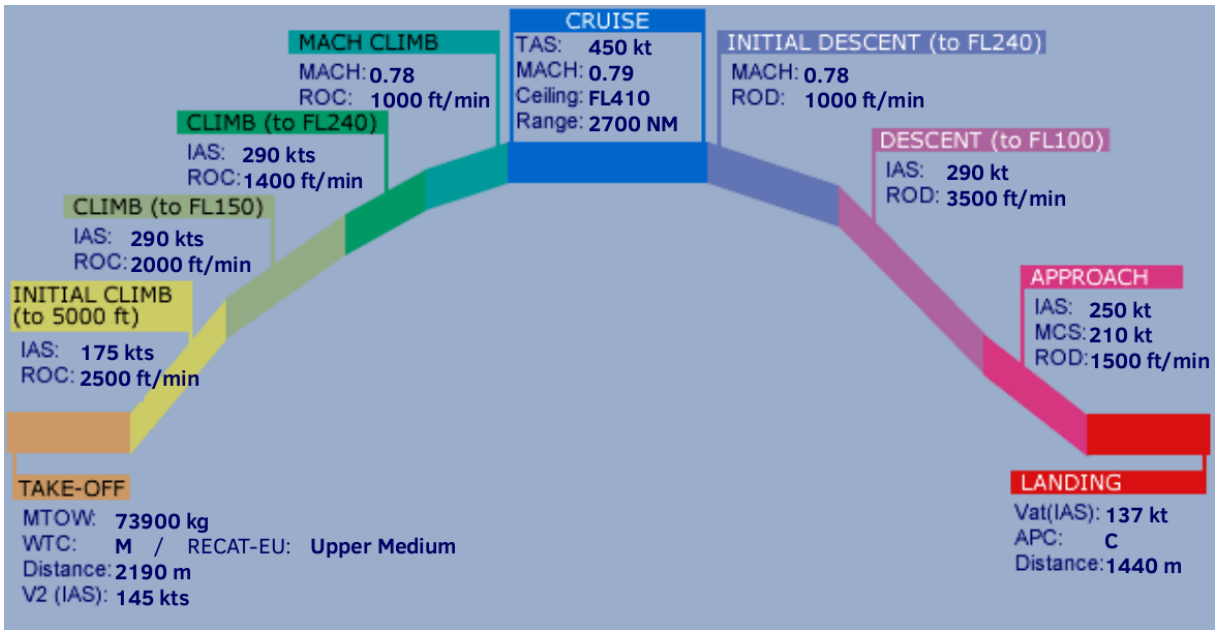

Figure 6.3: Aircraft performance for the Airbus A320-200 (**Eurocontrol 2019**)

The second option is to use a more generic approach and work with common practice and aviation regulations as a guideline to form an averaged model for approximating flight time of any given passenger jet aircraft. Assumptions regarding aircraft performance data are based on a comparison of BADA tables of four popular aircraft (**Eurocontrol 1998**): Airbus A320-200, Airbus A340, Boeing 737-200, and Boeing 747-400. Corresponding graphs can be found in Appendix D.

The following assumptions are made when estimating flight time (full calculation can be found in the 'Flight time' sheet in the Excel tool):

- LTO cycle is neglected
- Maximum IAS of 250 knots below FL100 by regulation
- Average ROC and ROD of 2 000 ft/min
- TAS varies linearly between 150 knots and 290 knots under FL100
- Between FL120 and FL300: variation between 360 knots and cruise speed
- Above FL300: constant cruise speed

The difference in DOC results by using this model instead of Eq. (6.1) is given in Figure 6.4. All calculations are done for the Airbus A320-200 at an altitude of 11 000 m. A difference of up to 7.9 % can be seen in the actual flight time at higher Mach numbers. This is because of the increased relative duration of the climbing and descending stages at shorter flight times. The annual DOC varies less than 3.5 % between the two methods, this could be considered acceptable. The seat-mile cost, which is used in the final combined model (see Chapter 8), varies up to about 4.1 %. This could be considered within boundaries given the not so accu-

rate nature of the DOC model. But in an effort to increase the correctness of the DOC or seat-mile cost model, the flight time estimation model will be used instead of Eq. (6.1).

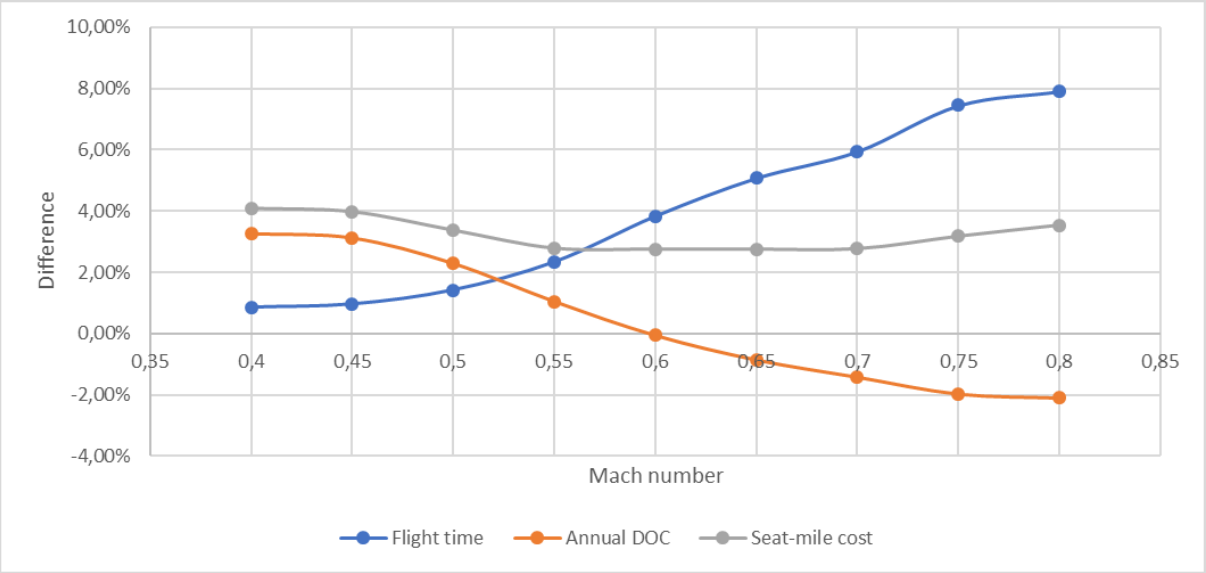

Figure 6.4: Difference in percentage between flight time estimation model and simple equation

6.2.3 Number of Flights per Year

The number of flights per year is an important parameter in calculating the annual DOC cost. It is used in the calculation of fuel cost, maintenance cost, staff cost, and fees and charges. Essentially every cost that is first calculated per flight and later changed to an annual cost. It is also a necessary factor to reform the annual DOC cost into seat-mile cost. The number of flights per year is based on annual aircraft utilization and flight time. And in turn the annual aircraft utilization $U_{a,f}$ is also based on flight time:

$$U_{a,f} = t_f \cdot \frac{k_{U1}}{t_f + k_{U2}} \tag{6.2}$$

The number of flights per year $n_{t,a}$ can then be defined as:

$$n_{t,a} = \frac{U_{a,f}}{t_f} = \frac{k_{U1}}{t_f + k_{U2}} \tag{6.3}$$

With k_{U1} and k_{U2} based on the type of aircraft:

Table 6.1: Factors for aircraft utilization equation (**Scholz 2015**)

Aircraft type	kU1 (in h)	kU2 (in h)
Short-/medium-range	3750	0,75
Long-range	4800	0,42

Annual aircraft utilization and number of flights per year can be reshaped into daily values by dividing both by 365. Daily aircraft utilization and number of flights per day can be used to compare aircraft or airlines and, in this case, to verify the correctness of the user's results when calculating annual aircraft utilization in the Excel tool. Data for American Airlines from **Swelbar 2018** indicates the following averages:

Table 6.2: Average daily aircraft utilization (**Swelbar 2018**)

Aircraft type	Daily aircraft utilization (h)	Number of flights per day
Short-/medium-range	8,2	4,5
Long-range	11,5	1,5

6.2.4 Seat-Mile Cost

The seat-mile cost is the direct operating cost for one seat in the aircraft over a distance of one NM. This metric is often used in an economic context to compare different aircraft models, independent of their fuselage size or design range. It is calculated as follows:

$$C_{s,m} = \frac{C_{a/c,a}}{n_{seat} \cdot n_{t,a} \cdot R_{DOC}} \tag{3.11}$$

6.2.5 Dollar Prices and Inflation

Every currency value in the DOC model is represented in U.S. Dollar (USD). All estimated USD values in the AEA1989 model are based on 1989 values. This means a correction is needed to achieve present date USD values. A compensation for inflation must be used. The inflation factor is defined as:

$$k_{INF} = (1 + p_{INF})^{n_{year} - n_{method}} \tag{6.4}$$

The annual mean inflation rate p_{INF} for the period 1989 – 2017 in the United States is 2.5547 % (**Worldbank 2019**). Multiplying all USD values in the model with an inflation factor is a basic rough compensation. In reality prices change due to a multitude of effects. Unions can demand higher crew wages; airport fees can change, or aircraft manufacturers can alter their prices. This means that the compensation for inflation only gives an approximate val-

ue. Fuel prices for example can hardly be approximated by an inflation factor, due to oil crises or political events strongly influencing the oil price. For this reason, the current fuel price must be added by the user. In conclusion, this correction for inflation means that all USD values in the DOC model are only an approximation.

6.3 Results DOC

DOC results can be represented as annual DOC or as seat-mile cost. Annual DOC returns a clear number of the cost paid by the airline for operating the aircraft, but this value differs a lot between aircraft of different sizes. Seat-mile cost is therefore the preferred output to keep the model as generic as possible. By dividing annual DOC by number of flights per year, DOC range and the number of seats for the seat-mile cost, different types of aircraft can be compared independent of their size.

6.3.1 Flight Time

The flight time is shown in hours.

		Mach number								
		0,4	**0,45**	**0,5**	**0,55**	**0,6**	**0,65**	**0,7**	**0,75**	**0,8**
Altitude (m)	**3000**	3,17	2,82	2,55	2,33	2,15	2,00	1,87	1,75	1,65
	3500	3,22	2,87	2,60	2,38	2,20	2,04	1,91	1,80	1,70
	4000	3,24	2,89	2,62	2,40	2,22	2,06	1,93	1,82	1,72
	4500	3,26	2,90	2,63	2,41	2,23	2,08	1,95	1,83	1,73
	5000	3,28	2,92	2,65	2,43	2,25	2,09	1,96	1,85	1,75
	5500	3,30	2,94	2,66	2,45	2,26	2,11	1,98	1,86	1,76
	6000	3,33	2,96	2,68	2,46	2,28	2,12	1,99	1,88	1,77
	6500	3,35	2,98	2,70	2,48	2,29	2,14	2,00	1,89	1,79
	7000	3,37	3,00	2,71	2,49	2,30	2,15	2,01	1,90	1,79
	7500	3,39	3,02	2,73	2,50	2,32	2,16	2,02	1,90	1,80
	8000	3,42	3,04	2,75	2,52	2,33	2,17	2,03	1,91	1,81
	8500	3,44	3,06	2,76	2,53	2,34	2,18	2,04	1,92	1,81
	9000	3,46	3,08	2,78	2,55	2,35	2,19	2,05	1,92	1,82
	9500	3,49	3,10	2,80	2,58	2,39	2,23	2,10	1,98	1,88
	10000	3,51	3,13	2,82	2,59	2,41	2,25	2,11	1,99	1,89
	10500	3,54	3,15	2,84	2,61	2,42	2,26	2,13	2,01	1,90
	11000	3,56	3,17	2,86	2,63	2,44	2,28	2,14	2,02	1,91
	11500	3,56	3,17	2,86	2,63	2,44	2,28	2,14	2,02	1,92
	12000	3,56	3,17	2,86	2,63	2,44	2,28	2,14	2,02	1,91
	12500	3,56	3,17	2,86	2,63	2,44	2,28	2,14	2,02	1,92

Figure 6.5: Results flight time in hours

The flight time is a result of TAS and cruise altitude. The dependency on cruise altitude (or flight level) can be seen in Figure 6.6. This means that different altitude zones will result in bigger or smaller variations in flight time, as can be seen for example when varying cruise al-

titude from 3000 m to 3500 m (a shift from around FL100 to FL115). This results in a substantial difference in flight time compared to other altitude zones. A lower cruise altitude also implicates less time spent during climb and descent.

The TAS itself depends on Mach number and altitude. A higher Mach number logically reflects a higher TAS. And the altitude influences the local speed of sound, which in turn influences the TAS. A higher altitude means a lower TAS for the same Mach number.

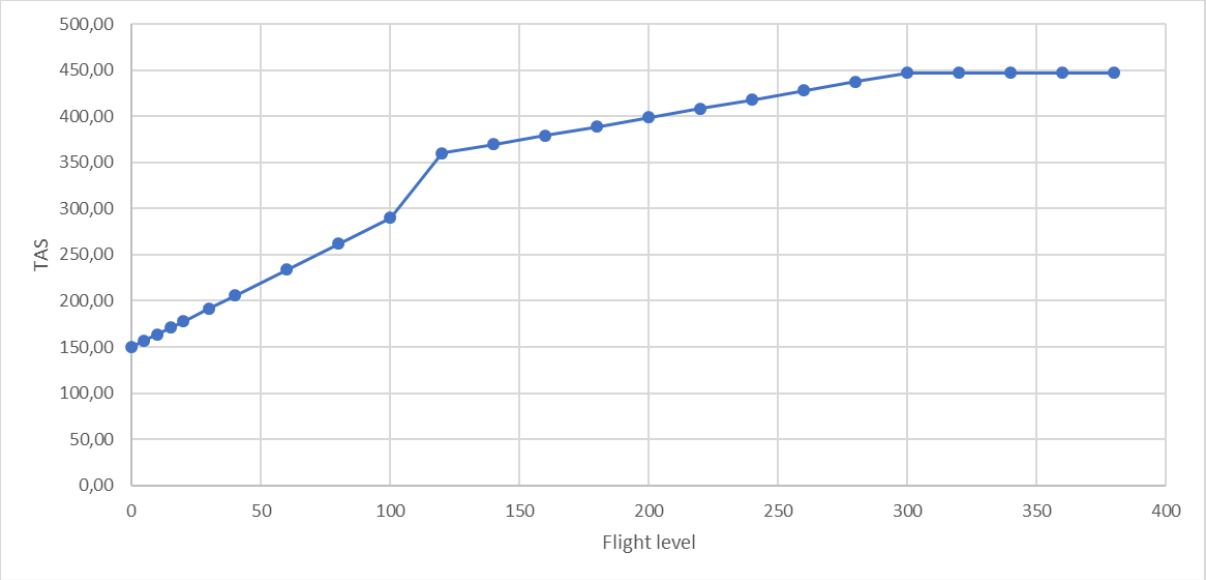

Figure 6.6: Airbus A320-200 TAS during climb and descent (approximation)

6.3.2 Annual DOC

The annual DOC is represented as a yearly cost in USD for the operation of one aircraft.

		Mach number								
		0,4	0,45	0,5	0,55	0,6	0,65	0,7	0,75	0,8
Altitude (m)	3000	3,10E+07	3,17E+07	3,24E+07	3,31E+07	3,39E+07	3,47E+07	3,55E+07	3,64E+07	3,75E+07
	3500	3,09E+07	3,16E+07	3,22E+07	3,29E+07	3,36E+07	3,44E+07	3,52E+07	3,60E+07	3,71E+07
	4000	3,09E+07	3,15E+07	3,22E+07	3,29E+07	3,35E+07	3,43E+07	3,50E+07	3,58E+07	3,68E+07
	4500	3,09E+07	3,15E+07	3,22E+07	3,28E+07	3,35E+07	3,41E+07	3,48E+07	3,56E+07	3,66E+07
	5000	3,09E+07	3,15E+07	3,21E+07	3,27E+07	3,34E+07	3,40E+07	3,47E+07	3,54E+07	3,63E+07
	5500	3,09E+07	3,15E+07	3,21E+07	3,27E+07	3,33E+07	3,39E+07	3,46E+07	3,53E+07	3,62E+07
	6000	3,10E+07	3,15E+07	3,21E+07	3,27E+07	3,33E+07	3,39E+07	3,45E+07	3,52E+07	3,60E+07
	6500	3,10E+07	3,15E+07	3,21E+07	3,26E+07	3,32E+07	3,38E+07	3,44E+07	3,51E+07	3,58E+07
	7000	3,11E+07	3,16E+07	3,21E+07	3,26E+07	3,32E+07	3,38E+07	3,43E+07	3,50E+07	3,57E+07
	7500	3,12E+07	3,16E+07	3,21E+07	3,26E+07	3,32E+07	3,37E+07	3,43E+07	3,49E+07	3,56E+07
	8000	3,12E+07	3,17E+07	3,21E+07	3,26E+07	3,31E+07	3,37E+07	3,43E+07	3,48E+07	3,55E+07
	8500	3,12E+07	3,17E+07	3,22E+07	3,26E+07	3,31E+07	3,37E+07	3,42E+07	3,48E+07	3,55E+07
	9000	3,12E+07	3,18E+07	3,22E+07	3,27E+07	3,32E+07	3,37E+07	3,42E+07	3,48E+07	3,54E+07
	9500	3,11E+07	3,19E+07	3,23E+07	3,27E+07	3,31E+07	3,35E+07	3,40E+07	3,45E+07	3,51E+07
	10000	3,11E+07	3,19E+07	3,24E+07	3,27E+07	3,31E+07	3,35E+07	3,40E+07	3,45E+07	3,50E+07
	10500	3,11E+07	3,19E+07	3,24E+07	3,28E+07	3,32E+07	3,36E+07	3,40E+07	3,44E+07	3,50E+07
	11000	3,10E+07	3,18E+07	3,24E+07	3,27E+07	3,31E+07	3,35E+07	3,39E+07	3,44E+07	3,49E+07
	11500	3,11E+07	3,18E+07	3,25E+07	3,28E+07	3,32E+07	3,36E+07	3,40E+07	3,44E+07	3,49E+07
	12000	3,11E+07	3,19E+07	3,26E+07	3,30E+07	3,33E+07	3,37E+07	3,41E+07	3,45E+07	3,50E+07
	12500	3,11E+07	3,19E+07	3,26E+07	3,31E+07	3,34E+07	3,38E+07	3,42E+07	3,46E+07	3,50E+07

Figure 6.7: Results annual DOC for one aircraft in USD

The annual DOC results follow the inverse pattern of the flight time, because a higher flight time means a lower number of flights per year. The number of flights per year has a heavy influence on all time-dependent (or cost index) components of the DOC: fuel, maintenance, crew costs, and fees and charges. All of these costs decrease with a lower number of flights per year.

Another observation is that the annual DOC follows the pattern of minimal fuel consumption slightly. Costs reach their lowest value in each column around the point of minimum fuel consumption for that column. The strength of this relationship depends on the actual fuel price and flight mission of the aircraft. A higher fuel price shows a clearer pattern towards minimum fuel consumption in the annual DOC results. Furthermore, short-/medium-range aircraft like the Airbus A320-200 depend less on fuel consumption than long-range aircraft. In the result for the Airbus A380 in Appendix E, a bigger variation is visible in annual DOC results per single column.

The annual DOC result conveys the idea that flying lower and slower would be an optimal flight condition. There are however two reasons that this is not the case. The first one is that flying slower would increase the flight time. At Mach 0.4 this would be almost double the flight time of a passenger jet aircraft nowadays. Passenger willingness to buy tickets for such

a flight would be substantially lower (this idea is further elaborated in Chapter 6.4). A second reason is that the increased flight time leads to a lower number of flights per year. This in turn negatively impacts the seat-mile cost and the ability of the airline to make a profit by selling tickets. This is one of the reasons why seat-mile cots is chosen as the representative economic metric instead of annual DOC.

The distribution of all DOC components is shown in Figure 6.8 for the regular flight conditions of the Airbus A320-200 (cruise speed of 0.78 M at 11 500 m altitude).

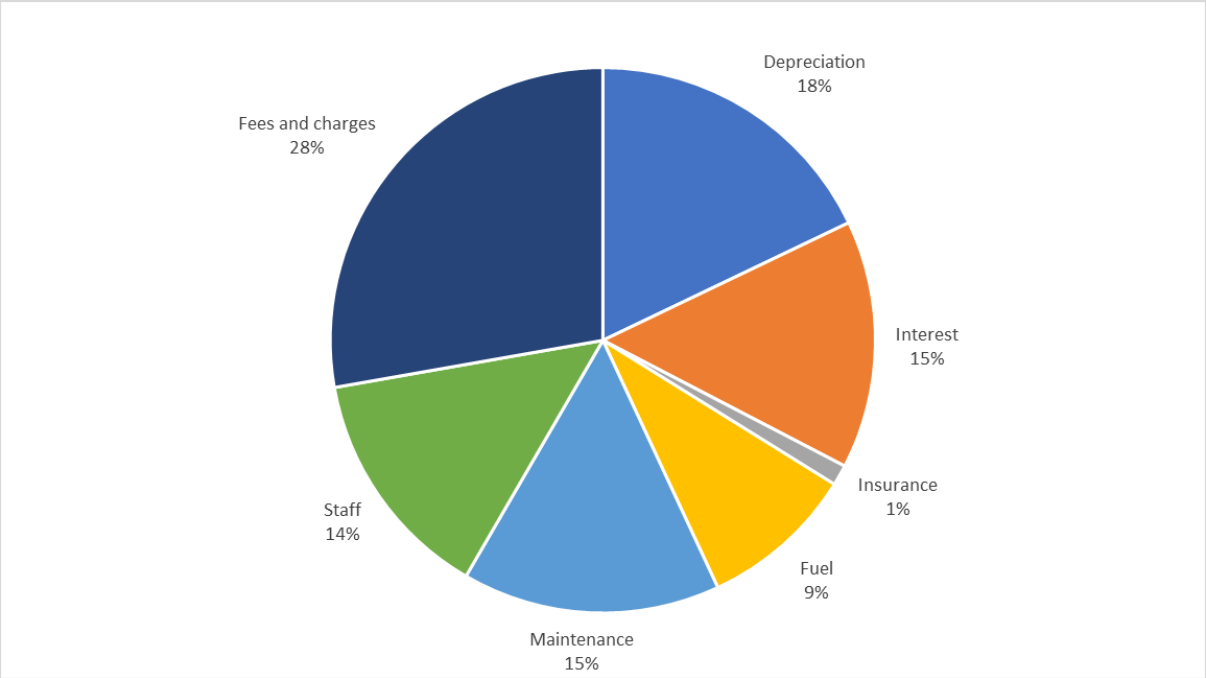

Figure 6.8: Annual DOC distribution for Mach 0.78 at 11 500 m

The first thing that stands out in the pie chart is the big slice of fees and charges. This seems abnormal but was researched by **Meyer 2004** and deemed to be realistic. The fees and charges share consists of landing fees, navigation or ATC fees, and ground handling fees. All USD values here are corrected for inflation from the 1989 values provided in the AEA1989 method.

A second observation is the low contribution of fuel costs to the total DOC. This is a result of the current low price of jet fuel (around 1.8 USD per gallon at the time of publication) and the short DOC range for this aircraft. See Figure 2.4 for the jet fuel price evolution over the last decades. Another reason for the low fuel cost is the fact that this is a short-/medium-range aircraft. The fuel cost share increases significantly once the DOC range is increased (see Appendix E for Airbus A380 case).

Figure 6.9 presents an overview of annual DOC distribution for four different flight parameter scenarios. The first observation is that depreciation, interest, and insurance stay at a constant

value since they only depend on the type of aircraft (short-/medium-range or long-range) and not on the flight time. Furthermore, fees and charges increase substantially with increasing Mach number due to the increase in number of flights per year (shorter flight time). This implies a greater number of LTO cycles and therefore an increase in all fees and charges: landing, navigation, and ground handling.

Fuel costs increase with number of flights per year and increasing fuel consumption to a lesser extent. Maintenance costs follow the same increase with an increasing number of flights per year. Staff costs, in contrary, decrease slightly due to the lower number of block hours.

	Case 1	Case 2	Case 3	Case 4
M	0,4	0,5	0,75	0,8
H (m)	3000	7000	11000	12500
Depreciation	$6 200 021,45	$6 200 021,45	$6 200 021,45	$6 200 021,45
Interest	$5 101 928,76	$5 101 928,76	$5 101 928,76	$5 101 928,76
Insurance	$423 617,79	$423 617,79	$423 617,79	$423 617,79
Fuel	$2 413 909,79	$2 691 784,30	$3 128 502,36	$3 396 793,16
Maintenance	$5 023 752,69	$5 106 346,31	$5 285 011,84	$5 320 396,10
Staff	$5 130 719,38	$5 031 588,64	$4 819 748,91	$4 778 910,89
Fees and charges	$6 674 835,27	$7 553 653,71	$9 443 810,82	$9 813 472,54
Flight time (h)	3,17	2,71	2,02	1,92
Seat-mile costs	$0,266	$0,244	$0,209	$0,205

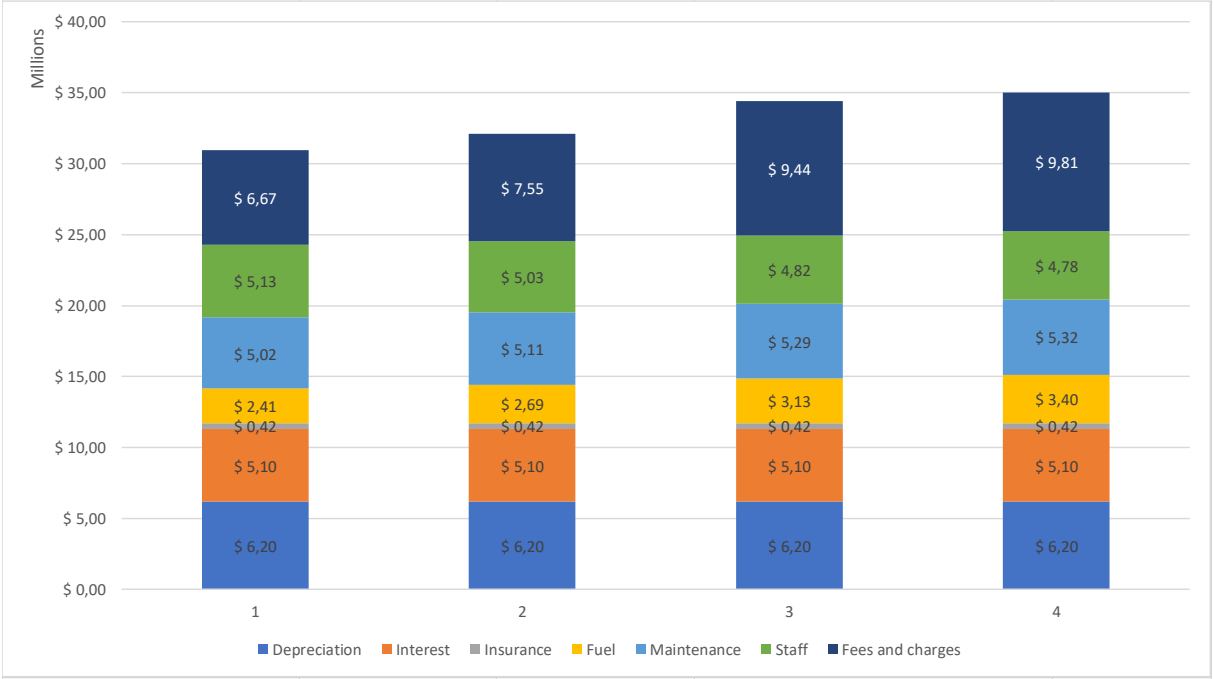

Figure 6.9: Breakdown of annual DOC for four flight parameter scenarios

6.3.3 Seat-Mile Cost

The seat-mile cost is shown as the cost in USD for one seat in the aircraft flown over a distance of one NM.

		Mach number								
		0,4	**0,45**	**0,5**	**0,55**	**0,6**	**0,65**	**0,7**	**0,75**	**0,8**
Altitude (m)	**3000**	0,266	0,248	0,235	0,224	0,216	0,209	0,204	0,200	0,198
	3500	0,269	0,251	0,237	0,226	0,218	0,211	0,205	0,201	0,199
	4000	0,271	0,252	0,238	0,227	0,218	0,211	0,206	0,202	0,199
	4500	0,272	0,253	0,239	0,228	0,219	0,212	0,206	0,202	0,199
	5000	0,274	0,254	0,240	0,229	0,220	0,213	0,207	0,202	0,199
	5500	0,276	0,256	0,241	0,229	0,220	0,213	0,207	0,203	0,199
	6000	0,277	0,257	0,242	0,230	0,221	0,214	0,208	0,203	0,199
	6500	0,279	0,258	0,243	0,231	0,222	0,214	0,208	0,203	0,200
	7000	0,281	0,260	0,244	0,232	0,222	0,215	0,208	0,203	0,199
	7500	0,283	0,262	0,245	0,233	0,223	0,215	0,209	0,203	0,200
	8000	0,286	0,264	0,247	0,234	0,224	0,216	0,209	0,204	0,200
	8500	0,287	0,265	0,248	0,235	0,225	0,216	0,209	0,204	0,200
	9000	0,288	0,268	0,250	0,237	0,226	0,217	0,210	0,204	0,200
	9500	0,290	0,270	0,252	0,239	0,228	0,220	0,213	0,207	0,203
	10000	0,291	0,272	0,253	0,240	0,229	0,221	0,214	0,208	0,203
	10500	0,293	0,273	0,255	0,242	0,231	0,222	0,215	0,209	0,204
	11000	0,294	0,274	0,256	0,243	0,232	0,223	0,215	0,209	0,204
	11500	0,294	0,274	0,258	0,243	0,232	0,223	0,216	0,209	0,205
	12000	0,294	0,274	0,258	0,244	0,233	0,224	0,216	0,210	0,205
	12500	0,295	0,274	0,259	0,245	0,234	0,224	0,217	0,210	0,205

Figure 6.10: Results seat-mile cost in USD

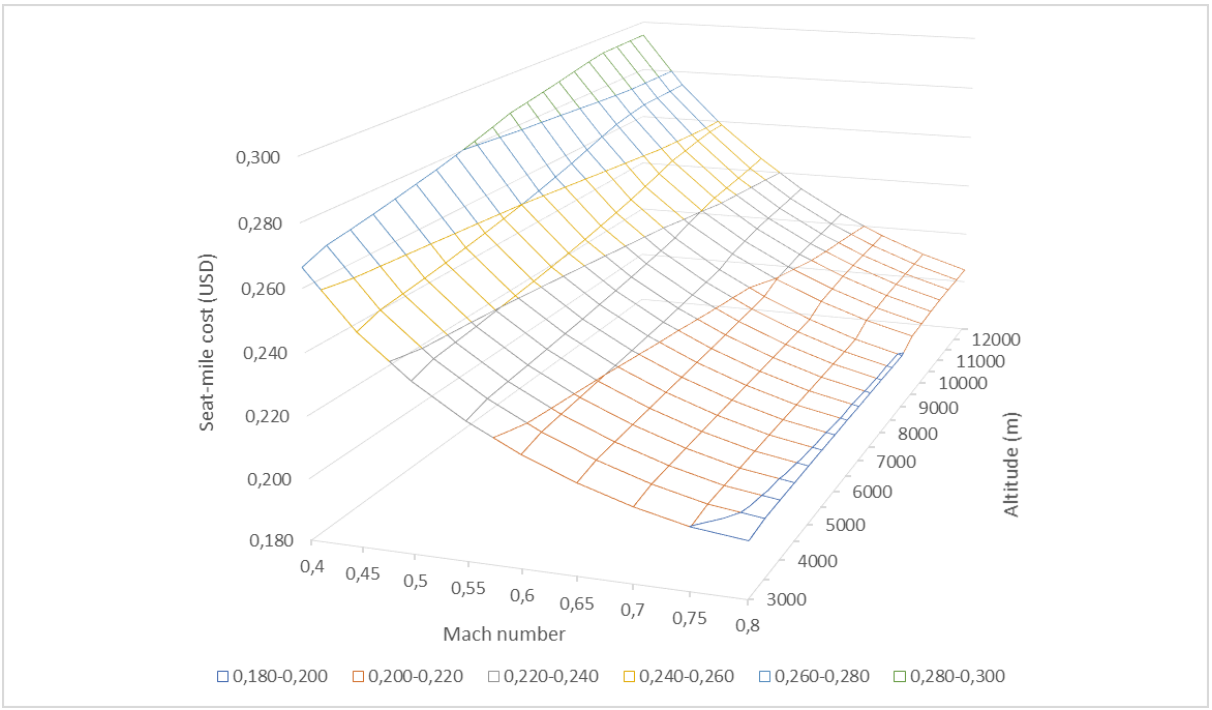

Figure 6.11: Contour plot of the seat-mile cost results

For seat-mile cost a general trend is visible towards high Mach number and low altitude. This follows the pattern of flight time entirely. Lower altitude means higher TAS for the same Mach number. Flight time is present in the seat-mile cost equation in the form of number of flights per year. Annual DOC evolves negatively towards lower altitude, but the influence of the number of flights per year on the seat-mile cost is higher and thus nullifies the negative influence of annual DOC.

$$C_{s,m} = \frac{C_{a/c,a}}{n_{seat} \cdot n_{t,a} \cdot R_{DOC}} \tag{3.11}$$

When looking at the seat-mile cost equation, annual DOC and number of trips per year are the only variable parameters when considering a single aircraft. DOC range could be altered to influence the seat-mile cost, but this is a question of operational flight planning done by the airline.

6.4 Added Value

In the annual DOC results can be seen that flying low and slow results in the lowest annual direct operating costs. DOC is purely built up out of economic data and questions can be asked here about the human factor in these results. When considering that a passenger jet aircraft would fly at about half the speed normally flown, would passengers still be willing to pay the same ticket price for a flight that takes twice as long? This customer willingness is difficult to put into numbers because it is highly subjective. In the work of **Nita 2013** a term called added value is used. This is an effort to add non-economic factors like performance, operating flexibility, or passenger comfort to the economic equation.

To decide on the weight of each of the added value factors, 22 questionnaires were taken by Nita from experts, aircraft design PhD students and aircraft design students. *The final weights were determined from the best answer (i.e. best consistency and high coefficients of determination) corrected by technical insight, expert views and the average of all answers* (**Nita 2013**). An overview of the added value factors and their final weights is given in Table 6.3. Cruise speed is the largest contributing factor to the added value, followed by passenger comfort factors like seat pitch and -width or overhead bin volume.

Table 6.3: Final attributed weights to the added value factor (**Nita 2013**)

												Absolute weights	Added Values scaled to 100 %
Economics	75	%	Equiv. ton-mile costs	100	%			%			%	75.00%	
Added Values	25	%	Performance	35	%	Airport performance	50	%	Landing field length	0	%	0.00%	0.00%
									Take-off field length	80	%	3.50%	14.00%
									Relative landing weight (m_{ML}/m_{MTO})	20	%	0.88%	3.50%
						Cruise performance	50	%	Cruise speed	100	%	4.38%	17.50%
			Passenger Comfort	55	%	Concerning all passengers	80	%	Seat pitch	30	%	3.30%	13.20%
									Seat width	20	%	2.20%	8.80%
									Armrest width	10	%	1.10%	4.40%
									Aisle width	5	%	0.55%	2.20%
									Aisle height	5	%	0.55%	2.20%
									Overhead bin volume per pax	20	%	2.20%	8.80%
									Aircraft gust sensibility	10	%	1.10%	4.40%
						Concerning part of the passengers	20	%	Sidewall clearance	10	%	0.28%	1.10%
									Number of "excuse-me" seats	90	%	2.48%	9.90%
			Cargo Handling	10	%	Concerning cargo	80	%	Containerized cargo (yes/no)	100	%	2.00%	8.00%
						Concerning cargo working conditions	20	%	Accessibility factor	50	%	0.25%	1.00%
									Cargo compartment height	50	%	0.25%	1.00%
											Check:	100.00%	100.00%

Although the added value approach does not give a comprehensive answer to the question if passengers would still be willing to pay the same ticket price for a flight that takes twice as long, it shows that the cruise speed of an aircraft is considered as an important added value. In conclusion, this is another reason why seat-mile cost is a more appropriate metric for calculating optimum economic benefit.

6.5 Conclusion DOC

In this chapter the economic impact of flying at different flight parameters is analyzed. The full method is based on the DOC method of **Scholz 2015**, which is in turn based on the AEA1989 method. The results are expressed in the form of annual cost and seat-mile cost of one aircraft.

The accuracy of the model largely depends on 1989 USD values for prices, fees, and charges adjusted for an average inflation or depends on statistical data. This produces a certain inaccuracy in the actual USD values. But again, as in Chapter 5, this does not pose a problem when only comparing different USD values for varying flight parameters to find a trend in DOC variation.

In general, the annual DOC and seat-mile cost follow a different and almost inverse pattern. Annual DOC decreases when flying slower and has a minimum value for each Mach number at around the point of minimum fuel consumption. The minimum value would be even more emphasized by higher fuel prices or for a long-range aircraft. This result conveys the idea that flying at a lower Mach number is beneficial in an economic context. However, this is not the case due to several reasons: a low passenger-willingness to pay for very slow flights (see

Chapter 6.4 about added value), a cutback in number of flights per year and the corresponding ticket income for the airline, and finally an increase in seat-mile cost for the same aircraft.

The main reason the annual DOC decreases with longer flight times is due to the lower number of flights per year that are possible and the corresponding lower fuel costs, maintenance costs, staff costs, and fees and charges. This is a logical consequence: operating any vehicle to transport passengers less than its full potential (be it an aircraft or some other means of transport) will decrease its operational costs. But this defeats the main purpose of the vehicle: generating as much revenue as possible during its limited lifespan.

Seat-mile cost follows the pattern of flight time. A minimal flight time results in a minimal seat-mile cost. This is because a lower flight time enables a higher number of flights per year. And therefore, cruise speed or cruise Mach number has a big influence on seat-mile cost. At an altitude of 11 500 m, the seat-mile cost is 30.47 % lower when flying at Mach 0.8 compared to Mach 0.4. Compared to this, the influence of cruise altitude is less distinct. It varies between 3.41 % and 9.58 % from high to low Mach numbers respectively.

It is clear that seat-mile cost portrays the economic effect of varying flight parameters better than the annual DOC. Imagine a fixed ticket price for a certain flight mission. A lower seat-mile cost means a higher return on this ticket. In this way, the lowest flight time ensures the optimal economic benefit for an aircraft. This results in a general outcome for DOC: a higher true airspeed during cruise (higher Mach number and lower altitude) results in the greatest number of flights per year and consequently in the lowest seat-mile cost possible. An added benefit of high TAS being at the lowest cruise altitude is that climb- and descent stages take up less time in this case. Which in turn further improves flight time.

Another observation that can be made from the results in this chapter is that fuel consumption has a minimal influence on annual DOC and especially on the seat-mile cost for this type of aircraft. As mentioned before, this is as a result of the current relatively low fuel price and because the Airbus A320-200 is a short-/medium-range aircraft. Meaning that it typically spends more time on the ground loading and unloading and less time in the air than a typical wide-body long-range aircraft (**Swelbar 2018**). Airlines could therefore be inclined towards less efficient (and thus probably less expensive) aircraft over expensive and efficient aircraft for their short- to medium-range flights.

7 Flight Parameter Optimization: Environmental Impact

7.1 General

The environmental impact of an aircraft can be defined in a number of different ways. The model is already narrowed down by the fact that only cruise flight is considered. Local air quality and noise pollution are not applicable at cruise altitudes. For this model, environmental impact is considered as a combination of resource depletion and engine emissions. With resource depletion equal to fuel consumption. Engine emissions are estimated with equivalent CO_2 mass, a metric used to combine the effects of CO_2, NO_x and AIC into one equation. Equivalent CO_2 mass is introduced and discussed in Chapter 3.5.

7.2 Important Parameters

The most influential parameters in the environmental impact calculation are represented in Figure 7.1. Inputs are green, important intermediate parameters in blue and the final results in grey. CO_2 and NO_x emissions are influenced by the aircraft's fuel consumption, AIC emission only by its range.

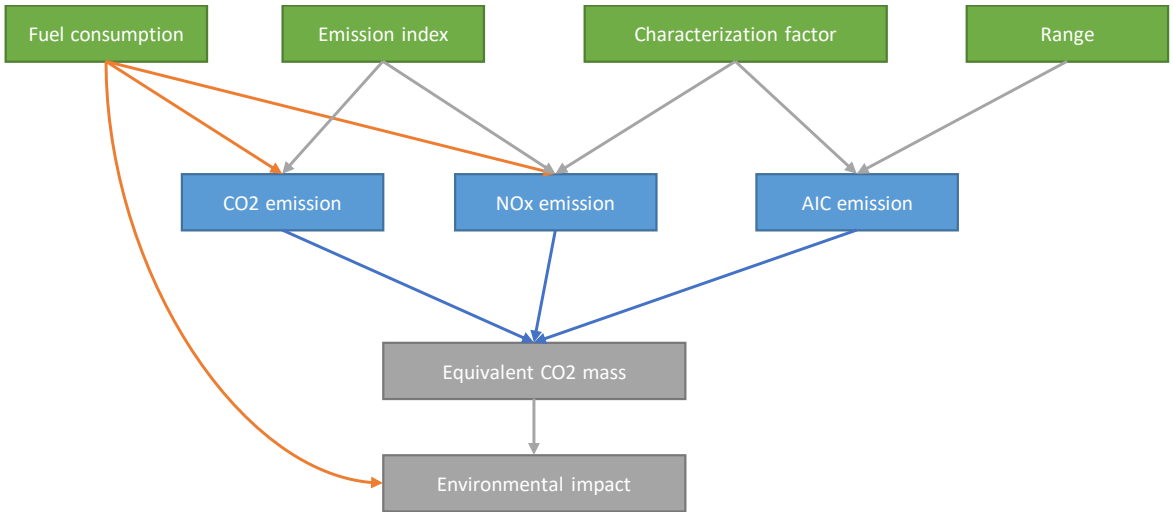

Figure 7.1: Flowchart of environmental impact calculation

7.2.1 Emission Index

The emission index of a specie is the mass (in g or kg) of this specie emitted per kg of fuel burned. The emission indices that are considered here are EI_CO_2 and EI_NO_x. The emission index of aircraft-induced clouds is hard to define because the formation of contrails depends on the altitude and distance flown and not on the mass of fuel burned. The emission index for CO_2 is independent of cruise altitude and equals a constant 3.16 kg CO_2 per kg of fuel. The emission index for NO_x on the other hand is dependent on the cruise altitude and is calculated with the Boeing fuel flow method 2 (**Baughcum 1996**). Application of this method in the Excel tool can be found in Chapter 4.7, the full calculation in Appendix B.

7.2.2 Characterization Factor

The characterization factor can be considered as a way to convert NO_x or AIC output into equivalent CO_2 mass. The equations are given in Chapter 3.5 and are based around sustained global temperature potential and an altitude-dependent forcing factor. The SGTP values can be found in Table 3.3 and the forcing factor values in Figure 3.4 or Appendix C.

7.3 Results Environmental Impact

7.3.1 Resource Depletion

Resource depletion is considered equal to fuel consumption as stated before. Fuel consumption results can be found in Chapter 5.3.3.

7.3.2 Emission Index NO_x

The emission index of NO_x is displayed as g of NO_x emitted per kg of fuel burned. Calculated using BFFM2 (see Chapter 3.5 and Appendix B), the emission index is mostly based on the fuel flow of the aircraft.

		Mach number								
		0,4	0,45	0,5	0,55	0,6	0,65	0,7	0,75	0,8
Altitude (m)	3000	13,38	13,63	14,49	15,85	17,72	20,31	23,65	28,19	35,71
	3500	13,66	13,75	14,45	15,65	17,35	19,72	22,80	27,00	33,95
	4000	14,00	13,92	14,46	15,51	17,04	19,21	22,05	25,92	32,35
	4500	14,39	14,14	14,53	15,42	16,79	18,77	21,38	24,95	30,89
	5000	14,85	14,42	14,66	15,40	16,60	18,40	20,80	24,09	29,57
	5500	15,39	14,77	14,84	15,43	16,49	18,11	20,30	23,32	28,39
	6000	15,99	15,19	15,10	15,54	16,44	17,89	19,88	22,66	27,34
	6500	16,68	15,68	15,42	15,71	16,46	17,75	19,56	22,10	26,41
	7000	17,46	16,25	15,82	15,95	16,56	17,69	19,32	21,64	25,60
	7500	18,34	16,90	16,29	16,27	16,73	17,71	19,17	21,28	24,92
	8000	19,33	17,65	16,86	16,68	16,99	17,82	19,11	21,02	24,36
	8500	20,44	18,51	17,51	17,17	17,34	18,01	19,14	20,87	23,93
	9000	21,68	19,48	18,27	17,76	17,78	18,30	19,27	20,82	23,61
	9500	23,06	20,57	19,15	18,46	18,32	18,69	19,51	20,88	23,42
	10000	24,60	21,80	20,14	19,27	18,97	19,19	19,86	21,06	23,37
	10500	26,33	23,18	21,27	20,20	19,74	19,81	20,33	21,37	23,44
	11000	26,26	23,12	21,21	20,14	19,68	19,75	20,27	21,31	23,38
	11500	29,01	25,39	23,16	21,85	21,20	21,13	21,53	22,46	24,41
	12000	32,12	27,98	25,37	23,80	22,96	22,73	23,00	23,82	25,64
	12500	35,65	30,91	27,89	26,02	24,96	24,57	24,70	25,40	27,10

Figure 7.2: Results emission index of NOx in g per kg of fuel

The general pattern of the EI_NO_x results is found in the uncorrected fuel flow results in Figure 7.3. There is a slight change in some of higher values because of the addition of a humidity factor for EI_NO_x. For a minimal emission of nitrogen oxides, flying lower and slower is the best approach. The shape somewhat follows the general shape of the fuel consumption results but shifted towards lower speed and altitude.

		Mach number								
		0,4	0,45	0,5	0,55	0,6	0,65	0,7	0,75	0,8
Altitude (m)	3000	0,48	0,49	0,53	0,59	0,66	0,77	0,92	1,11	1,43
	3500	0,50	0,50	0,53	0,59	0,66	0,76	0,89	1,07	1,37
	4000	0,52	0,52	0,54	0,59	0,65	0,75	0,87	1,04	1,32
	4500	0,55	0,54	0,55	0,59	0,65	0,74	0,86	1,01	1,28
	5000	0,58	0,56	0,57	0,60	0,65	0,73	0,84	0,99	1,24
	5500	0,61	0,58	0,58	0,61	0,66	0,73	0,83	0,97	1,20
	6000	0,65	0,61	0,61	0,63	0,67	0,73	0,83	0,95	1,17
	6500	0,69	0,64	0,63	0,64	0,68	0,74	0,82	0,94	1,14
	7000	0,74	0,68	0,66	0,66	0,69	0,75	0,82	0,93	1,12
	7500	0,79	0,72	0,69	0,69	0,71	0,76	0,83	0,93	1,10
	8000	0,85	0,77	0,73	0,72	0,74	0,78	0,84	0,93	1,09
	8500	0,92	0,82	0,77	0,76	0,77	0,80	0,85	0,94	1,09
	9000	0,99	0,88	0,82	0,80	0,80	0,83	0,87	0,95	1,09
	9500	1,08	0,95	0,88	0,85	0,84	0,86	0,90	0,97	1,10
	10000	1,18	1,03	0,95	0,90	0,89	0,90	0,93	1,00	1,11
	10500	1,29	1,12	1,02	0,97	0,94	0,95	0,97	1,03	1,14
	11000	1,30	1,14	1,04	0,98	0,96	0,96	0,99	1,04	1,15
	11500	1,51	1,31	1,19	1,12	1,08	1,08	1,10	1,15	1,26
	12000	1,76	1,52	1,37	1,28	1,23	1,22	1,23	1,28	1,39
	12500	2,05	1,76	1,58	1,47	1,41	1,38	1,39	1,43	1,53

Figure 7.3: Results corrected fuel flow in kg per second

7.3.3 Equivalent CO_2 Mass

The equivalent CO_2 mass is represented as kg of CO_2 emitted per NM flown, per seat. By dividing by the number of seats, the metric becomes more generic.

		Mach number								
		0,4	**0,45**	**0,5**	**0,55**	**0,6**	**0,65**	**0,7**	**0,75**	**0,8**
Altitude (m)	**3000**	0,118	0,106	0,101	0,101	0,103	0,108	0,115	0,126	0,145
	3500	0,121	0,107	0,101	0,099	0,101	0,105	0,111	0,121	0,139
	4000	0,125	0,109	0,102	0,099	0,099	0,102	0,108	0,117	0,133
	4500	0,129	0,112	0,102	0,098	0,098	0,100	0,105	0,113	0,128
	5000	0,134	0,114	0,104	0,099	0,097	0,098	0,102	0,109	0,123
	5500	0,146	0,124	0,111	0,105	0,102	0,103	0,106	0,112	0,126
	6000	0,156	0,130	0,115	0,107	0,103	0,104	0,107	0,114	0,129
	6500	0,171	0,140	0,123	0,113	0,108	0,108	0,110	0,117	0,132
	7000	0,220	0,182	0,160	0,148	0,141	0,140	0,143	0,149	0,167
	7500	0,271	0,227	0,201	0,187	0,179	0,176	0,177	0,184	0,200
	8000	0,346	0,293	0,262	0,244	0,234	0,230	0,231	0,236	0,252
	8500	0,458	0,391	0,352	0,329	0,316	0,310	0,310	0,315	0,332
	9000	0,587	0,502	0,453	0,424	0,407	0,399	0,397	0,401	0,419
	9500	0,710	0,607	0,547	0,512	0,490	0,479	0,475	0,478	0,494
	10000	0,852	0,723	0,649	0,605	0,578	0,563	0,556	0,557	0,572
	10500	0,975	0,806	0,710	0,653	0,618	0,597	0,587	0,586	0,601
	11000	1,003	0,810	0,702	0,638	0,599	0,576	0,565	0,565	0,582
	11500	1,123	0,873	0,733	0,650	0,599	0,569	0,553	0,550	0,566
	12000	1,270	0,939	0,755	0,646	0,579	0,539	0,516	0,509	0,524
	12500	1,504	1,079	0,843	0,704	0,618	0,566	0,536	0,523	0,535

Figure 7.4: Results equivalent CO2 mass in kg per NM flown, per seat

There is a relatively clear color transition around 7 000 m (about 23 000 ft) in these results. This is the point at which the influence of aircraft-induced clouds starts to rise rapidly and where the full warming effect of NO_x becomes available. The influence of AIC appears in the form of the forcing factor s and can be seen on Figure 3.4. On Figure 7.4, a vaguely visible orange colored band can be seen around 10 000 to 11 500 m (about 33 000 to 38 000 ft). This is the altitude associated with a maximum value of the forcing factor for AIC, and thus the biggest contribution. It also happens to be the most common cruise altitude zone for passenger jet aircraft nowadays.

Furthermore, in the green zone at lower altitude and moderate speed a shape resembling the fuel consumption pattern can be seen. This is because fuel consumption directly influences the amount of CO_2 and NO_x emitted (see Eq. (3.17)).

Equivalent CO_2 mass (Eq. (3.17)) is a rather complex metric that depends on numerous dependent and independent parameters. To get a better understanding of the influence of different emission contributors on the equivalent CO_2 mass, a comparison of different flight parameter scenarios is added below.

	Case 1	Case 2	Case 3	Case 4
M	0,55	0,8	0,5	0,75
H (m)	5000	4000	10000	11000
C02	106,33%	114,29%	24,90%	19,15%
NOx	-6,33%	-14,29%	18,02%	22,46%
AIC	0,00%	0,00%	57,08%	58,39%

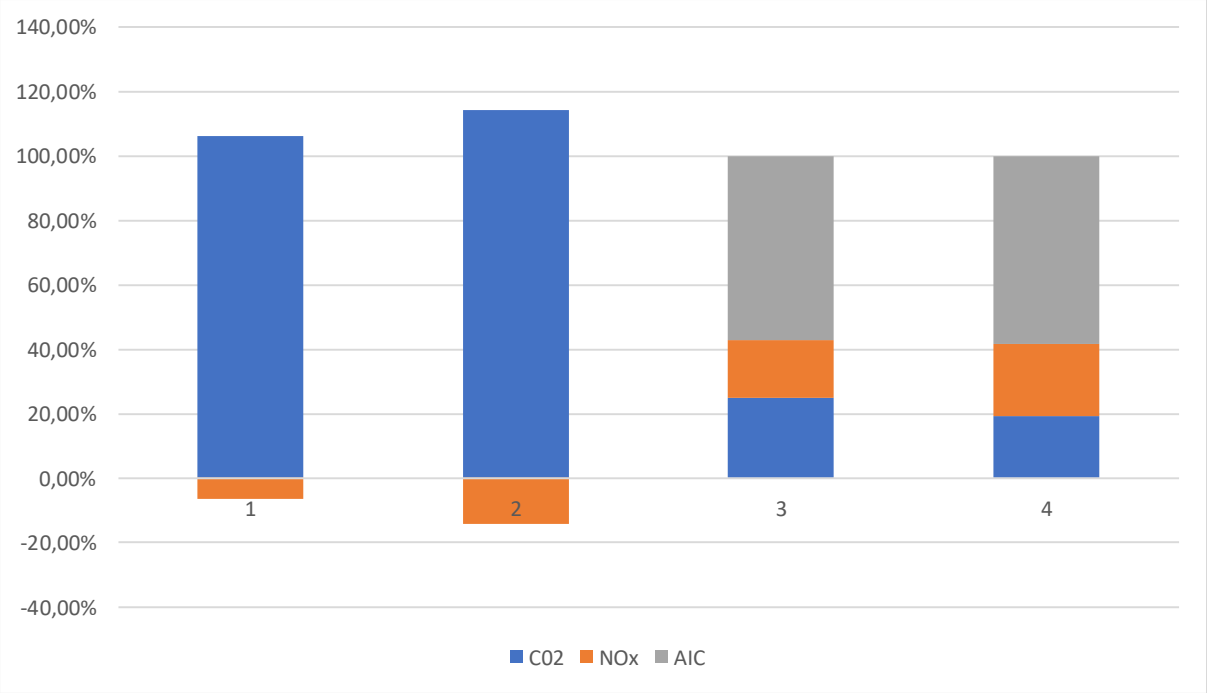

Figure 7.5: Importance of individual parameters in the equivalent CO2 mass equation

The first observation is that aircraft-induced clouds have zero or close to zero percent influence in the lower altitude zone. The reason being the low forcing factor values for AIC (see Figure 3.4). At higher altitudes the influence of AIC contributes for the majority of the environmental impact.

Another important note is that NOx has a negative contribution to the equivalent CO_2 mass at low altitudes. Nitrogen oxides can cause both a warming and a cooling effect. The warming effect occurs because of short ozone (O_3) and the cooling effect because of long ozone and methane (O_3 and CH_4 respectively). This phenomenon is visible in a cause effect form in Table 2.1 and in a quantitative form as SGTP values in Table 3.3. This cooling effect (or negative contribution) stops at around 6 000 m (about 19 500 ft).

7.3.4 Environmental Impact

The environmental impact is a combination of resource depletion and engine emissions. The impact of engine emissions is made quantitative by use of the equivalent CO_2 mass metric in the previous subchapter. Both resource depletion and engine emissions are normalized, multi-

plied by their respective weighting factor and added up to form the environmental impact. Weighting factors can be altered to change the importance of each contributor. Altering the weighting factors will result in a different outcome. The value of these weighting factors could be a topic of discussion, but for this result a neutral approach with 50 – 50 weighting factors (and thus an equal importance of resource depletion and engine emissions) is used.

		Mach number								
		0,4	**0,45**	**0,5**	**0,55**	**0,6**	**0,65**	**0,7**	**0,75**	**0,8**
Altitude (m)	**3000**	0,053	0,023	0,012	0,011	0,018	0,035	0,058	0,092	0,155
	3500	0,062	0,027	0,012	0,008	0,013	0,026	0,047	0,078	0,135
	4000	0,072	0,032	0,013	0,006	0,008	0,019	0,037	0,064	0,117
	4500	0,083	0,038	0,015	0,005	0,005	0,013	0,028	0,052	0,100
	5000	0,097	0,046	0,018	0,006	0,002	0,008	0,020	0,042	0,085
	5500	0,114	0,057	0,025	0,009	0,003	0,006	0,016	0,035	0,074
	6000	0,133	0,068	0,032	0,012	0,003	0,004	0,012	0,028	0,065
	6500	0,155	0,083	0,041	0,018	0,006	0,004	0,009	0,023	0,057
	7000	0,192	0,110	0,062	0,035	0,020	0,015	0,018	0,030	0,061
	7500	0,231	0,140	0,087	0,054	0,036	0,029	0,030	0,039	0,066
	8000	0,282	0,180	0,119	0,082	0,060	0,050	0,048	0,055	0,079
	8500	0,349	0,233	0,164	0,121	0,095	0,082	0,077	0,082	0,103
	9000	0,425	0,294	0,215	0,166	0,135	0,118	0,111	0,112	0,131
	9500	0,502	0,354	0,265	0,209	0,173	0,153	0,142	0,141	0,157
	10000	0,589	0,422	0,320	0,256	0,215	0,190	0,176	0,172	0,184
	10500	0,675	0,481	0,364	0,289	0,241	0,211	0,193	0,186	0,196
	11000	0,685	0,483	0,361	0,284	0,234	0,203	0,185	0,178	0,189
	11500	0,769	0,535	0,394	0,305	0,247	0,211	0,188	0,178	0,186
	12000	0,867	0,591	0,426	0,322	0,255	0,211	0,184	0,170	0,175
	12500	1,000	0,677	0,485	0,364	0,285	0,234	0,201	0,183	0,184

Figure 7.6: Results environmental impact (normalized between 0 and 1)

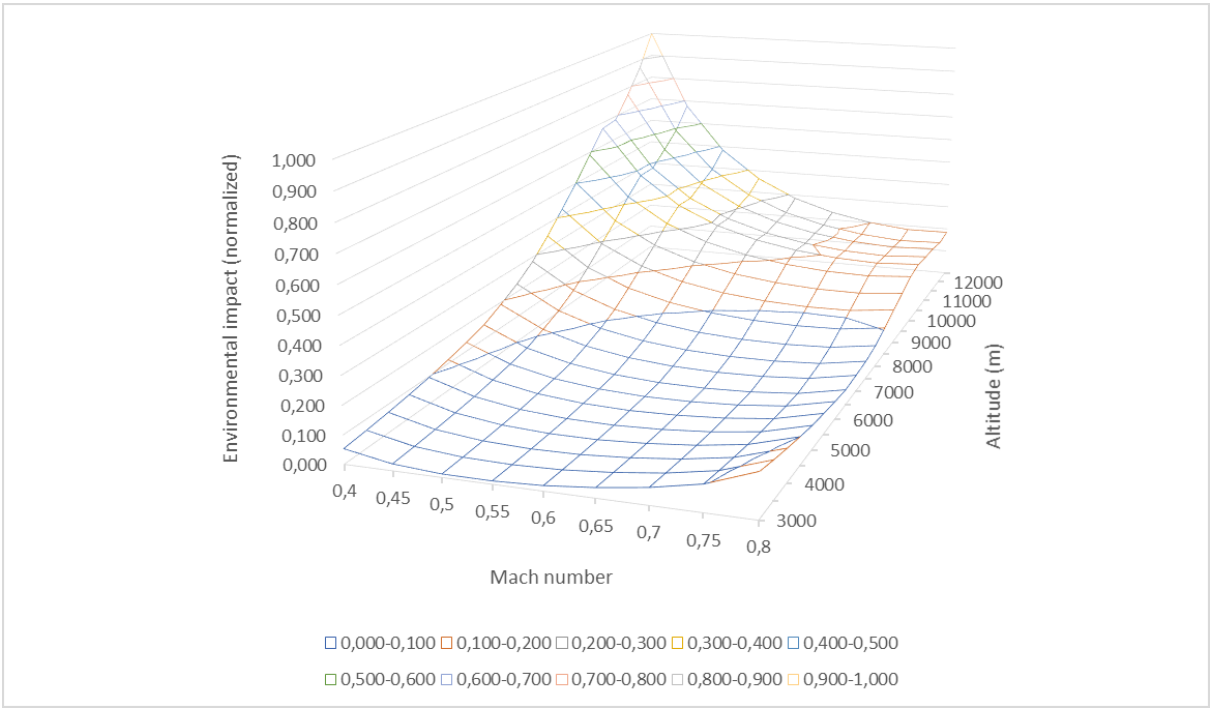

Figure 7.7: Contour plot of the environmental impact results

Due to these results being a combination of fuel consumption and equivalent CO_2 mass, a lot of similarities are found with both models. First, a clear altitude boundary can be seen where the green zone turns into yellow. The altitude has shifted from around 7 000 meter in the original equivalent CO_2 mass model to 8 000 meter here due to the shape of the fuel consumption results. Furthermore, the diagonal shape of the fuel consumption pattern from Chapter 5.3.3 is visible. This implies a reduced environmental impact at higher altitudes when flying faster, although this effect is rather limited. In conclusion, the results come down to flying significantly lower and slightly slower for a minimal environmental impact.

7.4 Conclusion Environmental Impact

In this chapter the environmental impact of an aircraft is represented in a quantitative way by combining resource depletion and engine emissions. Resource depletion is calculated as fuel consumption and engine emissions by way of equivalent CO_2 mass. The equivalent CO_2 mass is dependent on varying flight parameters by means of emission indices and altitude-dependent characterization factors. It combines the effects from CO_2 and non-CO_2 emissions into a single metric.

There exists a certain level of uncertainty for several contributors to the environmental impact of aircraft. Especially the influence of aircraft-induced cloudiness (AIC) in the form of contrails and cirrus clouds has a poor level of scientific understanding (see Figure 2.5). This and the fact that seasonal and location-based influences on contrail formation have been neglected, results in some inaccuracy in the final environmental impact results. This does not produce any issues when solely comparing results with each other to achieve a trend in environmental impact variation.

The main conclusion of the results in Figure 7.6 is that a reduction in cruise altitude would greatly reduce the environmental impact of aircraft. Looking at the equivalent CO_2 mass results (Figure 7.4), the common cruise altitude zone for jet aircraft nowadays (10 500 m to 11 500 m) results in the biggest equivalent CO_2 mass emission. Flying lower would greatly reduce the formation of contrails. In Figure 3.4 can be seen that the forcing factor of AIC shifts towards zero below 6 500 m, meaning no more formation of contrails and aircraft-induced cirrus clouds.

The problem with a lower cruise altitude is the decrease in overall engine efficiency and the corresponding increase in TSFC. Furthermore, the aircraft's aerodynamic efficiency is not optimized for this lower altitude. Meaning that it would be far out of the optimal dark green zone of the aerodynamic efficiency results in Figure 5.5, which in turn increases fuel consumption. A smaller wing surface resulting from an increase in wing loading will optimize the aircraft's aerodynamic efficiency for lower cruise altitudes. This scenario is analyzed in Chapter 8.3.

From an operational standpoint flying at lower altitudes also proves some challenges. A first issue relates to the historical reason of flying at higher altitudes: when flying at or around tropopause level an aircraft can fly over most weather phenomena, reducing turbulence and flying through thunderstorms. This is both a safety and passenger comfort measure. Additionally, bird strikes are extremely rare at tropopause level (90 % occurs under 3 000 ft according to **Cleary 2005**), further increasing safety at higher altitudes. Another reason is the added safety margin for an engine failure or other aircraft defect at high altitude. The flight crew has more time to follow necessary procedures, communicate, or come up with other measures if needed.

Changing the regular cruise altitude of an Airbus A320-200 of about 11 500 m to an altitude of 6 500 m at a constant Mach 0.78 would result in a decrease of equivalent CO_2 mass of 77.66 % and an increase of fuel consumption of 5.64 %. The increase of fuel consumption is mostly influenced by an increase of TSFC of 6.04 % and a decrease of the aerodynamic efficiency of 5.44 %. Combining equivalent CO_2 mass and resource depletion (fuel consumption) into the environmental impact would result in a decrease of 69.59 % in environmental impact.

A secondary conclusion is that the cruise Mach number must be reduced in order to minimize the environmental impact. Flying slower does not have a substantial impact on the equivalent CO_2 mass alone, but when combining the need of flying lower with resource depletion (fuel consumption results), it is clear that a reduction in cruise altitude requires a reduction in cruise speed in order to maintain minimum fuel consumption.

At an altitude of 6 500 m a cruise speed reduction to Mach 0.65 would result in a minimal environmental impact. Resulting in a further reduction of 82.61 % in environmental impact compared to flying at Mach 0.78 at the same altitude. This can be explained by the fuel consumption pattern in Figure 5.10: Mach 0.65 at 6 500 m is right in the optimal dark green zone while flying Mach 0.78 at this altitude results in an increase in fuel consumption of 11.86 %. The emitted equivalent CO_2 mass is reduced by 13.36 % with this cruise speed reduction.

The altitude of 6 500 m is used as an example in the previous paragraphs because of the lack of contrail formation and the fact that this is the optimum altitude for the combined model in Chapter 8. The actual flight parameters for a minimal environmental impact are Mach 0.6 at an altitude of 5000 m. Comparing this to the regular values of Mach 0.78 at 11 500 m, a reduction in environmental impact of 98.81 % would be possible. This is however a highly unrealistic flight scenario. The lower altitude poses problems as stated before and an even lower cruise Mach number results in a greater economic loss.

There is a range of other options to decrease the environmental impact of operating an aircraft apart from changing its flight parameters. New engine design to lower the thrust specific fuel consumption and thus the emission of CO_2 and NO_x is an option. Small improvements like

adding an electric motor to the nose wheel for ground handling at airports instead of using the aircraft engines for this (**DLR 2011**). Using biofuel or a mixture of biofuel and regular jet fuel is another option which is already being tested by multiple manufacturers, among them Boeing with their ecoDemonstrator program (**Jensen 2018**). Even fully electric or hybrid electric aircraft designs have been considered but will not be viable in the near future (**Scholz 2018**). The drawback of all these options is that a modification to the existing aircraft or a new aircraft design is necessary, or that they are simply not viable yet (e.g.: biofuel or electric aircraft). Having to invest in a new aircraft or extensive modifications makes all these options less attractive to airlines due to the long lifespan of their current aircraft. In contrast, small changes to flight parameters can be implemented right now without major challenges.

8 Flight Parameter Optimization: Combined Model

8.1 General

The combined model is a combination of seat-mile cost to represent the economic consequences and environmental impact for ecologic consequences. Fuel consumption will not be used as a direct input in the model because it is already heavily implemented in both DOC and environmental impact models.

Fuel consumption is present in DOC in the form of the Breguet factor, which determines the necessary fuel mass needed to complete the flight. It influences the environmental impact model in three ways. First, directly in the form of resource depletion, responsible for half of the environmental impact results (when using the default 50 – 50 weighting factors). Second, it is also used to calculate the aircraft's fuel flow, necessary for calculating the emission index of NO_x. Finally, fuel consumption is used to calculate the equivalent CO_2 mass with Eq. (3.17).

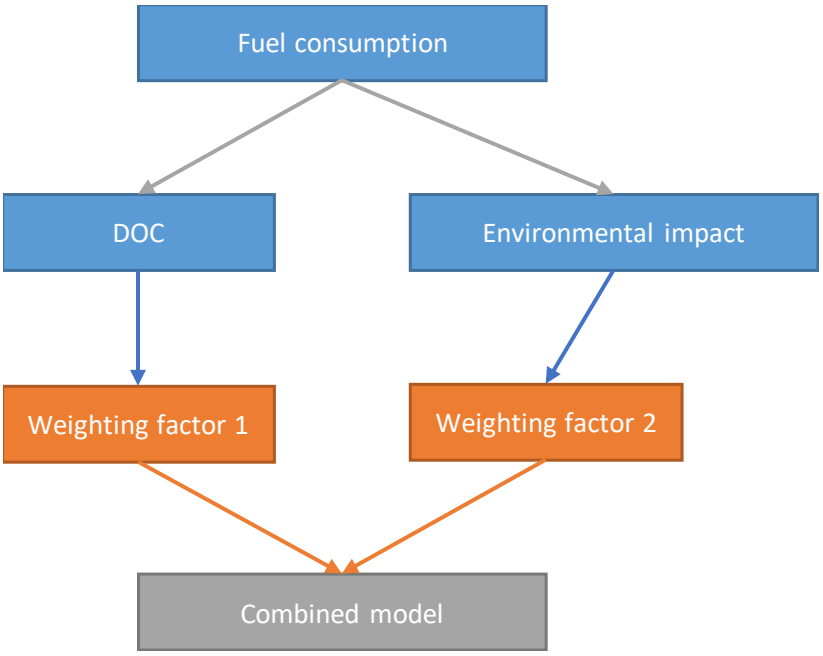

Figure 8.1: Flowchart combined model calculation

8.2 Results Combined Model

The results for the combined model can vary widely depending on the distribution of weighting factors. Two scenarios are presented here: a perhaps idealistic approach with a 50 – 50 weight distribution between economic and ecologic importance and a perhaps more realis-

tic approach of 80 % economic importance and 20 % ecologic importance. These are only arbitrary values and can be changed in the Excel tool to generate different results.

8.2.1 Equal Importance DOC and Environmental Impact Case

In this case the combined model is a result with equal weighting factors of 50 % for DOC and 50 % for environmental impact.

		Mach number								
		0,4	**0,45**	**0,5**	**0,55**	**0,6**	**0,65**	**0,7**	**0,75**	**0,8**
Altitude (m)	**3000**	0,381	0,271	0,196	0,141	0,101	0,075	0,060	0,056	0,078
	3500	0,401	0,287	0,208	0,151	0,109	0,080	0,062	0,056	0,073
	4000	0,413	0,295	0,213	0,154	0,110	0,080	0,060	0,051	0,065
	4500	0,426	0,303	0,219	0,157	0,111	0,079	0,057	0,047	0,057
	5000	0,441	0,314	0,225	0,161	0,114	0,079	0,056	0,043	0,050
	5500	0,459	0,326	0,234	0,168	0,118	0,081	0,056	0,041	0,045
	6000	0,477	0,339	0,243	0,173	0,121	0,083	0,056	0,039	0,040
	6500	0,498	0,354	0,253	0,181	0,126	0,086	0,056	0,038	0,036
	7000	0,527	0,376	0,270	0,194	0,137	0,094	0,063	0,042	0,038
	7500	0,558	0,400	0,288	0,209	0,149	0,104	0,071	0,048	0,041
	8000	0,595	0,429	0,312	0,229	0,166	0,118	0,082	0,057	0,048
	8500	0,635	0,466	0,342	0,254	0,187	0,137	0,098	0,071	0,060
	9000	0,680	0,507	0,376	0,282	0,212	0,158	0,117	0,088	0,074
	9500	0,726	0,548	0,410	0,315	0,243	0,189	0,148	0,117	0,103
	10000	0,777	0,592	0,447	0,346	0,270	0,213	0,169	0,136	0,119
	10500	0,828	0,629	0,480	0,372	0,291	0,230	0,183	0,148	0,128
	11000	0,839	0,635	0,483	0,373	0,291	0,229	0,182	0,147	0,128
	11500	0,882	0,662	0,505	0,388	0,301	0,236	0,186	0,149	0,127
	12000	0,932	0,691	0,526	0,401	0,309	0,239	0,186	0,146	0,122
	12500	1,000	0,734	0,556	0,428	0,328	0,254	0,197	0,154	0,128

Figure 8.2: Results combined model with equal importance of DOC and environmental impact (normalized between 0 and 1)

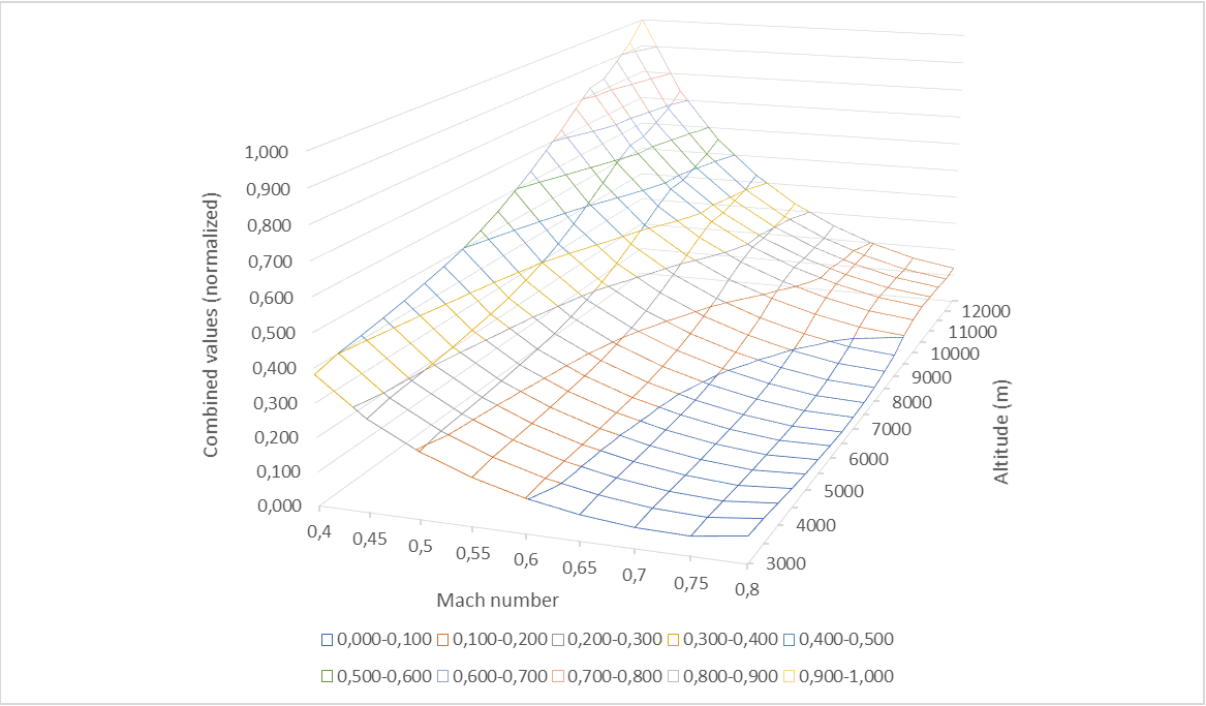

Figure 8.3: Contour plot of the combined model results (DOC and environmental impact)

The influence of the DOC is clear in the way that it shifts the optimum for minimum environmental impact towards the right, to a higher cruise Mach number. The shape from Figure 7.6 of the environmental impact results is still clearly visible with its tendency towards lower altitude. These two combine to an optimum result at a lower altitude and an unchanged cruise Mach number compared to regular flight parameters.

8.2.2 Emphasis on DOC Case

In this case the combined model is a result with a weighting factor of 80 % for DOC and 20 % for environmental impact.

		Mach number								
		0,4	**0,45**	**0,5**	**0,55**	**0,6**	**0,65**	**0,7**	**0,75**	**0,8**
Altitude (m)	**3000**	0,577	0,420	0,306	0,219	0,151	0,099	0,061	0,035	0,031
	3500	0,604	0,442	0,326	0,236	0,166	0,112	0,071	0,043	0,036
	4000	0,618	0,452	0,333	0,242	0,171	0,116	0,073	0,043	0,034
	4500	0,632	0,463	0,341	0,248	0,175	0,119	0,075	0,043	0,031
	5000	0,648	0,474	0,350	0,255	0,181	0,122	0,077	0,044	0,029
	5500	0,666	0,488	0,359	0,263	0,186	0,127	0,080	0,045	0,027
	6000	0,684	0,502	0,369	0,270	0,192	0,130	0,082	0,045	0,025
	6500	0,704	0,517	0,380	0,279	0,199	0,135	0,085	0,046	0,024
	7000	0,728	0,535	0,394	0,290	0,207	0,142	0,089	0,049	0,025
	7500	0,754	0,555	0,409	0,302	0,217	0,149	0,095	0,053	0,026
	8000	0,783	0,579	0,428	0,316	0,229	0,159	0,102	0,058	0,029
	8500	0,807	0,605	0,449	0,333	0,242	0,169	0,111	0,065	0,034
	9000	0,833	0,635	0,472	0,353	0,258	0,182	0,122	0,073	0,040
	9500	0,860	0,665	0,497	0,378	0,285	0,211	0,151	0,103	0,070
	10000	0,890	0,694	0,523	0,401	0,304	0,227	0,165	0,115	0,080
	10500	0,919	0,717	0,549	0,421	0,321	0,241	0,177	0,125	0,088
	11000	0,931	0,726	0,557	0,426	0,325	0,245	0,180	0,128	0,091
	11500	0,950	0,738	0,572	0,438	0,334	0,251	0,184	0,131	0,092
	12000	0,971	0,750	0,586	0,449	0,341	0,255	0,187	0,131	0,090
	12500	1,000	0,769	0,599	0,466	0,354	0,266	0,195	0,137	0,095

Figure 8.4: Results combined model with an emphasis on DOC (normalized between 0 and 1)

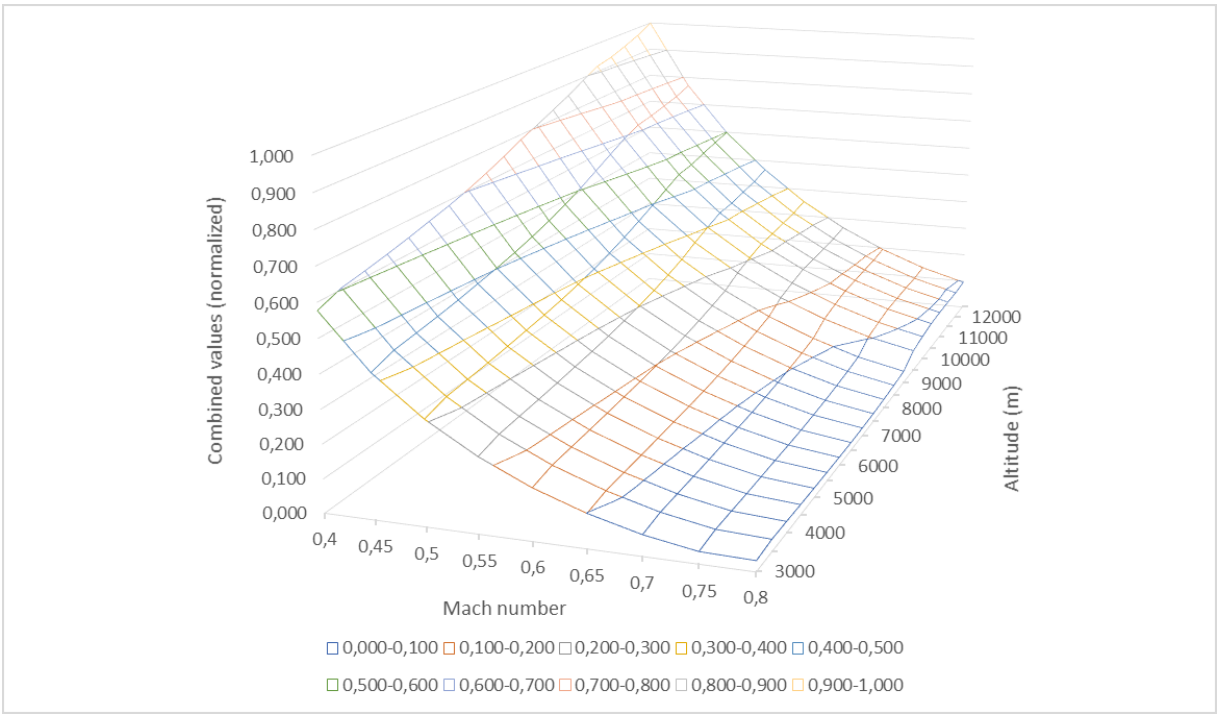

Figure 8.5: Contour plot of the combined model results (DOC)

In these results the shape of the environmental impact results is no longer clearly visible. All focus is aimed towards an economic optimum, which is achieved at the highest Mach number. There is still a slight shift towards the optimal altitude for environmental impact, but less visible than in the previous set of results in Chapter 8.2.1.

Another observation is that the normalized values around the optimum zone are lower than in the previous case. This is because the influence of environmental impact shifts the optimum zone towards a smaller Mach number. And with this influence less present than before, the optimum zone is mostly dictated by the DOC. Optimum DOC is at a maximum Mach number, therefore the values come closer to an optimum normalized value of zero.

8.3 Influence of the Wing Loading

In this chapter the combined model from Chapter 8.2 will be altered with a higher wing loading. Wing loading is defined as the ratio of an aircraft's mass (MTOW) over its wing surface. Wing loading and thrust-to-weight ratio are the two most important parameters to be optimized during preliminary aircraft design. Both are represented graphically in a matching chart with the aim to achieve the highest possible wing loading and lowest possible thrust-to-weight ratio. As can be seen in Figure 8.6, maximum wing loading is limited by the available landing field length and requires an increasing thrust-to-weight ratio for take-off (**Scholz 2015**).

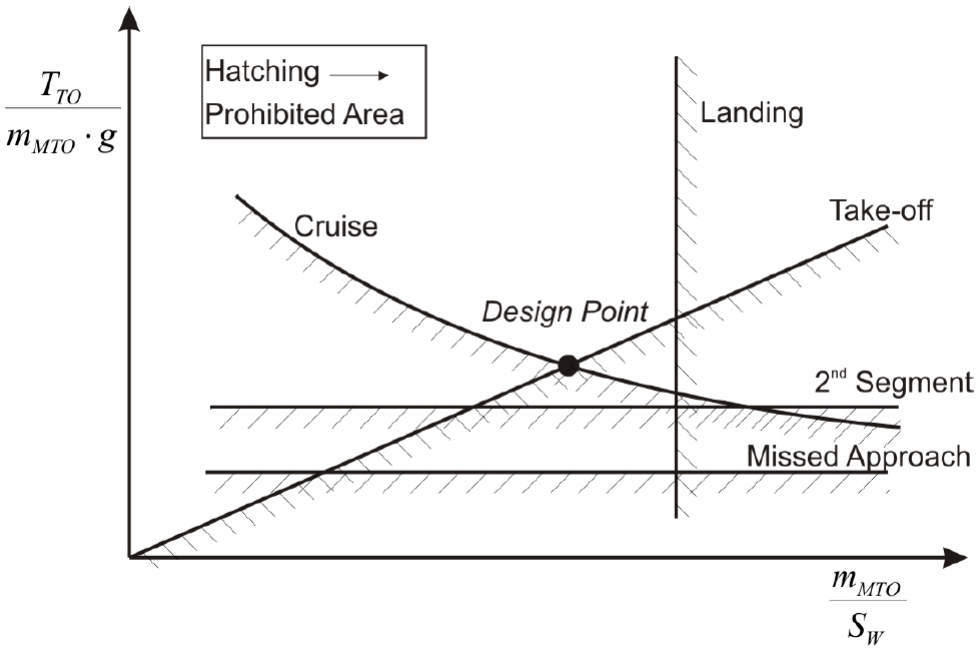

Figure 8.6: Illustrative example of a matching chart (**Scholz 2015**)

Wing loading influences the lift coefficient, as given in the following equation where the lift coefficient is represented in function of wing loading:

$$C_L(m/S) = \frac{2 \cdot g \cdot (m/S)}{\rho \cdot M^2 \cdot a^2} \tag{8.1}$$

This equation reveals that for a fixed altitude (represented by ρ and a) a higher wind loading will produce a higher lift coefficient. This optimizes the aerodynamic efficiency for lower altitudes, therefore shifting the zone of minimal fuel consumption to a lower altitude. The main purpose of choosing a higher wing loading for an aircraft is to lower its wing surface for the same MTOW. A smaller wing surface is optimal for flying at lower altitudes.

An increase in wing loading also means a required increase in landing field length. Landing field length is defined as the landing distance multiplied by a safety factor (1.667 for jet aircraft), as can be seen in Figure 8.7.

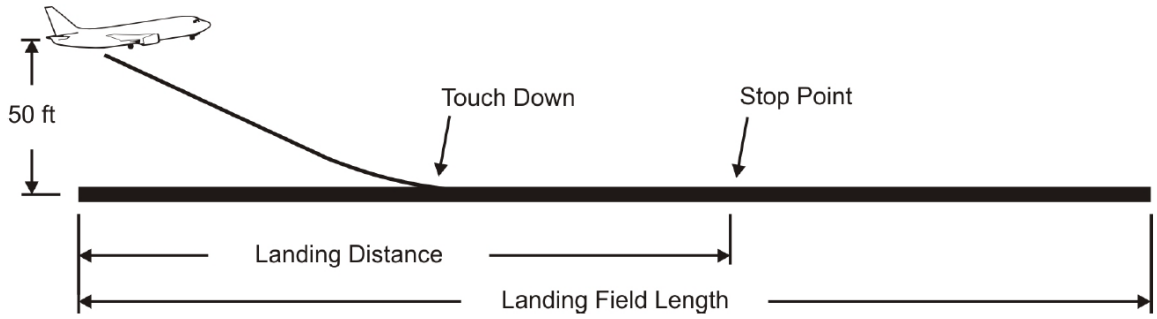

Figure 8.7: Landing field length (**Scholz 2015**)

The landing field length s_{LFL} relates to the ratio of maximum landing mass over wing surface in the following way:

$$\frac{m_{ML}}{S} = k_L \cdot \sigma \cdot C_{L,max,L} \cdot s_{LFL} \tag{8.2}$$

From this ratio the wind loading can be calculated by means of the maximum landing mass to maximum take-off mass ratio:

$$\frac{m_{MTOW}}{S} = \frac{m_{ML}/S}{m_{ML}/m_{MTO}} \tag{8.3}$$

When assuming the maximum lift coefficient during landing as constant, the landing field length is directly proportional with wing loading.

As an experiment, the original wing loading of the Airbus A320-200 of 600.49 kg/m^2 is increased with about 50 % to 900.74 kg/m^2. As a result of Eq. (8.2) and (8.3), the landing field length increases with 50 % as well. This makes it impossible for this aircraft to land at many airports where it normally would have been able to.

This 50 % increase in wing loading yields the following combined model results at 50 – 50 weighting factors for DOC and environmental impact:

		Mach number								
		0,4	**0,45**	**0,5**	**0,55**	**0,6**	**0,65**	**0,7**	**0,75**	**0,8**
Altitude (m)	**3000**	0,404	0,290	0,210	0,149	0,102	0,067	0,041	0,024	0,020
	3500	0,427	0,308	0,225	0,162	0,114	0,077	0,049	0,030	0,024
	4000	0,441	0,319	0,233	0,169	0,119	0,081	0,052	0,032	0,024
	4500	0,457	0,331	0,241	0,175	0,124	0,085	0,055	0,033	0,024
	5000	0,474	0,343	0,251	0,183	0,131	0,090	0,059	0,036	0,024
	5500	0,492	0,358	0,262	0,192	0,138	0,096	0,063	0,039	0,026
	6000	0,507	0,373	0,274	0,201	0,145	0,101	0,067	0,041	0,027
	6500	0,524	0,391	0,287	0,211	0,153	0,107	0,072	0,045	0,029
	7000	0,546	0,412	0,303	0,225	0,164	0,117	0,079	0,051	0,033
	7500	0,569	0,433	0,322	0,240	0,177	0,127	0,088	0,058	0,039
	8000	0,596	0,455	0,344	0,258	0,192	0,140	0,099	0,067	0,046
	8500	0,630	0,481	0,370	0,280	0,210	0,156	0,113	0,079	0,056
	9000	0,668	0,511	0,398	0,304	0,231	0,174	0,129	0,093	0,068
	9500	0,707	0,541	0,423	0,333	0,259	0,201	0,156	0,120	0,094
	10000	0,752	0,576	0,450	0,362	0,283	0,223	0,174	0,137	0,109
	10500	0,802	0,611	0,477	0,384	0,305	0,241	0,191	0,151	0,121
	11000	0,817	0,621	0,484	0,388	0,308	0,243	0,192	0,151	0,122
	11500	0,866	0,653	0,506	0,404	0,325	0,256	0,202	0,160	0,129
	12000	0,926	0,691	0,531	0,421	0,340	0,270	0,212	0,167	0,134
	12500	1,000	0,739	0,565	0,446	0,359	0,290	0,230	0,182	0,147

Figure 8.8: Results combined model for a 50 % higher wing loading

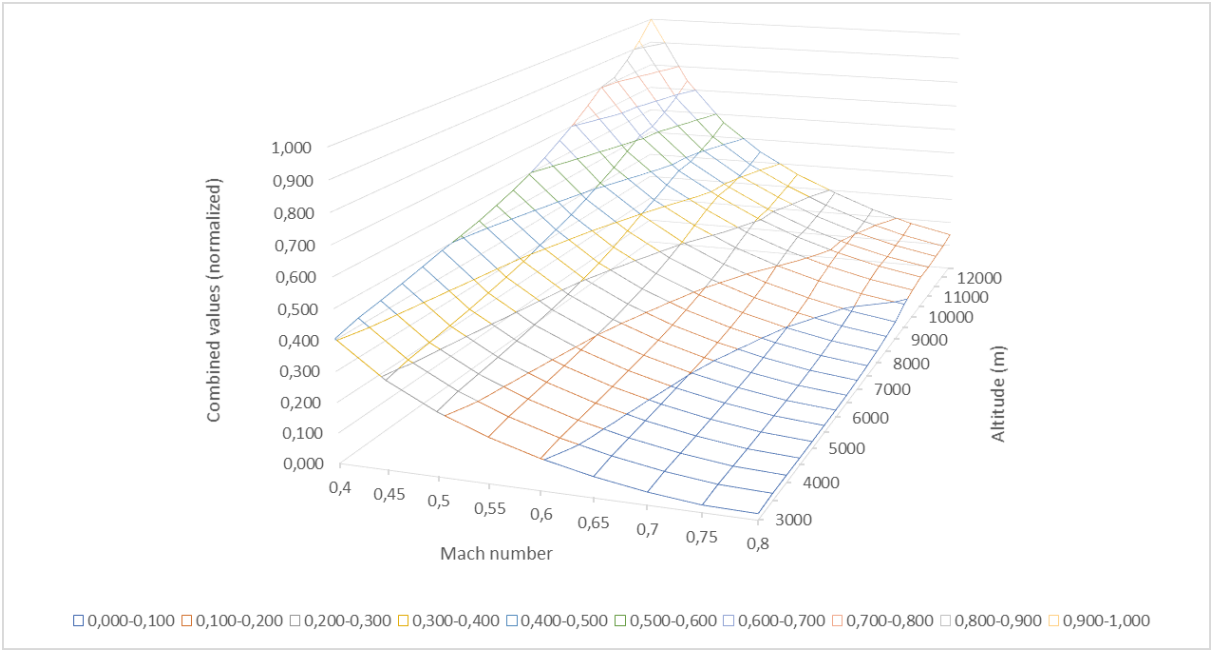

Figure 8.9: Contour plot of the combined model results (50 % higher wing loading)

In the following figures, the influence of a higher wing loading on fuel consumption, DOC, and environmental impact will be presented.

		Mach number								
		0,4	**0,45**	**0,5**	**0,55**	**0,6**	**0,65**	**0,7**	**0,75**	**0,8**
Altitude (m)	**3000**	9,76E-05	8,14E-05	7,24E-05	6,76E-05	6,57E-05	6,64E-05	6,89E-05	7,39E-05	8,45E-05
	3500	1,02E-04	8,44E-05	7,42E-05	6,86E-05	6,59E-05	6,59E-05	6,78E-05	7,20E-05	8,15E-05
	4000	1,08E-04	8,79E-05	7,64E-05	6,98E-05	6,64E-05	6,57E-05	6,70E-05	7,05E-05	7,90E-05
	4500	1,13E-04	9,18E-05	7,90E-05	7,14E-05	6,73E-05	6,59E-05	6,64E-05	6,92E-05	7,68E-05
	5000	1,20E-04	9,62E-05	8,19E-05	7,34E-05	6,84E-05	6,63E-05	6,62E-05	6,84E-05	7,49E-05
	5500	1,27E-04	1,01E-04	8,54E-05	7,57E-05	6,99E-05	6,71E-05	6,63E-05	6,78E-05	7,35E-05
	6000	1,35E-04	1,07E-04	8,93E-05	7,84E-05	7,17E-05	6,82E-05	6,68E-05	6,76E-05	7,24E-05
	6500	1,44E-04	1,13E-04	9,37E-05	8,16E-05	7,40E-05	6,96E-05	6,75E-05	6,77E-05	7,17E-05
	7000	1,54E-04	1,20E-04	9,87E-05	8,52E-05	7,66E-05	7,15E-05	6,87E-05	6,81E-05	7,13E-05
	7500	1,65E-04	1,27E-04	1,04E-04	8,94E-05	7,97E-05	7,37E-05	7,02E-05	6,90E-05	7,14E-05
	8000	1,77E-04	1,36E-04	1,11E-04	9,42E-05	8,33E-05	7,64E-05	7,21E-05	7,02E-05	7,18E-05
	8500	1,90E-04	1,45E-04	1,18E-04	9,95E-05	8,74E-05	7,95E-05	7,45E-05	7,18E-05	7,26E-05
	9000	2,04E-04	1,56E-04	1,25E-04	1,06E-04	9,21E-05	8,32E-05	7,73E-05	7,39E-05	7,39E-05
	9500	2,21E-04	1,68E-04	1,34E-04	1,12E-04	9,75E-05	8,74E-05	8,06E-05	7,65E-05	7,56E-05
	10000	2,39E-04	1,81E-04	1,44E-04	1,20E-04	1,03E-04	9,22E-05	8,45E-05	7,95E-05	7,79E-05
	10500	2,59E-04	1,95E-04	1,55E-04	1,28E-04	1,10E-04	9,77E-05	8,90E-05	8,31E-05	8,06E-05
	11000	2,58E-04	1,95E-04	1,55E-04	1,28E-04	1,10E-04	9,75E-05	8,87E-05	8,28E-05	8,03E-05
	11500	2,78E-04	2,10E-04	1,66E-04	1,37E-04	1,17E-04	1,03E-04	9,35E-05	8,68E-05	8,35E-05
	12000	3,00E-04	2,26E-04	1,78E-04	1,47E-04	1,25E-04	1,10E-04	9,89E-05	9,14E-05	8,72E-05
	12500	3,24E-04	2,43E-04	1,91E-04	1,57E-04	1,34E-04	1,17E-04	1,05E-04	9,65E-05	9,15E-05

Figure 8.10: Results fuel consumption in kg fuel per NM flown, per kg of aircraft MTOW (50 % higher wind loading)

The smaller wing surface that results from a higher wing loading will shift this aircraft's aerodynamic efficiency optimum to a lower altitude. Which consequently shifts the minimal fuel consumption optimum to a lower altitude. There will be a small increase in TSFC at lower altitude, but the improved aerodynamic efficiency outweighs this for the fuel consumption result.

		Mach number								
		0,4	**0,45**	**0,5**	**0,55**	**0,6**	**0,65**	**0,7**	**0,75**	**0,8**
Altitude (m)	**3000**	0,269	0,250	0,235	0,224	0,215	0,208	0,202	0,197	0,194
	3500	0,273	0,253	0,238	0,226	0,217	0,210	0,204	0,199	0,195
	4000	0,274	0,254	0,239	0,227	0,218	0,210	0,204	0,199	0,196
	4500	0,276	0,255	0,240	0,228	0,219	0,211	0,205	0,200	0,196
	5000	0,278	0,257	0,242	0,230	0,220	0,212	0,206	0,201	0,197
	5500	0,280	0,259	0,243	0,231	0,221	0,213	0,207	0,201	0,197
	6000	0,282	0,261	0,244	0,232	0,222	0,214	0,207	0,202	0,198
	6500	0,283	0,263	0,246	0,233	0,223	0,215	0,208	0,202	0,198
	7000	0,284	0,265	0,247	0,234	0,224	0,216	0,209	0,203	0,198
	7500	0,285	0,266	0,249	0,236	0,225	0,216	0,209	0,203	0,199
	8000	0,287	0,268	0,251	0,237	0,226	0,217	0,210	0,204	0,199
	8500	0,288	0,269	0,253	0,239	0,228	0,218	0,211	0,204	0,200
	9000	0,289	0,270	0,255	0,240	0,229	0,219	0,212	0,205	0,200
	9500	0,291	0,271	0,256	0,243	0,232	0,222	0,215	0,208	0,203
	10000	0,292	0,272	0,257	0,245	0,233	0,224	0,216	0,210	0,204
	10500	0,294	0,274	0,258	0,246	0,235	0,226	0,217	0,211	0,205
	11000	0,295	0,275	0,259	0,247	0,236	0,226	0,218	0,211	0,206
	11500	0,295	0,275	0,259	0,247	0,237	0,227	0,219	0,212	0,206
	12000	0,296	0,275	0,259	0,247	0,238	0,228	0,220	0,213	0,207
	12500	0,296	0,276	0,259	0,247	0,238	0,229	0,221	0,214	0,208

Figure 8.11: Results seat-mile cost in USD (50 % higher wing loading)

The seat-mile cost experiences a slight change by increasing wing loading. Seat-mile cost at lower altitudes decreases while it increases at higher altitudes compared to the regular wing loading case. Seat-mile cost depends on the annual DOC of an aircraft. The annual DOC in turn depends on fuel consumption results and the optimal zone here is shifted towards lower altitudes.

		Mach number								
		0,4	**0,45**	**0,5**	**0,55**	**0,6**	**0,65**	**0,7**	**0,75**	**0,8**
Altitude (m)	**3000**	0,071	0,035	0,015	0,004	0,000	0,001	0,007	0,018	0,040
	3500	0,081	0,041	0,019	0,006	0,001	0,000	0,004	0,013	0,034
	4000	0,092	0,049	0,024	0,009	0,002	0,000	0,003	0,010	0,028
	4500	0,105	0,057	0,029	0,013	0,003	0,000	0,001	0,007	0,024
	5000	0,119	0,067	0,036	0,017	0,006	0,001	0,001	0,006	0,020
	5500	0,136	0,079	0,044	0,023	0,010	0,004	0,002	0,005	0,018
	6000	0,156	0,092	0,054	0,030	0,015	0,007	0,004	0,005	0,016
	6500	0,178	0,108	0,065	0,038	0,021	0,011	0,006	0,007	0,016
	7000	0,209	0,131	0,083	0,053	0,033	0,021	0,015	0,014	0,022
	7500	0,243	0,156	0,103	0,069	0,047	0,033	0,025	0,023	0,029
	8000	0,284	0,188	0,129	0,091	0,066	0,050	0,040	0,036	0,040
	8500	0,338	0,230	0,163	0,119	0,091	0,072	0,061	0,055	0,057
	9000	0,400	0,277	0,201	0,152	0,119	0,098	0,084	0,076	0,077
	9500	0,464	0,326	0,240	0,185	0,148	0,123	0,107	0,097	0,096
	10000	0,539	0,381	0,284	0,221	0,180	0,151	0,132	0,120	0,117
	10500	0,624	0,439	0,327	0,254	0,206	0,173	0,150	0,136	0,131
	11000	0,642	0,448	0,331	0,255	0,205	0,171	0,148	0,133	0,128
	11500	0,738	0,510	0,373	0,285	0,227	0,188	0,161	0,143	0,136
	12000	0,855	0,583	0,421	0,319	0,250	0,204	0,172	0,151	0,141
	12500	1,000	0,678	0,488	0,368	0,288	0,234	0,197	0,172	0,159

Figure 8.12: Results environmental impact per NM flown per seat (50 % higher wing loading)

Comparing to the environmental impact with a regular wing loading, a decrease of the optimum value is visible. The optimal value with regular wing loading is 0.0022 normalized between 0 and 1. The optimal value for a higher wing loading is $3.74 \cdot 10^{-6}$, also normalized between 0 and 1. This value is significantly smaller because the zones of minimal fuel consumption and minimal environmental impact start to merge with a higher wing loading. Essentially, the higher wing loading brings fuel consumption and equivalent CO_2 mass optima closer to each other.

8.4 Conclusion Combined Model

In this chapter all three separate models have been combined into one model. The goal is to find optimum flight parameters for both economic and ecologic interests. The combined model is calculated for two cases: an equal importance of economic and ecologic benefits and a case with emphasis on the economic benefits.

The accuracy of this model is only as strong as the combined accuracies of all separate models. As mentioned before, all individual results are calculated with the same methods. Therefore, a comparison of results is still accurate enough to visualize a trend with changing flight parameters.

The general trend in both cases is a reduction in cruise altitude. This has a positive effect on seat-mile cost because of the increased TAS and on the environmental impact because of the

reduced equivalent CO_2 mass. A decrease in cruise Mach number on the other hand would benefit the environmental impact but would impose a penalty on the seat-mile cost. An important point to consider is that flying fast and low could be outside of the aircraft's permissible flight envelope (see Chapter 9.2).

In the 50 – 50 DOC and environmental model, the optimum combined value can be found at Mach 0.8 at 6 500 m. This results in a combined optimization of 71.30 % compared to the regular flight parameters (Mach 0.78 at 11 500 m). Mach 0.8 is close to the maximum operating Mach number of the aircraft but results in the optimum seat-mile cost. Corresponding to this speed, an altitude of 6 500 m results in the lowest environmental impact (see Figure 7.6). In the case of an emphasis on DOC, the optimum value is still at the same flight parameters but has an ever lower normalized value. This is because the optimal DOC zone is already at this point.

A higher wing loading implies a smaller wing surface when keeping the MTOW constant. This results in a shift of the minimum fuel consumption zone towards lower altitude, moving it closer to the zone of minimal equivalent CO_2 mass. An increase in wing loading will essentially merge the zones of minimum fuel consumption and minimum equivalent CO_2 mass. As a result, the normalized environmental impact values are significantly lower than in the normal wing loading case.

The optimal combined value with a 50 % higher wing loading can be found at Mach 0.8 at 3 000 m. This result in a combined optimization of 84.32 %, an increase of 13.02 % compared to the normal wing loading case. This is however at a greatly reduced altitude and will probably be outside of the aircraft's permissible flight envelope as mentioned before. Besides the flight envelope problem, flying at low altitudes generates safety and passenger comfort issues (see Chapter 7.4).

An important recent development that could alter the relationship between DOC and environmental impact is a CO_2 emissions standard for aircraft manufacturers. This standard is drafted by the ICAO and will be implemented starting in 2020 (scheduled date at the moment of publication). In short, the standard applies to all aircraft with an MTOW over 5 700 kilogram, which implies most aircraft types in the current global passenger jet fleet. It is based on fuel consumption during the cruise flight stage only. The standard covers three categories: newly designed aircraft which require a type certificate will have to comply by January 2020, all aircraft in production which require modifications will have to comply by the end of 2023, and finally all remaining in-production aircraft will have to comply by 2028 (**ATAG 2016**). The implication of this standard could be a shift of importance from economic to ecologic reasons.

9 Conclusions and Recommendations

9.1 Conclusions

The main goal of this work is to visualize and analyze the influence of cruise Mach number, cruise altitude, and aircraft wing loading on fuel consumption, DOC, and environmental impact. And subsequently combine these three objectives into one model. All calculations are done on the Airbus A320-200 as a reference aircraft, but the models are intended for any passenger jet aircraft.

Fuel consumption – Minimum fuel consumption is achieved by following a rising Mach number and rising altitude pattern. Each Mach number has its corresponding optimal altitude. A low Mach number must be flown at lower altitudes and an increasing Mach number requires an increase in altitude. Fuel consumption is predominantly influenced by the aerodynamic efficiency of the aircraft and to a lesser extent by the TSFC, Mach number and local speed of sound. A higher wing loading shifts the zone for minimal fuel consumption to lower altitudes due to a shift of the optimal lift coefficient (and aerodynamic efficiency) in the same direction.

Direct operating cost – Two metrics are available for calculating an aircraft's DOC: annual DOC and seat-mile cost. The annual DOC is minimal at minimal TAS (small Mach number, large altitude). However, this result does not represent the economic impact: it simply minimizes the amount of flights per year which reduces all time-dependent costs (fuel, maintenance, staff, and fees and charges), in this way also minimizing possible revenue generation by the aircraft. The more correct approach is to compare the seat-mile cost.

The seat-mile cost must be as low as possible to increase possible revenue gain. It is predominantly influenced by the aircraft's flight time. A shorter flight time implies a lower seat-mile cost, situating the optimum at the highest Mach number combined with a medium-low altitude. The higher wing loading case shifts optimal seat-mile cost from medium-low altitudes to the lowest altitude because of the change in annual DOC through fuel consumption.

Environmental impact – The environmental impact is expressed as a combination of resource depletion (equal to fuel consumption) and engine emissions (in the form of equivalent CO_2 mass). The emission of equivalent CO_2 mass peaks at the cruise altitude zone used by passenger jet aircraft nowadays. A reduction of cruise altitude from 11 500 m to 6 500 m would reduce the formation of AIC to almost none. For the Airbus A320-200, this and other beneficial effects of flying at a lower altitude (e.g. lower emission of NO_x) would reduce equivalent CO_2 mass by 77.66 % with an increase in fuel consumption of 5.64 %. If a variation in Mach number would also be applied from Mach 0.78 to Mach 0.65 at 6 500 m, a fur-

ther reduction of equivalent CO_2 mass of 13.36 % and a reduction in fuel consumption of 11.86 % are achieved.

A higher wing loading optimizes the normalized environmental impact results even more. This is because the zones of minimum fuel consumption and minimum equivalent CO_2 mass merge with increasing wing loading.

Combined model – In the combined model results are generated for two cases: one where economic and ecologic benefits have an equal importance and one with an emphasis on the economic benefits. In both cases the general trend is a reduction in cruise altitude and an unaltered cruise Mach number compared to present-day conditions. An emphasis on economic interest yields lower (and thus better) results in the optimal zone than the case with equal importance. This is because the optimum is already mostly influence by DOC. Therefore, decreasing the importance of environmental impact will further optimize the results. A higher wing loading shifts the optimal zone towards lower altitudes.

Operational limitations – Flying at a lower cruise altitudes comes with certain complications. As mentioned in Chapter 7.4 most of these are related to aircraft safety or passenger comfort: no possibility to fly over weather phenomena, a higher chance of bird strikes, and less reaction time in case of emergency. When coupled with low Mach number, there is the added possibility that the aircraft is flying outside of its permitted flight envelope. Load factors here can be higher than the structural limit of the aircraft or it could be flying below stall speed.

9.2 Recommendations

When considering varying cruise Mach number and altitude for an aircraft, the flight envelope should be kept in mind. In this thesis optimal theoretical values are proposed for several goals, but there is no guarantee that the aircraft could actually operate at these flight conditions. As an example: flying at low Mach number and high altitude could be well below the aircraft's stall speed and flying at high Mach number and low altitude could result in ambient conditions above the aircraft's structural limit (the cabin pressure differential would be too high). Therefore, a protection could be built into all models that ensures the results to be within the considered aircraft's flight envelope.

As mentioned in Chapter 6.2.2, flight time has a considerable influence on the seat-mile cost and various DOC categories. This means that an improvement on the approximating flight time model introduced in Chapter 6.2.2 would yield an improved accuracy in both seat-mile cost and annual DOC results. The model could be enhanced by including BADA data for more and more modern aircraft (more up-to-date BADA data is not publicly available at the time of publication) and by modelling the data with more fitting and complex equations.

Finally, the influence of the ICAO's CO_2 standard (as described in Chapter 8.4) or possible future environmental taxes could be included in a quantitative way in the weighting factors of DOC and environmental impact. This standard could shift importance from economic to ecologic consequences or change ecologic into economic consequences.

References

AIRBUS, 2002. *Getting to grips with aircraft performance*. Blagnac, France: Airbus S.A.S. Available at: https://bit.ly/2x5k8rr, archived as: https://perma.cc/2KRG-2W9K

AIRBUS, 2005a. *A320 Aircraft characteristics / Airport and maintenance planning*. Blagnac, France: Airbus S.A.S. Available at: https://bit.ly/2IjsDUY, archived as: https://perma.cc/S8XL-P92S

AIRBUS, 2005b. *A380 Aircraft characteristics / Airport and maintenance planning*. Blagnac, France: Airbus S.A.S. Available at: https://bit.ly/2Rt6Uy3, archived as: https://perma.cc/K9EP-NHU6

ANDERSON, John D., 1989. *Introduction to flight*. New York, NY: McGraw-Hill.

ATAG, 2016. *Q&A: The ICAO CO_2 Standard for Aircraft*. Air Transport Action Group. Available as PDF at: https://bit.ly/2XuqEa5, archived as: https://perma.cc/4NSC-DZQ4

BAUGHCUM, Steven L., TRITZ, Terrance G., HENDERSON, Stephen C., et al., 1996. *Scheduled Civil Aircraft Emission Inventories for 1992: Database Development and Analysis*. Hampton, Virginia: NASA Langley Research Center, NASA contractor report 4700. Available at: https://go.nasa.gov/2IXUDhb, archived as: https://perma.cc/ZR6G-3T2D

BENSEL, Artur, 2018. *Characteristics of the Specific Fuel Consumption for Jet Engines*. Hamburg, Germany: Department of Automotive and Aeronautical Engineering, HAW Hamburg, Project. Available at: https://bit.ly/2FlGQQG, archived as: https://perma.cc/5V3M-732P

BLAKE, W. and Performance Training Group, 2009. *Jet transport performance methods, D6-1420*. Seattle, WA: Flight Operations Engineering, Boeing Commercial Airplanes. Available at: https://bit.ly/2XlSTI1, archived as: https://perma.cc/JH88-6E2W

BOEING, 2018. Boeing Commercial Market Outlook. Seattle, WA: Boeing Commercial Airplanes. Available at: https://bit.ly/2FoJqWW, archived as: https://perma.cc/T9BS-FBX3

BURZLAFF, Marcus, 2017. *Aircraft Fuel Consumption – Estimation and Visualization*. Hamburg, Germany: HAW Hamburg, project. Available at: https://bit.ly/2XsH2aU, archived as: https://perma.cc/L65B-BTN4

CLEARY, Edward C., DOLBEER, Richard A., 2005. *Wildlife Hazard Management at Airports*. Washington D.C.: Federal Aviation Administration. Available at: https://bit.ly/2JZdTvx, archived as: https://perma.cc/744P-7EF2

DLR, 2011. *DLR Airbus A320 ATRA taxis using fuel cell-powered nose wheel for the first time*. News Archive DLR. Available at: https://bit.ly/31LuYAY, archived as: https://perma.cc/NDM6-7LUH

EUROCONTROL, 1998. *Aircraft Performance Summary Tables for the Base of Aircraft Data (BADA) Revision 3.0*. Eurocontrol Experimental Centre. Available at: https://bit.ly/31WyjgT, archived as: https://perma.cc/CV3G-4JSW

EUROCONTROL, 2019. Aircraft Performance Database. 2019/06/21, Website. Available at: https://bit.ly/2ItpbZo, archived as: https://perma.cc/6MRT-LTXJ

FAA, 2017. *Reduced Vertical Separation Minimum (RVSM)*. Federal Aviation Administration. Available at: https://bit.ly/31IP4Mh, archived as: https://perma.cc/XS5R-L4R9

FAR Part 1, 2005. *Federal Aviation Regulations, Part 1, Definitions and Abbreviations*. Washington D.C.: Federal Aviation Administration. Available at: https://bit.ly/2Kr81Ol, archived as: https://perma.cc/89JV-SUXJ

FICHTER, Christine, MARQUART, Susanne, SAUSEN Robert, et al., 2005. *The impact of cruise altitude on contrails and related radiative forcing.* In: Meteorologische Zeitschrift. Berlin, Germany: Gebrueder Borntraeger. Vol. 14, No. 4, pp. 563-572. Available at: https://bit.ly/2IV9MjA, archived as: https://perma.cc/H2FA-46T4

GREWE, Volker, LINKE, Florian, 2017. *Eco-efficiency in aviation*. Metereologische Zeitschrift, Vol. 26, No. 6, pp. 689-696. Available at: https://bit.ly/2G4xvNl, archived as: https://perma.cc/85YM-NK8K

HERRMANN, Steffen, 2010. Untersuchung des Einflusses der Motorenzahl auf die Wirtschaftlichkeit eines Verkehrsflugzeuges unter Berücksichtigung eines optimalen Bypassverhältnisses. Berlin, Germany: Technical University, Institute for Aerospace Sciences, Department of Aircraft and Lightweight Design, Thesis.

HULL, David G., 2007. *Fundamentals of Airplane Flight Mechanics*. Berlin, Germany: Heidelberg.

HURT, Harry H. Jr., 1965. *Aerodynamics for Naval Aviators*. Direction of Commander, Naval Air Systems Command. Available at: https://bit.ly/2WTNsLS, archived as: https://perma.cc/6CLR-BVQL

IATA, 2010. *IATA economic briefing: Airline fuel and labor cost share*. Montréal, Canada: International Air Traffic Association. Available at: https://bit.ly/2LbskyT, archived as: https://perma.cc/B8SA-SXAG

ICAO, 2019. *Aircraft Engine Emissions Databank*. ICAO Doc 9646- AN/943, Excel database. Available at: https://bit.ly/31q4STV, archived as: https://perma.cc/SYJ7-824H

EIA, 2019. U.S. Energy Information Administration. 2019/06/12, Website. Available at: https://bit.ly/2IqZWql, archived as: https://perma.cc/EXR9-WN8X

JACKSON, Paul, 2007. *Jane's All the World's Aircraft 2007-2008*. Surrey, UK: Jane's Information Group Limited.

JARDINE, N. Christian, 2005. *Calculating the Environmental Impact of Aviation Emissions*. Oxford, UK: Environmental Change Institute, Oxford University Centre for the Environment. Available at: https://bit.ly/2N93v90, archived as: https://perma.cc/A6ZV-TGWD

JENKINSON, R. Lloyd, SIMPKIN, Paul, RHODES, Darren, 1999. *Civil Jet Aircraft Design*. Oxford, UK: Butterworth-Heinemann.

JENSEN, Bret, LONGACRE, Jordan, 2018. 2018 ecoDemonstrator to begin flight testing. News Archive Boeing. Available at: https://bit.ly/2XsSGCI, archived as: https://perma.cc/4SLY-WKJH

KIM, Brian, FLEMING, Gregg, BALASUBRAMANIAN, Sathya, et al., 2005. SAGE: System for assessing Aviation's Global Emissions Version 1.5. Washington D.C.: Federal Aviation Administration, Technical Manual. Available at: https://bit.ly/2ZBlbLU, archived as: https://perma.cc/AP6Y-7C8H

MEYER, Silvia, 2004. *Ein Vergleich von DOC-Methoden hinsichtlich der Kosten für Gebühren*. Hamburg, Germany: HAW Hamburg, Project. Available at: https://bit.ly/2x3cCxg, archived as: https://perma.cc/3XBZ-GP78

NASA, 1976. *U.S. Standard Atmosphere*. Washington, D.C.: U.S. Government Printing Office. Available at: https://bit.ly/2FmUbIr, archived as: https://perma.cc/PWX4-LFQV

NEUBAUER, Scott C., MEGONIGAL, Patrick J., 2015. *Moving Beyond Global Warming Potentials to Quantify the Climatic Role of Ecosystems*. In: Ecosystems, Vol. 18, No. 6, pp. 1000-1013. Available at: https://doi.org/10.1007/s10021-015-9879-4, archived as: https://perma.cc/ZHX3-V2QG

NITA, Mihaela Florentina, 2013. *Contributions to Aircraft Preliminary Design and Optimization*. München, Germany: Verlag Dr. Hut, Dissertation. Available at: https://bit.ly/2RmZWL2, archived as: https://perma.cc/EZE4-K34F

PENNER, Joyce E., LISTER, David H., GRIGGS, David J., et al., 1999. *Aviation and the Global Atmosphere*. Cambridge, UK: Cambridge University Press, Report. Available at: https://bit.ly/2It6FjI, archived as: https://perma.cc/6SPT-4ZV2

PONATER, Michael, MARQUART, Susanne, SAUSEN, Robert, 2002. Contrails in a comprehensive global climate model: Parameterization and radiative forcing results. In: Journal of Geophysical Research: Atmospheres. Vol. 107, pp. ACL 2-1 – ACL 2-15. Available at: https://bit.ly/2RvDdwd, archived as: https://perma.cc/9SX6-BLEE

ROBERSON, William; ROOT, Robert; ADAMS, Dell; 2007. *Fuel conservation strategies: Cruise flight*. In: Aero. Seattle, WA: The Boeing Company. Vol. Q04, pp. 23-27. Available at: https://bit.ly/2IsBJ31, archived as: https://perma.cc/656C-3XY3

ROUX, Elodie, 2002. Modèles Moteur... Réacteurs double flux civils et réacteurs militaires à faible taux et dilution avec PC. Toulouse, France: ISAE-SUPAERO, Report. Available at: https://bit.ly/2RoAJ2M, archived as: https://perma.cc/ECB8-WJFA

SAUSEN, Robert, ISAKSEN, Ivar, GREWE, Volker, et al., 2005. *Aviation radiative forcing in 2000: an update on IPCC (1999)*. In: Meteorologische Zeitschrift. Berlin, Germany: Gebrueder Borntraeger. Vol. 14, No. 4, pp. 555-561. Available at: https://bit.ly/2IuAtwt, archived as: https://perma.cc/62S6-6P27

SCHOLZ, Dieter, 2012. *Flugmechanik 1: Unterlagen zur Vorlesung*. Hamburg, Germany: HAW Hamburg, Lecture notes. Available at: https://bit.ly/2IrXoIL, archived as: https://perma.cc/AY6Y-7AME

SCHOLZ, Dieter, 2015. *Aircraft design*. Hamburg, Germany: HAW Hamburg, Lecture notes. Available at: https://bit.ly/2Kwd8N4, archived as: https://perma.cc/H5GK-HN3N

SCHOLZ, Dieter, 2017. *Der spezifische Kraftstoffverbrauch von Flugtriebwerken (TSFC und PSFC)*. Hamburg, Germany: HAW Hamburg, Memo. Available at: https://bit.ly/2XjUzSk, archived as: https://perma.cc/5E23-PJEN

SCHOLZ, Dieter, 2018. *Evaluating Aircraft with Electric and Hybrid Propulsion*. Presentation from the Electric & Hybrid Aerospace Symposium 2018 in Cologne. Available at: https://bit.ly/2MWBcuz, archived as: https://perma.cc/S2QK-W86J

SCHWARZ, Emily Dallara, KROO, Ilan M., 2009. Aircraft Design: Trading Cost and Climate Impact. Available at: https://doi.org/10.2514/6.2009-1261, archived as: https://perma.cc/5S8U-RPM8

SCHWARZ, Emily Dallara, 2011. Aircraft Design for Reduced Climate Impact. Stanford, UK: Stanford University, Dissertation. Available at: https://stanford.io/2ZDuifo, archived as: https://perma.cc/683N-3RQG

SETO, L., 2009. *Cost index*. Seattle, WA: Boeing Commercial Airplanes, Flight Operations Engineering. Available at: https://bit.ly/2IQZ8dy, archived as: https://perma.cc/5SXJ-NYC8

SPAKOVSZKY, Z. S., 2006. *16.Unified: Thermodynamics and Propulsion*. Lecture notes digitalized by MIT. Cambridge, MA: Massachusetts Institute of Technology. Available at: https://bit.ly/31U6QfJ, archived as: https://perma.cc/M6DD-TZTU

SWELBAR, William S., BELOBABA, Peter P., 2018. *Airline Data Project*. Cambridge, MA: MIT Global Airline Industry Program. Available at: https://bit.ly/2II0FUd, archived as: https://perma.cc/GWJ3-XN3W

VAN ENDERT, Lynn, 2017. *Definition of an Ecolabel for Aircraft*. Hamburg, Germany: HAW Hamburg.

WHITELEGG, John, 2000. *Aviation: the social, economic and environmental impact of flying*. London, UK: Ashden Trust. Available at: https://bit.ly/31Ul2p4, archived as: https://perma.cc/BL4K-BYB9

WORLDBANK, 2019. *Inflation, consumer prices (annual %) for the United States*. The World Bank Database. Available at: https://bit.ly/2x6Pjmi, archived as: https://perma.cc/EPA9-4YX9

YOUNG, Trevor M., 2001. *Lecture Notes Flight Mechanics Course ME 4726*. Limerick, Ireland: University of Limerick.

YOUNG, Trevor M., 2018. *Performance of the Jet Transport Airplane: Analysis Methods, Flight Operations, and Regulations*. Hoboken, NJ: Wiley.

All links viewed on 2019-06-20 or later.

Appendix A – TSFC Model by Herrmann

All equations are established by **Herrmann 2010**.

$$SFC = \frac{0.697\sqrt{\frac{T(h)}{T_0}}\left(\phi - \vartheta - \frac{\chi}{\eta_{comp}}\right)}{\sqrt{5\,\eta_{noz}\left(1+\eta_{fan}\,\eta_{turb}\,BPR\right)\cdot\left(G+0.2\,M^2\,BPR\,\frac{\eta_{comp}}{\eta_{fan}\cdot\eta_{turb}}\right)} - M\,(1+BPR)}$$

$$G = \left(\phi - \frac{\chi}{\eta_{comp}}\right)\cdot\left(1 - \frac{1.01}{\eta_{gasgen}^{\frac{\gamma-1}{\gamma}}\cdot(\chi+\vartheta)\cdot\left(1-\frac{\chi}{\phi\cdot\eta_{comp}\cdot\eta_{turb}}\right)}\right)$$

$$\vartheta = 1+\frac{\gamma-1}{2}\cdot M^2 \;;\quad \phi = T_{TE}/T(h) \;;\quad \chi = \vartheta\cdot\left(OAPR^{\frac{\gamma-1}{\gamma}}-1\right) \;;\quad \eta_{gasgen} = 1-\frac{0.7M^2(1-\eta_{inlet})}{1+0.2M^2}$$

Turbine entry temperature in cruise: $T_{TE} = \frac{-8000\ \mathrm{K}\cdot\mathrm{kN}}{T_{TO}} + 1520\ \mathrm{K}$

$$OAPR = 2.668\cdot10^{-5}\ 1/\mathrm{kN}\cdot T_{TO} + 3.517\cdot BPR + 0.05566$$

$$\eta_{comp} = \frac{-2\ \mathrm{kN}}{2\ \mathrm{kN}+T_{TO}} - \frac{0.1171}{0.1171+BPR} - M\cdot0.0541 + 0.9407$$

$$\eta_{turb} = \frac{-3.403\ \mathrm{kN}}{3.403\ \mathrm{kN}+T_{TO}} + 1.048 - M\cdot0.1553$$

$$\eta_{inlet} = 1-(1.3+0.25\,BPR)\cdot\Delta p/p$$

$$\eta_{fan} = \frac{-5.978\ \mathrm{kN}}{5.978\ \mathrm{kN}+T_{TO}} - M\cdot0.1479 - \frac{0.1335}{0.1335+BPR} + 1.055$$

$$\eta_{noz} = \frac{-2.032\ \mathrm{kN}}{2.032\ \mathrm{kN}+T_{TO}} + 1.008 - M\cdot0.009868$$

$T(h)$ is the temperature at altitude, $T_0 = 288$ K, T_{TO} is the take-off thrust of one engine and $\Delta p/p \approx 0.02$ is the inlet pressure loss, the ratio of specific heats $\gamma = 1.4$. Efficiencies are only valid for $T_{TO} > 80$ kN.

HERRMANN, Steffen: *Untersuchung des Einflusses der Motorenzahl auf die Wirtschaftlichkeit eines Verkehrsflugzeuges unter Berücksichtigung eines optimalen Bypassverhältnisses*. Berlin, Technical University, Institute for Aerospace Sciences, Department of Aircraft and Lightweight Design, Thesis, 2010

Appendix B – Boeing Fuel Flow Method 2

This method is adapted from **Baughcum 1996** and **Kim 2005**. The aim is to generate a value for the emission index of NO_x in function of the aircraft's fuel flow. The method will be explained in a step-wise manner.

1. The aircraft's engine should be looked up in the ICAO's Aircraft Engines Emission Database (**ICAO 2019**). The ICAO values for fuel flow must be adjusted for installation effects on the aircraft. The correction factors are:

- $r = 1.010$ for take-off
- $r = 1.013$ for climbout
- $r = 1.020$ for approach
- $r = 1.100$ for idle

2. In this step the adjusted fuel flow data and the corresponding EI_NO_x values from ICAO 2019 must be plotted in a log-log plot. An example is given:

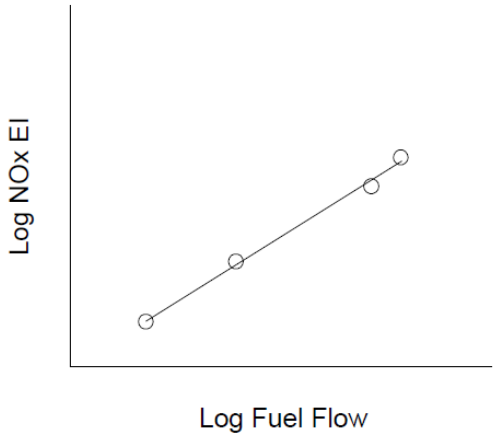

Figure B.1: Example of the log-log plot of EI_NOx in function of fuel flow (**Kim 2005**)

3. The aircraft's uncorrected fuel flow (in kg/s) must be calculated as follows:

$$W_f = f \cdot V \qquad (B.1)$$

With: V in km/s

Then the corrected fuel flow must be calculated with the following equation from Boeing:

$$W_{ff} = \frac{W_f}{\delta} \cdot \left(\theta^{3.8} \cdot e^{0.2 \cdot M^2}\right) \qquad (B.2)$$

4. A linear trendline is plotted over the log-log plot in Excel. The equation from the trendline is then used to calculate the corresponding EI_NO_x value and has the following general structure:

$$EI_{NO_x,graph} = a \cdot W_{ff} + b \tag{B.3}$$

5. In this final step the calculated $EI_{NO_x,graph}$ value from step 4 is uncorrected in order to reflect the at-altitude flight conditions. This is done by using different factors which take the effect of humidity into account:

$$k_H = -19 \cdot \left(\frac{0.37318 \cdot p_v}{p - 0.6 \cdot p_v} - 0.0063\right) \tag{B.4}$$

With:

$$p_v = 6895 \cdot 0.014504 \cdot 10^{\beta} \tag{B.5}$$

With:

$$\beta = 7.90298 \cdot (1 - k_T) + 3.00571 + 5.02808 \cdot \log_{10}(k_T)$$
$$+1.3817 \cdot 10^{-7} \cdot \left[1 - 10^{11.344 \cdot (1 - k_T)}\right] + 8.1328 \cdot 10^{-3} \cdot \left[10^{3.39149 \cdot (1 - k_T)} - 1\right] \tag{B.6}$$

With:

$$k_T = \frac{373.16}{T + 0.01}$$

Finally, EI_NO_x can be calculated:

$$EI_{NO_x} = EI_{NO_x,graph} \cdot e^{k_H} \cdot \left(\frac{\delta^{1.02}}{\theta^{3.3}}\right)^{0.5} \tag{B.7}$$

Appendix C – Forcing Factor Data

All values are compiled in **Van Endert 2017**, based on a graph from **Schwarz 2011**. In the original graph, data only started above 17 000 feet, but according to Schwarz the forcing factor at lower altitudes can be set equal to the first available value above it. This principle is applied to the data in red.

Table C.1: Forcing factor for aircraft-induced clouds

Altitude (ft)	Forcing factor
16000	0,0284495
17470,3	0,0284495
19547,9	0
21529,7	0
23511,4	0,173542
25525,1	0,395448
27506,8	0,799431
29456,6	1,25178
31598,2	1,70982
33547,9	2,10526
35529,7	1,82077
37543,4	1,53343
39557,1	0,967283
41538,8	0,793741

Table C.2: Forcing factor for short ozone

Altitude (ft)	Forcing factor
16000	0,469417
17502,3	0,469417
19484	0,55761
21497,7	0,620199
23479,5	0,711238
25525,1	0,711238
27506,8	0,813656
29520,5	0,930299
31502,3	1,00996
33484	1,13229
35561,6	1,42816
37575,3	1,62447
39589,0	1,8037
41538,8	1,93172

Table C.3: Forcing factor for long ozone and methane

Altitude (ft)	Forcing factor
16000	0,86771
17470,3	0,86771
19484	0,924609
21497,7	0,955903
23543,4	0,961593
25525,1	0,944523
27538,8	0,927454
29520,5	0,927454
31534,2	0,941679
33516	0,975818
35561,6	1,14083
37543,4	1,21479
39589	1,20341
41570,8	1,20341

Appendix D – Flight Time Estimation

Flight time estimation is based on BADA data from **Eurocontrol 1998** and represented by the following four figures.

TAS for climb and descent follows a pretty similar pattern for these aircraft (see figure D.1 and figure D.2). The true airspeed will be approximated by two linear zones and a constant speed zone. A variation from 150 knots to 289 knots below FL100, a variation from about 360 knots to cruise speed between FL120 and FL300 and a zone of constant cruise speed above FL300.

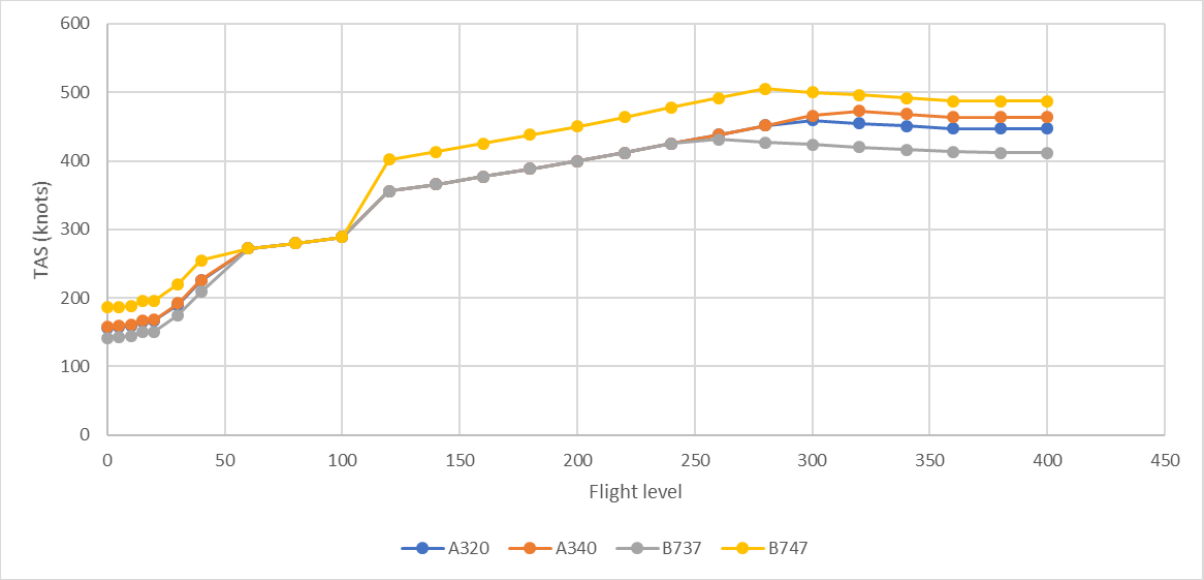

Figure D.1: TAS during climb based on BADA data (**Eurocontrol 1998**)

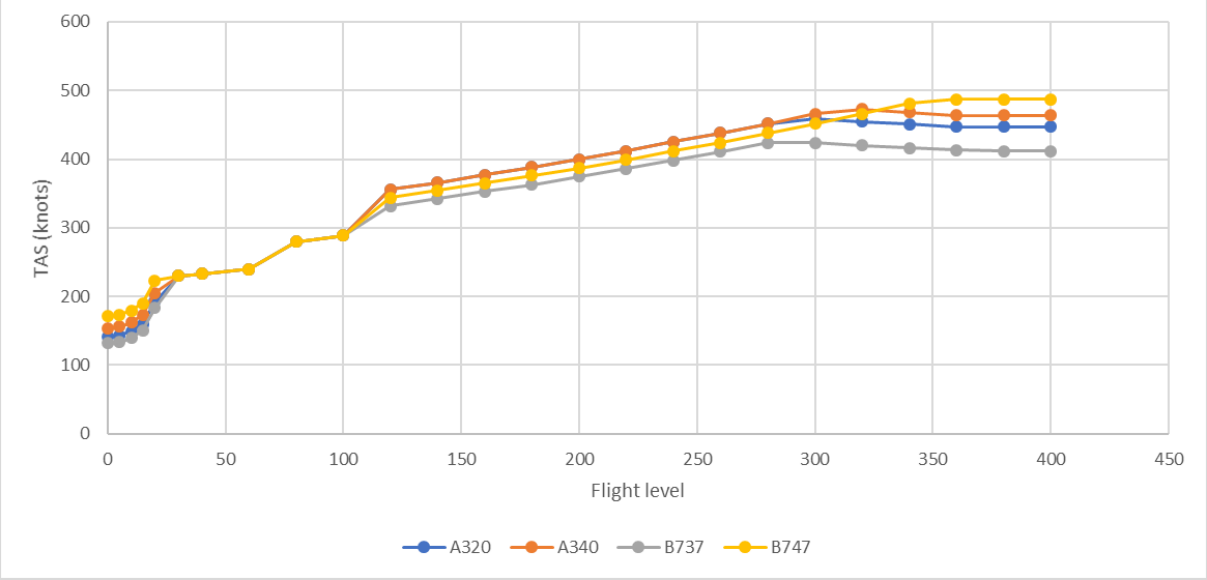

Figure D.2: TAS during descent based on BADA data (**Eurocontrol 1998**)

Rate of climb and rate of descent follow a more irregular pattern (see figure D.3 and figure D.4). A rough approximation will be made of an average ROC and ROD of 2 000 ft/min.

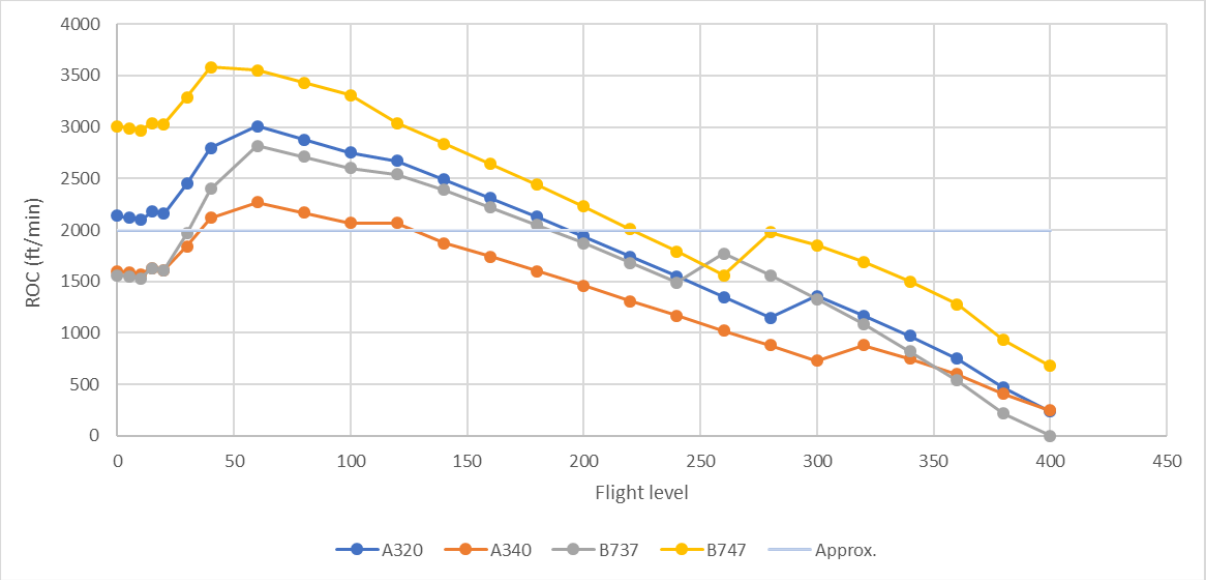

Figure D.3: Rate of climb based on BADA data (**Eurocontrol 1998**)

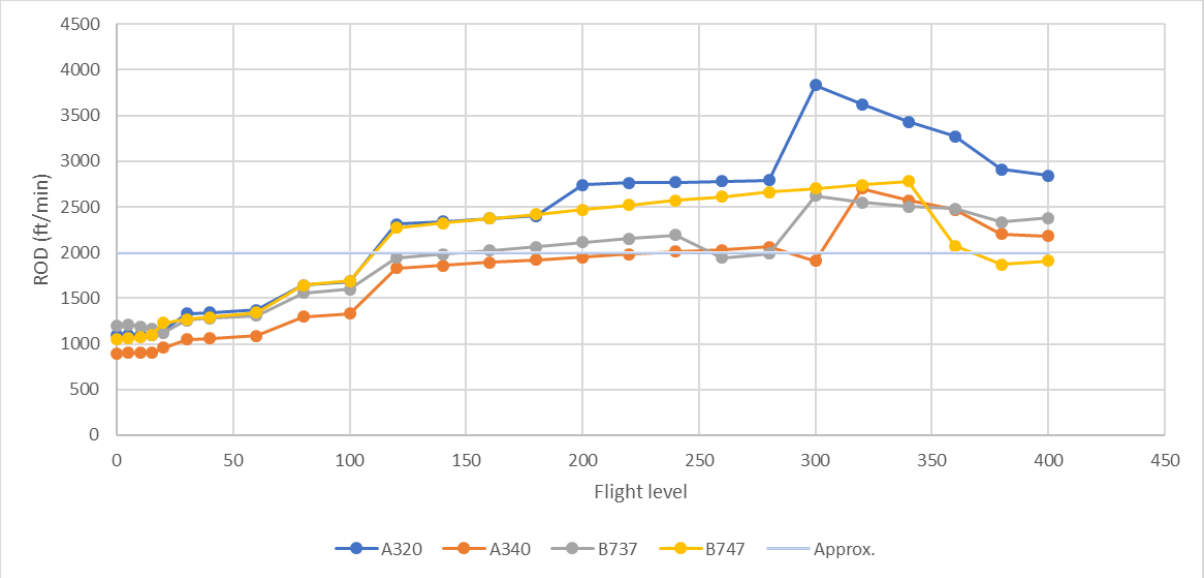

Figure D.4: Rate of descent based on BADA data (**Eurocontrol 1998**)

Based on this data, the following approximating equations are produced:

Below FL100:

$$TAS = 1.4 \cdot FL + 150 \tag{D.1}$$

At FL120:

$$TAS = 360 \tag{D.2}$$

Between FL120 and FL300:

$$TAS = \frac{TAS_{CR} - 360}{180} \cdot (FL - 120) + 360 \tag{D.3}$$

Above FL300:

$$TAS = TAS_{CR} \tag{D.4}$$

For the Airbus A320-200 this result in the average TAS during climb and descent as displayed in Figure 6.6.

Appendix E – Case Study: Airbus A380-800

In this appendix the procedure of calculating minimal fuel consumption, DOC, and environmental impact from Chapter 5 to 8 is repeated for the case of an Airbus A380-800. Only the final results for fuel consumption, DOC, environmental impact, and the combined model will be displayed. All aircraft data are found in **Airbus 2005b**.

		Mach number										
		0,4	0,45	0,5	0,55	0,6	0,65	0,7	0,75	0,8	0,85	0,9
Altitude (m)	3000	8,05E-05	7,02E-05	6,53E-05	6,36E-05	6,41E-05	6,65E-05	7,07E-05	7,68E-05	8,54E-05	9,99E-05	1,66E-04
	3500	8,36E-05	7,20E-05	6,61E-05	6,37E-05	6,35E-05	6,52E-05	6,87E-05	7,40E-05	8,17E-05	9,48E-05	1,55E-04
	4000	8,71E-05	7,41E-05	6,72E-05	6,39E-05	6,31E-05	6,41E-05	6,71E-05	7,16E-05	7,84E-05	9,02E-05	1,45E-04
	4500	9,12E-05	7,66E-05	6,86E-05	6,45E-05	6,30E-05	6,34E-05	6,57E-05	6,95E-05	7,55E-05	8,61E-05	1,37E-04
	5000	9,57E-05	7,95E-05	7,03E-05	6,54E-05	6,31E-05	6,29E-05	6,46E-05	6,78E-05	7,30E-05	8,25E-05	1,29E-04
	5500	1,01E-04	8,28E-05	7,24E-05	6,66E-05	6,36E-05	6,28E-05	6,38E-05	6,64E-05	7,09E-05	7,93E-05	1,22E-04
	6000	1,06E-04	8,66E-05	7,49E-05	6,81E-05	6,44E-05	6,29E-05	6,33E-05	6,53E-05	6,91E-05	7,66E-05	1,16E-04
	6500	1,13E-04	9,08E-05	7,78E-05	7,00E-05	6,55E-05	6,34E-05	6,32E-05	6,45E-05	6,77E-05	7,42E-05	1,10E-04
	7000	1,20E-04	9,57E-05	8,12E-05	7,23E-05	6,70E-05	6,42E-05	6,33E-05	6,41E-05	6,66E-05	7,23E-05	1,05E-04
	7500	1,28E-04	1,01E-04	8,50E-05	7,51E-05	6,89E-05	6,53E-05	6,39E-05	6,40E-05	6,59E-05	7,08E-05	1,01E-04
	8000	1,36E-04	1,07E-04	8,94E-05	7,82E-05	7,11E-05	6,68E-05	6,47E-05	6,43E-05	6,55E-05	6,97E-05	9,70E-05
	8500	1,46E-04	1,14E-04	9,44E-05	8,19E-05	7,38E-05	6,87E-05	6,60E-05	6,49E-05	6,55E-05	6,89E-05	9,38E-05
	9000	1,57E-04	1,22E-04	1,00E-04	8,61E-05	7,70E-05	7,11E-05	6,76E-05	6,59E-05	6,59E-05	6,86E-05	9,12E-05
	9500	1,69E-04	1,30E-04	1,06E-04	9,09E-05	8,06E-05	7,39E-05	6,96E-05	6,73E-05	6,67E-05	6,87E-05	8,91E-05
	10000	1,82E-04	1,40E-04	1,14E-04	9,63E-05	8,49E-05	7,71E-05	7,21E-05	6,91E-05	6,79E-05	6,92E-05	8,76E-05
	10500	1,97E-04	1,51E-04	1,22E-04	1,03E-04	8,97E-05	8,10E-05	7,51E-05	7,14E-05	6,96E-05	7,02E-05	8,67E-05
	11000	1,96E-04	1,50E-04	1,21E-04	1,02E-04	8,95E-05	8,08E-05	7,50E-05	7,12E-05	6,94E-05	6,99E-05	8,64E-05
	11500	2,11E-04	1,61E-04	1,30E-04	1,09E-04	9,46E-05	8,49E-05	7,83E-05	7,39E-05	7,15E-05	7,14E-05	8,62E-05
	12000	2,27E-04	1,73E-04	1,39E-04	1,16E-04	1,00E-04	8,95E-05	8,21E-05	7,70E-05	7,40E-05	7,33E-05	8,66E-05
	12500	2,45E-04	1,86E-04	1,48E-04	1,24E-04	1,07E-04	9,47E-05	8,64E-05	8,06E-05	7,70E-05	7,57E-05	8,75E-05

Figure E.1: Results fuel consumption A380 in kg fuel per NM, per kg of MTOW

		Mach number										
		0,4	0,45	0,5	0,55	0,6	0,65	0,7	0,75	0,8	0,85	0,9
Altitude (m)	3000	0,174	0,158	0,146	0,137	0,130	0,125	0,121	0,118	0,117	0,117	0,116
	3500	0,176	0,160	0,147	0,138	0,131	0,125	0,121	0,118	0,117	0,117	0,117
	4000	0,178	0,161	0,148	0,139	0,131	0,126	0,121	0,118	0,116	0,116	0,117
	4500	0,180	0,162	0,149	0,140	0,132	0,126	0,121	0,118	0,116	0,115	0,117
	5000	0,182	0,164	0,150	0,140	0,132	0,126	0,121	0,118	0,115	0,115	0,117
	5500	0,184	0,165	0,152	0,141	0,133	0,127	0,122	0,118	0,115	0,114	0,117
	6000	0,185	0,167	0,153	0,142	0,134	0,127	0,122	0,118	0,115	0,114	0,117
	6500	0,186	0,169	0,155	0,143	0,135	0,128	0,122	0,118	0,115	0,113	0,117
	7000	0,188	0,171	0,156	0,145	0,136	0,129	0,123	0,118	0,115	0,113	0,117
	7500	0,189	0,173	0,158	0,146	0,137	0,129	0,124	0,119	0,115	0,113	0,117
	8000	0,190	0,175	0,160	0,148	0,138	0,130	0,124	0,119	0,116	0,113	0,117
	8500	0,192	0,176	0,162	0,149	0,139	0,131	0,125	0,120	0,116	0,113	0,117
	9000	0,193	0,177	0,164	0,151	0,141	0,133	0,126	0,121	0,116	0,114	0,117
	9500	0,195	0,178	0,165	0,153	0,143	0,134	0,128	0,122	0,118	0,115	0,117
	10000	0,196	0,180	0,166	0,155	0,144	0,136	0,129	0,123	0,118	0,115	0,117
	10500	0,198	0,181	0,168	0,157	0,146	0,137	0,130	0,124	0,119	0,116	0,117
	11000	0,199	0,182	0,168	0,158	0,147	0,138	0,131	0,125	0,120	0,116	0,118
	11500	0,199	0,182	0,169	0,158	0,148	0,139	0,132	0,125	0,120	0,117	0,117
	12000	0,200	0,183	0,169	0,159	0,150	0,140	0,133	0,126	0,121	0,117	0,118
	12500	0,201	0,183	0,170	0,159	0,150	0,142	0,134	0,127	0,122	0,118	0,118

Figure E.2: Results seat-mile cost A380 in USD

Altitude (m) \ Mach number	0,4	0,45	0,5	0,55	0,6	0,65	0,7	0,75	0,8	0,85	0,9
3000	0,052	0,022	0,008	0,003	0,005	0,011	0,023	0,039	0,063	0,102	0,276
3500	0,060	0,027	0,011	0,003	0,003	0,007	0,017	0,032	0,053	0,088	0,248
4000	0,070	0,033	0,014	0,004	0,002	0,004	0,012	0,025	0,043	0,075	0,223
4500	0,082	0,040	0,018	0,006	0,001	0,002	0,009	0,019	0,035	0,064	0,200
5000	0,095	0,049	0,022	0,008	0,002	0,001	0,005	0,014	0,029	0,054	0,179
5500	0,110	0,059	0,029	0,012	0,004	0,001	0,004	0,011	0,024	0,047	0,164
6000	0,129	0,072	0,038	0,018	0,008	0,003	0,005	0,010	0,021	0,043	0,156
6500	0,150	0,086	0,048	0,025	0,012	0,006	0,006	0,010	0,019	0,039	0,146
7000	0,177	0,105	0,062	0,036	0,020	0,012	0,010	0,012	0,021	0,039	0,144
7500	0,204	0,124	0,075	0,045	0,027	0,017	0,013	0,014	0,020	0,036	0,134
8000	0,236	0,147	0,092	0,058	0,037	0,024	0,018	0,018	0,022	0,037	0,129
8500	0,280	0,177	0,115	0,076	0,051	0,035	0,028	0,025	0,028	0,041	0,132
9000	0,331	0,213	0,141	0,096	0,067	0,049	0,039	0,034	0,036	0,047	0,135
9500	0,385	0,251	0,169	0,118	0,084	0,062	0,050	0,043	0,043	0,052	0,135
10000	0,451	0,297	0,203	0,144	0,105	0,080	0,064	0,055	0,053	0,061	0,139
10500	0,540	0,358	0,248	0,178	0,133	0,102	0,083	0,072	0,067	0,073	0,149
11000	0,572	0,379	0,263	0,190	0,142	0,111	0,091	0,079	0,075	0,082	0,164
11500	0,685	0,455	0,319	0,233	0,177	0,139	0,115	0,101	0,094	0,099	0,181
12000	0,832	0,554	0,390	0,287	0,220	0,176	0,147	0,129	0,120	0,123	0,205
12500	1,000	0,667	0,471	0,349	0,270	0,217	0,182	0,160	0,148	0,149	0,230

Figure E.3: Results environmental impact A380 per NM flown, per seat (normalized)

Altitude (m) \ Mach number	0,4	0,45	0,5	0,55	0,6	0,65	0,7	0,75	0,8	0,85	0,9
3000	0,376	0,269	0,194	0,140	0,101	0,073	0,057	0,049	0,053	0,071	0,156
3500	0,391	0,280	0,201	0,145	0,103	0,074	0,055	0,045	0,046	0,044	0,144
4000	0,406	0,290	0,208	0,149	0,105	0,074	0,052	0,040	0,038	0,038	0,132
4500	0,422	0,301	0,216	0,154	0,108	0,074	0,051	0,037	0,032	0,032	0,121
5000	0,440	0,314	0,225	0,160	0,111	0,076	0,050	0,034	0,027	0,027	0,111
5500	0,460	0,328	0,235	0,167	0,116	0,078	0,051	0,033	0,023	0,023	0,104
6000	0,477	0,345	0,247	0,176	0,122	0,082	0,053	0,033	0,022	0,021	0,100
6500	0,494	0,363	0,261	0,186	0,130	0,087	0,056	0,034	0,021	0,020	0,096
7000	0,515	0,384	0,277	0,198	0,139	0,094	0,061	0,037	0,022	0,019	0,095
7500	0,536	0,406	0,293	0,211	0,149	0,102	0,066	0,040	0,023	0,018	0,091
8000	0,560	0,424	0,313	0,226	0,161	0,111	0,073	0,045	0,025	0,018	0,089
8500	0,589	0,446	0,336	0,244	0,175	0,122	0,082	0,052	0,030	0,021	0,088
9000	0,624	0,472	0,362	0,265	0,192	0,135	0,093	0,060	0,037	0,024	0,087
9500	0,659	0,497	0,382	0,288	0,211	0,152	0,107	0,072	0,047	0,026	0,090
10000	0,701	0,529	0,406	0,313	0,232	0,169	0,121	0,084	0,057	0,030	0,091
10500	0,755	0,567	0,436	0,341	0,256	0,190	0,139	0,099	0,070	0,037	0,098
11000	0,776	0,582	0,448	0,351	0,264	0,198	0,146	0,106	0,076	0,041	0,107
11500	0,836	0,624	0,478	0,374	0,290	0,218	0,163	0,121	0,089	0,050	0,115
12000	0,913	0,676	0,517	0,404	0,320	0,243	0,185	0,140	0,106	0,061	0,128
12500	1,000	0,735	0,560	0,437	0,347	0,273	0,210	0,161	0,125	0,075	0,142

Figure E.4: Results combined values A380 (normalized)

The A380-800 shows a trend towards a higher Mach number and a slightly higher cruise altitude than the A320-200. The higher Mach number is because of the aircraft's higher optimal cruise Mach number of Mach 0.85 compared to the A320's Mach 0.78. The higher cruise altitude follows from the aircraft's optimized design for higher altitude. The A380-800 is a wide-body long-range aircraft which is optimized to fly slightly faster and higher than a single aisle aircraft like the A320-200. The fact that it is built for long-range flight missions also explains why the seat-mile cost is significantly lower than the A320's seat-mile cost.